

**STREAM SUB-REACH DIFFERENTIATION: THE INFLUENCE OF LAND
MANAGEMENT**

by

Noelle Richardson

B.Sc., University of British Columbia, 2016

A THESIS SUBMITTED IN PARTIAL FULFILLMENT OF
THE REQUIREMENTS FOR THE DEGREE OF

MASTER OF SCIENCE

in

THE COLLEGE OF GRADUATE STUDIES

(Earth and Environmental Science)

THE UNIVERSITY OF BRITISH COLUMBIA

(Okanagan)

March 2020

© Noelle Richardson, 2020

The following individuals certify that they have read, and recommend to the College of Graduate Studies for acceptance, a thesis/dissertation entitled:

STREAM SUB-REACH DIFFERENTIATION: THE INFLUENCE OF LAND
MANAGEMENT

submitted by Noelle Richardson in partial fulfillment of the requirements of
the degree of Master of Science.

Dr. Bernard Bauer, Irving K. Barber School of Arts and Sciences

Supervisor

Dr. Craig Nichol, Irving K. Barber School of Arts and Sciences

Supervisory Committee Member

Dr. Robert Newbury, Irving K. Barber School of Arts and Sciences

Supervisory Committee Member

Dr. Dwayne Tannant, University of British Columbia

University Examiner

Abstract

Agricultural land-use practices impart unique biophysical signatures on streams at the scale of a farm or ranch. As such, Alderson Creek, a groundwater-fed stream that traverses several small agricultural land holdings, might be segmented into a series of sub-reaches, the boundaries of which align roughly with property divisions. A research project was designed to assess whether land management influences have implications on stream characteristics and aquatic health at the scale of agriculturally segmented landscapes.

A series of biophysical and chemical indicators of water quality were monitored regularly at several cross-sections along Alderson Creek. An assessment of the overall water quality was conducted with the use of time-series plots and downstream trends. Discriminant analysis (DA) tests were executed with various combinations of the measured variables. The intent was to identify sub-reach membership based on statistical similarities and differences. The results indicate that there is some evidence for sub-reach differentiation. Clustering of cross-sections was evident in the raw data (i.e., box-plots) as well as in statistical tests (i.e., discriminant analysis), although sub-reaches weren't delineated exactly as expected. Some sub-reaches were different from one another because land uses were distinctly different (R5 from R4). However, some sub-reaches were not clearly differentiable because land use was not distinctly different and there was some transference of water quality from upstream to downstream (R2 versus R1). Overall, this study determined that sub-reach differentiation is influenced by local influences (at the scale of a cross-section or monitoring site), downstream effects (reach scale), and land use practices (property or sub-reach scale).

Research undertaken in this thesis contributes to the literature on the role of human influences on stream health and to the understanding of scales of influence. Researchers as well as land-owners benefit from knowledge about the scale at which agricultural land uses may impact stream health as well as the potential benefits of rehabilitation. The implementation of best-management practices such as riparian rehabilitation along a small segment of a stream bounded by property lines, rather than an entire water course, does lead to overall improvements of water quality and ecosystem health.

Lay Summary

Rivers and streams are increasingly influenced by human land use. Alderson Creek is a groundwater-fed stream that runs through agricultural fields near Armstrong, BC. There are five agricultural properties through which Alderson Creek flows, dividing it into five sections that are referred to as 'sub-reaches'. Land adjacent to Alderson Creek is used for livestock husbandry and crop production, which are known to affect water quality, aquatic and riparian wildlife, and vegetation cover. Water quality indicators, such as temperature, were used in this study to assess stream health as it relates to land management. A comparison of water quality parameters between the sub-reaches provides an understanding of the dynamic behavior of the stream in time and space as well as the scale of impact. With increasing interest in stream rehabilitation, the research contributes to a broader understanding of the drivers of ecological change in streams.

Table of Contents

Abstract.....	iii
Lay Summary	iv
List of Tables	vii
List of Figures.....	viii
Acknowledgements	xii
Chapter 1. Introduction	1
1.1. PROJECT OVERVIEW	1
1.2. OBJECTIVE AND HYPOTHESIS	1
1.3. STUDY AREA.....	2
Chapter 2. Literature Review	6
2.1. LAND USE AND AGRICULTURAL IMPACTS ON WATER QUALITY IN STREAMS	6
2.2. SCALE CONSIDERATIONS IN STREAM SYSTEMS	9
2.3. STREAM HEALTH AND WATER QUALITY INDICATORS	12
2.3.1. <i>Temperature</i>	13
2.3.2. <i>Dissolved Oxygen</i>	14
2.3.3. <i>Electrical Conductivity</i>	15
2.3.4. <i>Turbidity</i>	15
2.3.5. <i>pH</i>	16
2.3.6. <i>Nitrogen</i>	17
2.3.7. <i>Macroinvertebrate Abundance</i>	17
2.3.8. <i>Macrophyte Density</i>	20
Chapter 3. Experimental Design	22
3.1. FIELD METHODS	22
3.1.1. <i>Sub-Reach Description and Sample Site Locations</i>	22
3.1.2. <i>Temperature</i>	28
3.1.3. <i>Conductivity, Turbidity, pH, Dissolved Oxygen</i>	29
3.1.4. <i>Nitrogen</i>	31
3.1.5. <i>Macrophytes and Macroinvertebrates</i>	32
3.2. LABORATORY METHODS.....	37
3.2.1. <i>Nitrogen</i>	37
3.2.2. <i>Macrophytes and Macroinvertebrates</i>	38
3.3. DATA ANALYSIS METHODS	42
3.3.1. <i>Temperature</i>	42
3.3.2. <i>Conductivity, Turbidity, pH, Dissolved Oxygen, Nitrogen, Macrophyte Density and Macroinvertebrate Abundance</i>	44
3.4. STATISTICAL ANALYSIS	44
Chapter 4. Results	49
4.1. GENERAL OBSERVATIONS AND DATA TRENDS	49
4.1.1. <i>Temperature</i>	49
4.1.2. <i>Conductivity, pH, Turbidity, Dissolved Oxygen</i>	53
4.1.2.1 <i>Conductivity</i>	54

4.1.2.2	<i>pH</i>	56
4.1.2.3	<i>Turbidity</i>	58
4.1.2.4	<i>Dissolved Oxygen</i>	61
4.1.3.	<i>Nitrogen, Macrophytes, Macroinvertebrates</i>	63
4.1.3.1	<i>Nitrogen</i>	63
4.1.3.2.	<i>Macrophyte Density</i>	65
4.1.3.3.	<i>Macroinvertebrate Density</i>	66
4.2.	SUB-REACH DIFFERENTIATION	70
4.3.	DISCRIMINANT ANALYSIS	75
Chapter 5.	Discussion	89
5.1.	SUB-REACH DIFFERENTIATION IN ALDERSON CREEK	89
5.2.	DISCRIMINATING POWER OF DA VARIABLES FOR SUB-REACH DIFFERENTIATION	91
5.3.	OPTIMIZED SUB-REACH DIFFERENTIATION	97
5.4.	GENERAL DOWNSTREAM TRENDS VERSUS LOCALIZED EFFECTS	100
5.5.	SUB-REACH DIFFERENTIATION AND LAND MANAGEMENT	101
5.6.	EXPERIMENTAL DESIGN CONSIDERATIONS	103
Chapter 6.	Conclusions	105
Bibliography	109
Appendix A:	Instrument Calibration	117
TEMPERATURE	117
CONDUCTIVITY, TURBIDITY, pH, DISSOLVED OXYGEN	119
Appendix B:	Nitrogen Concentration Calculation	120
Appendix C:	Discriminant Analysis Results	121
DISCRIMINANT VARIABLES: CONDUCTIVITY, TEMPERATURE, pH, TURBIDITY (EXCLUDING XS 34/35)	121
DISCRIMINANT VARIABLES: CONDUCTIVITY, TEMPERATURE, pH, TURBIDITY (EXCLUDING R5)	123
DISCRIMINANT VARIABLES: MACROPHYTE DENSITY, pH, TEMPERATURE	124
DISCRIMINANT VARIABLES: MACROINVERTEBRATES IN CONTROL BASKETS, pH, TEMPERATURE, TURBIDITY, CONDUCTIVITY	125
DISCRIMINANT VARIABLES: MACROINVERTEBRATES IN CUMULATIVE BASKETS, pH, TEMPERATURE, TURBIDITY, CONDUCTIVITY	126
DISCRIMINANT VARIABLES: MACROINVERTEBRATES IN KICK NETS, pH, TEMPERATURE, TURBIDITY	127
DISCRIMINANT VARIABLES: DO, pH, TEMPERATURE	128
DISCRIMINANT VARIABLES: DO, pH, TEMPERATURE, CONDUCTIVITY (EXCLUDING R5)	129
DISCRIMINANT VARIABLES: NITROGEN, pH, TEMPERATURE	130
DISCRIMINANT VARIABLES: NITROGEN, pH, TEMPERATURE, CONDUCTIVITY	131

List of Tables

Table 2.1. Water quality rating and disturbance level based on the EPT richness (Lenat 1988) and the Hilsenhoff index of Biotic Integrity (Hilsenhoff 1977).	19
Table 2.2. Ranking system to assess sparsity or density of macrophytes according to the percent cover.....	21
Table 3.1. Land-use type and land characteristics observed in each sub-reach along Alderson Creek.	24
Table 3.2. Cross-sections that were monitored within the proposed sub-reaches (R1 to R5) along Alderson Creek.	28
Table 3.3. Onset HOBO temperature pendant specifications (Onset Computer Corporation 2011-2017).	28
Table 3.4. An example of the spreadsheet used to analyze the measured parameters along Alderson Creek.	44
Table 3.5. Combinations of discriminant variables that were used in eight discriminant analysis tests are indicated by check marks.....	48
Table 4.1. A summary of canonical discriminant functions based on variances in pH, turbidity, conductivity, and temperature to differentiate between sub-reaches along Alderson Creek.	78
Table 4.2. Standardized canonical discriminant function coefficients for pH, turbidity, conductivity, and temperature discriminant variables for each discriminant function.	79
Table 4.3. Loadings of each parameter on the respective functions, shown for the analysis that included pH, temperature, and turbidity.	81
Table 4.4. Loadings of each parameter on the respective functions, shown for the analysis that included pH, temperature, conductivity, and DO.	83
Table 4.5. Loadings of each parameter on the respective functions, shown for the analysis that included pH, temperature, conductivity, and macrophyte density.....	84
Table 4.6. Loadings of each parameter on the respective functions, shown for the analysis that included macroinvertebrate abundance, pH, turbidity, and temperature, separated into results from control baskets and from cumulative baskets.	86
Table 4.7. Results from a discriminant analysis performed with various combinations of environmental parameters as the discriminating variables.	87

List of Figures

Figure 1.1. Location of Alderson Creek (red) relative to Fortune Creek and Armstrong, British Columbia.	3
Figure 1.2. Annual recurrence of in-stream aquatic vegetation, which slows water flow and chokes the creek.	4
Figure 2.1. The extent a ‘damaged’ reach (red) transfers downstream (yellow) into a rehabilitated reach (green) in (A)).	9
Figure 2.2. A meandering stream reach made up multiple pool-riffle sequences, with possible sub-reach distinctions, delineated from local scale controls.	12
Figure 3.1. Alderson Creek, located northeast of Armstrong in British Columbia, flows north from a groundwater spring into Fortune Creek.	22
Figure 3.2. R1 through R5 of Alderson Creek.	25
Figure 3.3. Locations of temperature pendant sampling sites in Alderson Creek..	27
Figure 3.4. HOBOware shuttle attached to the temperature pendants in the creek to download data stored on the pendants.	29
Figure 3.5. Locations of nitrogen sampling along Alderson Creek.	31
Figure 3.6. Locations of macroinvertebrate sampling and macrophyte density analysis along Alderson Creek.	32
Figure 3.7. A quadrat, placed onto the center of the creek, defines the 1 m ² area used to count the percent of squares occupied by vegetation.	33
Figure 3.8. Artificial substrate basket consisting of river stone.	34
Figure 3.9. Artificial substrate baskets placed along the right bank at site 2, XS 15, relative to the encircled blue quadrat flag on the lower left-hand side of the image.	35
Figure 3.10. Collection of artificial substrate baskets.	36
Figure 3.11. Kick net method to collect macroinvertebrate samples in Alderson Creek.	36
Figure 3.12. Samples prepared for nitrogen analysis of the five proposed sub-reaches and the sample upstream from XS 35 (left) as well as the KNO ₃ standard solutions (right).	38
Figure 3.13 Left: macroinvertebrates samples preserved in 95% ethanol..	39
Figure 3.14. Features of an Ephemeroptera (left) and four examples of Ephemeroptera genera (right).	40

Figure 3.15. Features of the top and bottom view of a Plecoptera (left) and four examples of Plecoptera genera (right).....	41
Figure 3.16. Features of a Trichoptera (left), examples of larvae cases, and three examples of Trichoptera genera with their respective cases (right).....	42
Figure 3.17. Seven-day moving averages of air temperature between April and December 2015, 2016 and 2017.....	43
Figure 4.1. Temperature measurements at 10-minute intervals recorded at cross-XS 1, 34, and 35 along Alderson Creek.....	51
Figure 4.2. Daily average temperature at XS 1, 34, and 35 as well as air temperature throughout 2016 and 2017 field seasons.....	52
Figure 4.3. Box-plots of temperature data illustrate the mean, median, interquartile range, and dispersion of measurements as a function of location.....	53
Figure 4.4. Raw data measurements of conductivity at XS 1, 4, 34, and 35 along Alderson Creek during 2015, 2016, and 2017 field seasons.	54
Figure 4.5. Conductivity measurements averaged across seasons.....	55
Figure 4.6. Box-plots of conductivity data illustrate the mean, median, interquartile range, and dispersion of measurements.	55
Figure 4.7. Raw data measurements of pH at XS 1, 4, 34, and 35 along Alderson Creek during 2015, 2016, and 2017 field seasons.....	56
Figure 4.8. pH measurements averaged across seasons. The average for summer, fall, winter, and spring are plotted at each cross-section.	57
Figure 4.9. Box-plots of pH data illustrate the mean, median, interquartile range, and dispersion of measurements.....	57
Figure 4.10. Raw data measurements of turbidity at XS 1, 4, 34, and 35 along Alderson Creek during 2015, 2016, and 2017 field seasons.	58
Figure 4.11. Turbidity measurements averaged across seasons.....	59
Figure 4.12. Box-plots of turbidity data illustrate the mean, median, interquartile range, and dispersion of measurements.....	60
Figure 4.13. Frequency distribution of all turbidity measurements (n = 799) recorded between 2015 and 2017 along Alderson Creek.....	60
Figure 4.14. Raw data measurements of dissolved oxygen (mg/L) at XS 1, 4, 34, and 35 along Alderson Creek between May to December 2017.	61

Figure 4.15. Dissolved oxygen measured in mg/L at each cross-section along Alderson Creek.	62
Figure 4.16. Dissolved oxygen and temperature recorded at 30-minute intervals using the HACH HQ40d DO probe, between 1:50 pm October 1 st , 2017 and 12:20 pm October 2 nd , 2017.....	63
Figure 4.17. Nitrate concentration averaged across seasons.....	64
Figure 4.18. Raw nitrate concentrations between May and December 2017 at the cross-sections representing each sub-reach (R1-R5).....	65
Figure 4.19. Maximum, minimum, mean, median and interquartile range of in-stream macrophyte density.	66
Figure 4.20. Maximum, minimum, mean, median and interquartile range of the total EPT counted in the control baskets from 2015-2017.....	68
Figure 4.21. Maximum, minimum, mean, median and interquartile range of the total EPT counted in the cumulative baskets from 2015-2017.	68
Figure 4.22. Maximum, minimum, mean, median and interquartile range of the total EPT counted in the kick net samples from 2015-2017.	69
Figure 4.23. Range of total individual invertebrate species, Ephemeroptera, Plecoptera, and Trichoptera counted at each sample site, in cumulative baskets, from 2015-2017.	70
Figure 4.24. Maximum, minimum, mean, median and interquartile range of conductivity, pH, turbidity, temperature, dissolved oxygen, and nitrate concentration.	72
Figure 4.25. Maximum, minimum, mean, median and interquartile range of number of macroinvertebrates counted in each sub-reach.	74
Figure 4.26. Maximum, minimum, mean, median, and interquartile range of number of macrophyte density observed in each sub-reach.....	74
Figure 4.27. Comparison of stream temperature when manually measured with handheld probes (Oakton PCTestr35) and from in-stream temperature pendants at XS 4 (top) and XS 30 (bottom).....	76
Figure 4.28. Centroids for each sampling site (i.e., cross section) on a combined-group plot....	80
Figure 4.29. Centroids for each sampling site (i.e., cross section) on a combined-group plot....	81
Figure 4.30. Centroids for each sampling site (i.e., cross section) on a combined-group plot....	82
Figure 4.31. Centroids and casewise results for each sampling site (i.e., cross section) on a combined-group plot.....	84

Figure 4.32. Centroids and casewise results for each sampling site (i.e., cross section) on a combined-group plot.....	85
Figure 5.1. Average loading of variables in DA tests.....	92
Figure 5.2. Centroids (large circles) and casewise results (small circles) for each cross-section on a combined-group plot.....	97
Figure 5.3 Centroids (large circles) and casewise results (small circles) for each cross-section on a combined-group plot.	99
Figure 5.4. XS 35 (left) and the culvert at XS 34 (right).	101
Figure 8.1. Regression analysis for the calibration of temperature pendant 1 in A) 2016 and B) 2017..	118
Figure 8.2. Residuals of temperature pendant data plotted against the true temperature to evaluate variance in A) 2016 and B) 2017.	119

Acknowledgements

I would first and foremost like to thank my supervisor, Dr. Bernard Bauer, for his guidance, encouragement and support through every stage of this project. Dr. Bauer pushed me to be a more inquisitive scholar and he provided me with thoughtful insight and feedback when needed. I am also thankful for the support of the rest of my supervisory committee, Dr. Craig Nichol and Dr. Robert Newbury who have both broadened my knowledge, challenged me, and provided advise. I would like to extend my appreciation to Dr. Jeff Curtis, Dr. Jason Pither, and Dr. Ian Walker who have lent their time, knowledge and laboratory space. I am indebted to the work of Justine Walker, who performed the first season of field data collection and participated in the development of the experimental design for the research. I am grateful for the extraordinary effort of the undergraduate and graduate students who assisted in field work including Lisa Hettrich, Spencer Belcourt, Kim MacRae, Taylor McRae, Nicholas Tochor, Matt Dows, Tom Campbell, and Ashleigh Duffy as well as Megan Ludwig for help and guidance through the nitrogen analysis. I am also extremely grateful to my family and friends who have supported me through two undergraduate programs and one graduate program, and for believing in me. The research was funded in part by the Governments of Canada and British Columbia through the Investment Agriculture Foundation of BC under *Growing Forward 2*, a federal-provincial-territorial initiative. Significant contributions (cash and in-kind) came from sources internal to the University of British Columbia Okanagan, especially the UBC O Work Study Program and the Department of Earth, Environmental, and Geographic Sciences, in addition to the Graduate Entrance Scholarship and University Graduate Fellowship award.

Chapter 1. Introduction

1.1. Project Overview

Rivers and streams are increasingly influenced by human factors, especially land-management practices that alter the hydrological and geomorphic condition of the watershed. Agricultural land-use activities, such as livestock grazing, crop cultivation, and drainage modification, may impact stream characteristics, imparting unique anthropogenic signatures on the stream. Rivers are divided into a range of spatial and temporal scales for the purpose of careful study using field empiricism. One of the standard approaches fluvial geomorphologists use is to identify relatively homogeneous sections of uniform morphology known as ‘reaches’ (Brierley and Fryirs 2005). Criteria used to characterize river reaches include hydro-geomorphic attributes such as flow velocity and depth, channel width, substrate size, lithology, planform geometry, and bank condition, in addition to several biotic and physico-chemical parameters that are geared to assessing stream habit potential or aquatic health (Fryirs and Brierley 2013). Anthropogenic overprints or signatures influence these criteria and affecting the characteristics of rivers within reach scales. For instance, a river that may appear as a uniform reach at a regional scale, might actually be segmented into a series of ‘sub-reaches’ the boundaries of which align roughly with fence lines, property markers, road crossings, or sub-division edges.

This thesis considers the circumstances at Alderson Creek, a 2 km creek near Armstrong, British Columbia. Alderson Creek flows through several agricultural properties, each of which has different agricultural management practices, such as cattle grazing, forage crop production, and fallow field. The thesis examines whether differences in land management in agricultural settings influence stream characteristics at sub-reach scales, or between properties.

1.2. Objective and Hypothesis

The objective of the thesis is to assess whether land-management decisions influence biotic and abiotic parameters in an agricultural watershed to the extent that a small first-order stream can be segmented into sub-reaches, which map on to land ownership pattern. The research thesis intends to integrate theories about the controls and indicators of stream health and the impacts of

agricultural land use adjacent to streams. Moreover, the research assesses dynamic behaviour of the study stream in time and space in an attempt to discern the scale of impact as land use becomes increasingly human dominated. The research is motivated by the interests of fluvial geomorphologists, local government agencies, and individual land holders in improving the state of an aquatic ecosystem wherein the implementation of beneficial-management practices (BMPs), such as riparian rehabilitation, are recognized to improve water quality and ecosystem health (Thorp and Covich 2015). Inter-connectivity of streams would suggest that localized improvements from BMPs on one property would transfer downstream only a short distance if the downstream property is not managed effectively, but the scale at which riparian rehabilitation is likely to be effective has not been tested stringently.

This thesis, which investigates whether Alderson Creek might be segmented into a series of sub-reaches that display distinct characteristics as a reflection of land management influences on water quality, provides insight into the scale at which BMPs may be effective. The extent of BMPs and the use of appropriate management practices may be guided with a better understanding of the reasons for which stream sub-reach characteristics are distinct. The overarching research question addresses whether land management practices can have implications for stream characteristics in agricultural landscapes, including aquatic health, at sub-reach scales. The corresponding null hypothesis is that sample sites will not cluster into groups that align with land management practices reflected in property boundaries. The results contribute to ongoing discussions in Geomorphology and Ecohydrology about the importance of scale in understanding fluvial processes, which has important implications for natural resources management, river restoration, and civic planning.

1.3. Study Area

Alderson Creek is located northeast of the City of Armstrong in the North Okanagan valley of British Columbia (Figure 1.1). Alderson Creek is approximately 2 km in length, arising from a groundwater spring and flowing north through an agricultural landscape into Fortune Creek. Fortune Creek drains through a deeply incised canyon before emerging onto a broad alluvial fan covering the main valley. Alluvial fans consist of deposits of boulders, gravels, and lenses of

sand, silt, and clay, contributing to a complex hydrogeologic system (Fulton 1995). On alluvial fans, surface flow can infiltrate into shallow substrate to arise downslope, consistent with what is observed at Alderson Creek where water from the Fortune Creek canyon migrates along the shallow aquifer system and comes back to the surface downslope of a small housing subdivision at the head of Alderson Creek. An additional branch into Alderson creek flows from the east with its source in the mountains draining into a drainage ditch parallel to Alderson Creek. The branch joins in a wetland area with mature trees near the top of Alderson Creek, North of McLeod Rd (see Figure 1.1). During the summer, this tributary typically ceases to flow.



Figure 1.1. Location of Alderson Creek (red) relative to Fortune Creek and Armstrong, British Columbia. Green arrows indicate flow direction. Used with permission. Copyright © 2018 Esri, ArcGIS Online, DigitalGlobe, GeoEye, Earthstar Geographics, CNES/Airbus DS, USDA,

USGS, AeroGRID, IGN, and the GIS User Community GIS User Community. All rights reserved.

The groundwater source from the alluvial fan matrix has implications for normal farm operations, including perennially wet and swampy zones, which pose significant risks and liability for animals, machinery, and production. In addition, Alderson Creek is not prone to major fluctuations in discharge that arise from spring-freshet, which serves as an important function in long-term evolution of river systems. Absence of large discharges during the freshet leads to insufficient flow capacity for scouring of the channel bottom which can lead to enhanced deposition of fine-grained silt and clay. Livestock access to the stream causes bank erosion, contributing to additional and unnatural inputs of sediment into the system. Fine-grained sediments on shallow stream beds stimulate annual growth of watercress and other aquatic vegetation that chokes the channel (Figure 1.2). This further slows water flow and leads to even more deposition of fine-grained silt and clay. Stream connectivity with adjacent landscape is intensified because even small precipitation events could lead to overbank flows and flooding of low-lying land, generating water quality concerns.



Figure 1.2. Annual recurrence of in-stream aquatic vegetation, which slows water flow and chokes the creek. The image on the left was taken on May 6, 2016 and the image on the right was taken on July 13, 2016.

The hydrology that influences the flow of Alderson Creek and management of adjacent agricultural properties are interconnected. Managing agricultural operation (i.e., preventing livestock access to the creek and using a riparian buffer to provide bank stabilization and intercept overland flow) lessen negative impacts on the creek, such as accretion of fine-grained sediment. This could help reduce vegetation build-up and increase flow capacity of the creek, in turn helping to mitigate overbank flows and flooding, as well as concerns for water quality and aquatic biota.

The following research expands on a preliminary investigation into the water quality regime along Alderson Creek by Walker (2016). In addition to the work by Walker (2016), preliminary field investigations indicated that livestock grazing (cattle and horses) and forage production (hay and alfalfa) are the main agricultural activities taking place along Alderson Creek. Properties through which Alderson Creek flows implement grazing or forage production but differ in how they are managed and in their natural vegetation. Given the variability between property management and adverse implications of agricultural operations along Alderson Creek, the creek is a suitable candidate to assess stream health and sub-reach scale.

Chapter 2. Literature Review

2.1. Land Use and Agricultural Impacts on Water Quality in Streams

Human use of land is typically directed at accommodating the needs and pressures arising from an expanding population, often involving a change from native ecosystems to agricultural landscapes. Changes in the natural environment of streams disrupt ecosystem structure as a result of pollution, water withdrawal or diversion of stream water as well as modification of the geomorphology of the stream channel (Thorp and Covich 2010). Stream sedimentation, nutrient enrichment, contaminant pollution, riparian clearing and loss of large wood are principal mechanisms influenced by land-use activities, each of which present harmful effects on stream condition (Allan and Castillo 2007). Agricultural land use in particular, including livestock husbandry and application of fertilizers to aid crop production, are known to affect water quality, aquatic and riparian wildlife, and vegetation cover (Belsky et al. 1999; Kauffman and Krueger 1984). Agricultural activities lead to a loss of vegetation and natural land cover along stream banks, which modifies hydrologic conditions, alters the thermal regime, and increases bank and channel erosion (Christensen et al. 2011; Kelly et al. 2016; Roni et al. 2002). Water chemistry in soils, groundwater, and streams is affected through the supply, removal and processing of chemical constituents such as nitrogen (Flotemersch et al. 2016; Stone et al. 2016). The impacts of human-dominated land use on stream health and community composition have been demonstrated in shifts of stream biota to pollution-tolerant taxa, warm water-tolerant species, and an overall decreased diversity and abundance (Kelly et al. 2016). A study comparing aquatic conditions in native forests to pastured land, for instance, found that reaches through pastures were exposed to more light, had warmer water, greater nutrient levels, algal biomass, and fine sediment, and were negatively correlated to the number of taxa (Quinn et al. 1997).

Awareness and understanding of the issues surrounding agricultural land use and aquatic ecosystem health have shifted attitudes towards implementation of beneficial management practices (BMPs) to restore fluvial environments to some degree of their former character or to establish a new functional environment (Brierley and Fryirs 2005). Stream restoration and rehabilitation are processes to help recover an ecosystem that has been damaged, degraded, or destroyed (Perini and Sabbion 2017). Stream restoration involves returning the aquatic system to

its original, undisturbed state, but this is not always obtainable (Roni and Beechie 2013). Stream rehabilitation, alternatively, involves improving some aspects of the system but not to pre-impact conditions (Roni and Beechie 2013). Rehabilitation activities typically involve returning straightened channels to meandering planforms, increasing complexity of channel features, and the stabilization of riparian zones (Thorp and Covich 2010). A riparian zone refers to the area of land adjacent to streams consisting of various types of vegetation including trees, shrubs and grasses. The riparian zone is a critical interface between land-water interactions because bank vegetation performs important ecological and geomorphic functions. Riparian zones regulate the sediment load and water chemistry of flows moving from land to stream. Reducing nitrate inputs has an effect on in-stream macrophyte growth, macroinvertebrate abundance and water chemistry (Hill 2000; Carline and Walsh 2007; Thorp and Covich 2010). Riparian vegetation also stabilizes the stream banks and moderates temperature (Allan and Castillo 2007). Cultivation and livestock grazing next to the streambank impact the ecological functioning of riparian vegetation (Hill 2000; Roni et al. 2002), and therefore stream rehabilitation is often aimed at repairing and planting riparian vegetation as well as isolating riparian zones from adjacent properties to prevent livestock access. Research has shown that the installation of riparian cover, streambank fencing, and manure management are beneficial for riparian vegetation health, soil and water quality, stability of banks, and recovery of aquatic insects to pre-impact conditions (Miller 2015; Thorp and Covich 2015; Bledose et al. 2011).

The effectiveness of rehabilitation efforts is related to scale because physical, biological, and chemical processes that reflect human activities are scale dependent (Christensen et al. 2011; Kelly et al. 2016). There is limited guidance, however, as to the scale at which rehabilitation will be successful (Bledose et al. 2011; Anderson et al. 2004). Stream condition may be localized or cumulative depending on the condition and extent of upstream riparian zones (Lee et al. 2001). Implementation of BMPs, such as riparian rehabilitation, along an entire water course rather than on a small segment of a stream would seem to have a better chance of leading to overall improvements in water quality and ecosystem health. If a downstream segment is not managed effectively, benefits accruing from the upstream rehabilitation would remain localized upstream and not be transferred downstream. Alternatively, localized rehabilitation might be beneficial at

mitigating the accumulation of negative effects downstream by improving the quality of water from the outset.

Emphasis is often placed on local scale rehabilitation because it is easier to address select habitat characteristics and it is more practical than rehabilitating an entire watershed (Allan and Castillo 2007; Roni et al. 2002). There is disagreement, however, on whether basin-level factors or local factors have a larger effect on stream condition (Lee et al. 2001). A study of the physical habitat and biotic integrity of a stream as a function of the type of riparian cover found that conditions locally were more influential than conditions upstream, although the conditions upstream do play a role (Lee et al. 2001). The extent of influence that upstream conditions has on downstream reaches depends on how quickly things change in the downstream direction although quantifying this is not simple. During rehabilitation designs, there are no set guidelines for the smallest scale at which stream rehabilitation should be practiced in order to make a difference. Imagine a stream where the upstream reach has no riparian cover and the downstream reach has a healthy vegetated riparian ecosystem. Poor aquatic conditions in reach 1 are transferred downstream into reach 2 (reaches 1 and 2, respectively, in scenario A) of Figure 2.1). The extent of rehabilitation activities that are required on reach 1 to make a difference is not known, but it would be useful to understand the smallest scale at which rehabilitation activities might eliminate the transfer of poor aquatic conditions into the second reach while also minimizing degradation in the upstream reach. Rehabilitation implemented on a smaller area in reach 1 (scenario B) in Figure 2.1) does not reduce the distance that poor aquatic conditions are ‘felt’ downstream as much as if they were implemented on a larger area (scenario C) in Figure 2.1). The downstream influence will likely be relative to size of deteriorated or rehabilitated land in reach 1. Rehabilitation along the entire length of a stream or reach is not always possible, therefore knowing the minimal effort required to have a positive effect would be useful. As such, a better understanding of the scale-dependent influence of land use on stream condition is critical for rehabilitation designs, and also beneficial for channel modelling and stream characterization (Bledose et al. 2011). If water quality and biological characteristics in a stream align with land-use type, for instance, planning and implementation of BMPs may be effective even if implemented only on those properties in which physico-chemical and biological conditions are poor.

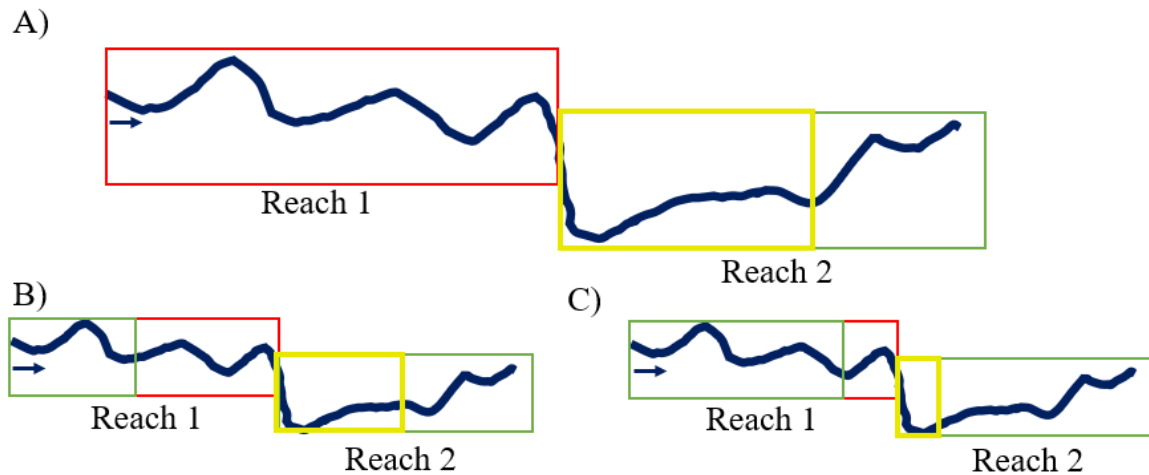


Figure 2.1. The extent a ‘damaged’ reach (red) transfers downstream (yellow) into a rehabilitated reach (green) in (A)). There aren’t universal methods to determine the distance that degradation in reach 1 is ‘felt’ downstream in reach 2. Rehabilitation efforts implemented on a greater extent of a reach will likely reduce the degree of negative effects felt downstream (illustrated in B) and C)).

2.2. Scale Considerations in Stream Systems

Physical, biological, and chemical processes in streams are scale dependent. Streams traverse a range of landscapes and they take various forms with respect to geomorphic structure and hydrologic pattern (Thorp and Covich 2010). The three major zones in a stream system--the upland zones, transfer zones, and depositional zones--are interconnected. However, each of these three zones exhibits a distinct character as the water flows from its source in mountainous terrain through alluvial environments to a valley bottom, for example (Couper 2007; Nagle 2000). The morphology of a stream is the product of processes at watershed scales (river network) to micro-habitat scales (e.g., pools and riffles). To understand the hydrologic and geomorphologic behaviour of rivers and streams, they are often classified into spatial ‘units’ based on spatial criteria including hydro-geomorphic attributes and differences in river structure. Large-scale units are made up of successively smaller-scale units, a spatial hierarchy used in characterizing streams (de Boer 1992). Hierarchical frameworks ensure that studies are carried out at the appropriate scale based on the objective and allow for data to be integrated between sites and scales (Frissell et al. 1986). Understanding the processes acting at different scales has implications for stream management.

Several hierarchical frameworks have been proposed (de Boer 1992; Gurnell et al. 2016; Frissell et al. 1986; Newson and Newson 2000), but the spatial divisions (levels) are not clearly defined and vary by author (Gurnell et al. 2016). Stream attributes are used to delineate levels, ranging from large-scale regional features such as geology, climate, geomorphology, and river form, to hydro-geomorphic attributes such as depth and width, flow velocity, and bank condition, to smaller scale abiotic and biotic parameters that relate to habitat potential or aquatic health (Bailey 1983). Top-level scales typically consist of the entire watershed, which is successively divisible into stream systems, stream segments, reaches, and points (Frissell et al. 1986; Wolter et al. 2016; de Boer 1996; Newson and Newson 2000). Watershed characteristics are classified based on biology, lithology, basin topography, climate, and geomorphology, all of which affect the form of the river, including slope, sediment sizes and discharge patterns (Schumm and Lichty 1965; Bailey 1983; Frissell et al. 1986; Couper 2007). Small systems are constrained by higher level scales, such as the dependence of pool-riffle morphology on slope, sediment and water inputs (Frissell et al. 1986).

Stream management is often focused on the reach scale, a longitudinal section of the stream with relatively homogeneous conditions (e.g., a wide braided reach with gravel bars and low-lying banks versus a meandering reach with distinct cut banks, point bars, and riparian vegetation) (Gurnell et al. 2016). Criteria used to characterize stream reaches include relief and slope, morphological structures and processes, hydro-geomorphic attributes such as flow velocity, depth, channel width, bed substrate size, bank condition and riparian vegetation (Frissell et al. 1986; Newson and Newson 2000; Couper 2007). Reaches are made up of smaller units, referred to as pool-riffle systems (Frissell et al. 1986), functional units (Newson and Newson 2000), or geomorphic units (Gurnell et al. 2016), which are in turn made up of smaller scale units called microhabitats (Frissell et al. 1986), hydraulic units (Brierley and Fryirs 2005), or river elements (Gurnell et al. 2016). Reaches are delineated by breaks in channel slope, local side slope, valley floor width, bank material, and bed channel material, whereas pool-riffle systems are characteristic bedforms (e.g., bed topography, depth) with distinct water surface slope, velocity structure, and plant composition (aquatic and riparian) (Gurnell et al. 2016; Frissell et al. 1986). Microhabitats consist of isolated elements (e.g., patches of plants) in zones of consistent flow depth, river stage, and sediment size and type (Gurnell et al. 2016).

Upper level controls such as geomorphic processes shape channel features at the reach scale whereas individual features influence the details of functional units and microhabitats (Allan and Castillo 2007). Processes at an intermediate scale (i.e., local controls) present a gap in the spatial hierarchy between reach scales and functional units. A reach, for instance, that is made up of multiple pool-riffle units (Figure 2.2), may also be divisible into sub-reaches, distinct in channel width, bank condition and riparian vegetation. The term sub-reach is seldom used in the literature. Gurnell et al. (2016) described a sub-reach as a synonym for a geomorphic unit. González-Pinzon et al. (2014) and Majerova et al. (2015) studied streams at the reach, sub-reach, and habitat scales, but did not define what a ‘sub-reach’ meant. In each case, the term sub-reach is classified somewhere between a reach and a microhabitat or point scale. Sub-reaches are divisions of what may appear as a uniform river reach at regional scales but exhibit distinctions at scales larger than microhabitats. Alderson Creek, for example, appears as a homogeneous river reach due to its steady slope, sediment calibre and size, consistent morphology and planform geometry (i.e., all of Alderson Creek is mapped as a first-order stream in the Water Atlas of Canada). Alderson Creek does, however, exhibit homogeneous sub-sections that display distinct attributes, such as riparian and in-stream vegetation and bank condition, in addition to biotic and physico-chemical parameters indicative of stream health. Sub-reaches may be bounded by culverts or other artificial obstructions (Roni et al. 2002). Sub-reach distinctions in the hierarchical framework of rivers and streams could be relevant to understanding the implications of human activities on stream health and geometry.

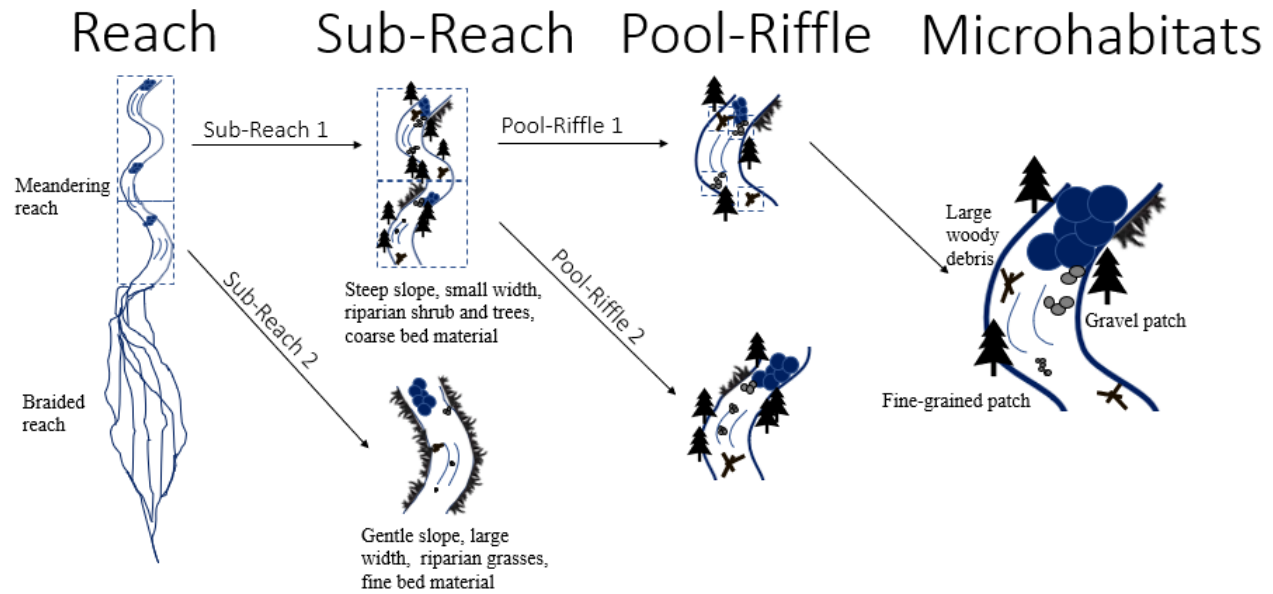


Figure 2.2. A meandering stream reach made up multiple pool-riffle sequences, with possible sub-reach distinctions, delineated from local scale controls.

2.3. Stream Health and Water Quality Indicators

Monitoring water quality parameters is valuable in assessing how an ecosystem will adapt to anthropogenic activity. Agricultural practices, which may lead to habitat loss, degradation of stream banks, and fragmentation, can have implications for stream health (Brierley and Fryirs 2005). Stream health can be defined as the ability of a stream and its associated ecosystem to perform ecological processes and functions (Brierley and Fryirs 2005). Measurable biophysical and chemical parameters are used as indicators of stream health, and specific criteria are selected to evaluate flow regime, stream connectivity, and aquatic habitat (Flotemersch et al. 2016; Palmer et al. 2005; Newson and Large 2006; Woolsey et al. 2007). Common physico-chemical indicators of stream health include temperature, dissolved oxygen, electrical conductivity (hereafter referred to as conductivity), turbidity, acidity (measured as pH), and nutrients or pollutants (e.g., nitrogen), while biological indicators include macrophyte and macroinvertebrate abundances and species composition and density (Collins et al. 2013; Newson and Large 2006). Several of these parameters are interrelated. For instance, increases in conductivity reduce oxygen solubility whereas increases in turbidity raise water temperature, which in turn lowers dissolved oxygen (Richter and Kolmes 2005; Welch 1952). Macroinvertebrate communities and

macrophyte survival are limited by temperature, dissolved oxygen, and turbidity, but macrophyte abundance also influences dissolved oxygen and stream temperature. The significance of these parameters in assessing stream health and the water quality guidelines are described below.

2.3.1. Temperature

Temperature is a fundamental control on the structure and function of ecological communities (Flotemersch et al. 2016). It has direct influences on fish metabolism, feeding, and growth, as well as indirect influences on other ecosystem characteristics (e.g., oxygen solubility) (Parkinson et al. 2016). Fish that are stressed by warm water are less able to deal with a second stressor (Richter and Kolmes 2005). Temperature thresholds vary by species and life stage. Salmon and trout, for example, require temperatures below 21°C for migration and between 12-17°C for rearing and spawning, and salmon and trout survival is limited by a mean daily temperature of 20°C and a maximum daily temperature of 22°C-24°C (Richter and Kolmes 2005). Temperatures above 26°C are lethal for all salmon and trout species in the Pacific Northwest (Richter and Kolmes 2005).

Temperature of stream water is dependent on several factors including climatic drivers (e.g., air temperature and thermal radiation from the sun), canopy conditions, inflow sources (e.g., groundwater), stream morphology (i.e., slope and elevation), stream discharge, and land use (Steel et al. 2016). Stream temperature directly responds to air temperatures and solar radiation inputs, although a delay in stream maximum and minimum temperatures reflects the fact that water takes more energy and more time to heat up (or cool down) than air or soil because of the unique thermal properties of water (i.e., large specific heat capacity). Riparian shading and large amounts of suspended sediments (i.e., turbidity) intercept solar radiation and prevent stream temperature from heating up during the day. Cooler groundwater inputs decrease stream temperature, and warm overland flow increases stream temperature. Vegetation removal, stream outputs and inputs (i.e., groundwater and overland flow), and disruption of stream connectivity are by-products of land-use practices that can influence stream temperature (Flotemersch et al. 2016).

2.3.2. Dissolved Oxygen

Dissolved oxygen (DO) in water is usually measured as mass concentration (mg/L) or as percent (%) oxygen saturation. The concentration of dissolved oxygen will vary depending on temperature, pressure and salinity (Waldron and Wiley 1996). The percentage of dissolved oxygen is relative to that when completely saturated at the temperature, pressure, and salinity at the time of measurement. For instance, warm water will retain less dissolved in its fully saturated state so water that is 100% saturated will contain a smaller DO concentration (mg/L) if it is warm compared to cool water. Guidelines for dissolved oxygen thresholds for aquatic life are not typically given in percent saturation. A stream may be near 100% saturation, but the concentration of dissolved oxygen can be below the threshold for fish survival because the stream is warm, for example. Typical stream water contains less than 10 mg/L of DO and the maximum concentrations (to be 100% saturated) is 15 mg/L at 0°C or 8 mg/L at 25°C (Ministry of Environment 1998). A 30-day average of 8 mg/L and an instantaneous minimum of 5 mg/L is required for all aquatic life at all life stages other than buried embryo, which is a more sensitive stage that requires a minimum DO of 9 mg/L (Ministry of Environment 2018).

DO concentration is also affected by the hydraulic characteristics of the stream, metabolic activity of organisms, and the presence of organic matter (Waldron and Wiley 1996). Atmospheric inputs, inflowing water, natural re-aeration, and photosynthesizing plants produce dissolved oxygen in streams (Ministry of Environment 1998). DO is lost through atmospheric exchange, the respiration of animals and plants, and the decomposition of mucky bottom materials and suspended organic matter (Welch 1952; Waldron and Wiley 1996). Dissolved oxygen concentration exhibits seasonal and daily cycles (Ministry of Environment 1998). DO concentration is least in the early morning because plants are not producing oxygen overnight but are still using up oxygen for respiration (Ministry of Environment 2018). DO concentration are reduced in the summer because colder water holds more oxygen. Increases in plant productivity facilitated by the release of nutrients leads to the consumption of DO (Ministry of Environment 1998). An oxygen-deficient environment inhibits respiratory metabolism and survival of most aquatic organisms.

2.3.3. Electrical Conductivity

Conductivity is a measure of electrical conductance of water, proportional to the concentration of ionic material in the water, such as calcium, sodium, potassium, magnesium, and chlorine (Talling 2008; Allan and Castillo 2007). Variation in conductivity stems from differences in concentration of ions in solution but is also related to temperature and stream flow. Ionic contributions are sourced from groundwater, dissolution of rocks and soil, agricultural runoff or from increased overland runoff as a result of paved surfaces. Conductivity increases with temperature because of increased ionic mobility and molecular solubility in warmer temperatures (Talling 2008; Welch 1952). Furthermore, conductivity is often inversely related to stream flow (Waldron and Wiley 1996), so high conductivities are expected when stream flow is least in late summer and early fall and low conductivities are expected when flow is greatest, such as in spring. This is particularly true when groundwater is a large contributor. Groundwater inputs are greater during low flows, which increases conductivity. Conductivity values range between 50-1500 microSiemens per centimeter ($\mu\text{S}/\text{cm}$) in freshwater lakes and streams (Ministry of Environment 1998; Talling 2008). Most conductivity probes are temperature compensated, with conductivity values reported at 25°C (Allan and Castillo 2007). Guidelines for aquatic life, livestock and wildlife are specific to the type of ion present (e.g., long-term maximum of Cl^- is 150 mg/L). Conductivity extending out of the natural range of a system may indicate pollution and can have detrimental impacts on aquatic life as many freshwater organisms are not adapted to varying levels of dissolved ions.

2.3.4. Turbidity

Turbidity is a measure of the transparency of water, and it indicates the presence of suspended matter including silt, clay, organic material, and micro-organisms (Ministry of Environment 1998). Increased turbidity limits light penetration, which reduces photosynthetic potential and productivity, raises temperature, clogs respiratory mechanisms of aquatic organisms, and provides a medium for growth and transport of pathogens and contaminants (Welch 1952). Turbidity will increase as a result of erosion from the stream bank, stream channel, and upland or riparian areas, caused by rainfall, storm events as well as physical disturbances (e.g., livestock destabilizing banks).

Freshwater turbidity ranges from 0-1000 Nephelometric Turbidity Units (NTU) (Ministry of Environment 2018) although water with a turbidity of 50 NTU is markedly cloudy. Criteria for drinking water and criteria for aquatic life, wildlife, and livestock depend on background NTU, which is the condition of the natural state of the system. A 10% change in turbidity when background turbidity is >50 NTU is problematic for drinking water, aquatic life, and livestock, whereas a 20% change in background turbidity is problematic for wildlife (Ministry of Environment 2018). When background turbidity is <50 NTU a change of 1 NTU is problematic for untreated drinking water and a change of 5 NTU is problematic for treated drinking water, aquatic life, wildlife, and livestock (Ministry of Environment 2018). Regardless of background level, a change of 8 NTU for a duration of 24 hours, or a change of 2 NTU for a duration of 30 days are problematic for aquatic life (Ministry of Environment 2018).

2.3.5. pH

Acidic conditions reduce species diversity and abundance, ecosystem processes (Allan and Castillo 2007), but organisms also respond to various physiological, chemical and indirect effects that accompany a lowered pH (Allan and Castillo 2007). pH is a measure of the concentration of free hydrogen ions in a solution (Gupta 2011). pH ranges from zero (acidic) to 14 (basic); a pH of 7 is neutral. The concentration of hydrogen ions in stream water is influenced by acid rain, lime compounds, acidic soils, and runoff from industrial activities (Ministry of Environment 1998). Hydrogen ions alter the charge environment of other molecules, modifying the solubility and biological availability of chemical constituents in stream water. Changes in pH indicate chemical changes in stream water (Gupta 2011), which may be indicative of pollution or other environmental factors that are harmful to plants and animals adapted to specific pH range.

British Columbia water quality guidelines recommend a pH range of 6.5-9 for aquatic life, wildlife, and agriculture (Ministry of Environment 2018) but other literature suggests a healthy pH range is 5.5-9 (Gupta 2011; Waldron and Wiley 1996). Freshwater that is strongly acidic (pH<5) or strongly basic (pH>9) is thought of as harmful, although the level of harm depends on species and other environmental factors (e.g., what is causing acidic or basic conditions) (Ministry of Environment 1998). Fish mortality increases at a pH<4 and reproduction is affected at a pH between 4-5 (Gupta 2011). Macroinvertebrates, described in Section 2.3.7, also have pH

thresholds: Ephemeroptera (mayfly) abundance decreases if $\text{pH} < 5$ and Plecoptera (stonefly) and Trichoptera (caddisfly) abundances decrease if $\text{pH} < 4$ (Courtney and Clements 1998).

2.3.6. Nitrogen

In excess, nitrogen inputs can lead to eutrophication of the system, enhancing primary production and favouring the growth of aggressive, invasive, weedy, plant species, which in turn alter dissolved oxygen, habitat availability and aquatic biodiversity (Cao et al. 2006; Kelly et al. 2016). Sources of nitrogen include atmospheric diffusion, industrial pollution, runoff from fertilized fields, N-fixing crops, animal waste, microbial processes, and groundwater inputs (Waldron and Wiley 1996; Allan and Castillo 2007). Nitrogen inputs vary seasonally. Decreased nitrogen concentrations are expected during the growing season due to nitrogen uptake by plants and when bacterial communities are more abundant (i.e., summer) due to increased N-fixation. Nitrogen increases are expected in the spring from freshet or rainstorms flushing nitrate into stream water that has accumulated in soils (Allan and Castillo 2007).

Nitrogen exists in several forms including ammonia, nitrite, and nitrate (Ministry of Environment 1998). The amount, impact and guidelines differ for each form, however, nitrates are the most stable and are the principal form found in natural waters (Ministry of Environment 1998). Ammonia and nitrites occur in very small amounts in natural waters (less than 0.1 mg/L and 0.001 mg/L, respectively) and do not contribute to excess phytoplankton and macrophyte growth compared to nitrates. Guidelines for nitrates are a long-term average of 3 mg/L and a short-term maximum of 32.8 mg/L (Ministry of Environment 2018).

2.3.7. Macroinvertebrate Abundance

Aquatic insects are abundant and diverse in freshwater systems, and they function as food and as predators in the aquatic environment (Thorp and Covich 2010). Macroinvertebrates are one of the most abundant groups of insects, and are spineless animals that inhabit the bottom of streams and are visible to the eye (Taccogna and Munro 1995). The community composition is a function of the stream conditions (Thorp and Covich 2010). Dissolved oxygen, stream chemistry, and substrate type have major influences on the species type and abundance of insects present in an

aquatic system. Typically, low dissolved oxygen, large thermal fluctuations, acidic conditions and large conductivities limit diversity, but species-specific preferences are helpful to evaluate stream condition (Thorp and Covich 2010). Substrate is one of the most important factors influencing macroinvertebrate abundance, as it provides habitat, shelter, and food (Thorp and Covich 2010).

Ephemeroptera-Plecoptera-Trichoptera (EPT) are commonly used to indicate stream health since EPT species are pollution sensitive taxa (Lear et al. 2011; Lenat 1988). EPT are found in unpolluted waters, including small streams, fast flowing rivers, ponds, and lakes, some inhabit buried silt and sandy areas while others inhabit exposed rocks and debris (Clifford 1991). EPT are good bio-indicators as they are abundant in freshwater, exhibit high diversity, are an important part of the food chain, and their abundance is influenced by water quality (Thorp and Covich 2010). Ephemeroptera larvae are an important source of food for fish and they inhabit lotic (streams) or lentic (lakes) water where they crawl on substrate. Their gills are used for the uptake of oxygen (Thorp and Covich 2010). Tolerance to pollution and habitat differ by species, although Ephemeroptera are known to inhabit cleaner and cooler waters. Plecoptera prefer cool-water and swift moving streams. They inhabit a variety of substrate types but are common in decaying leaves and detritus, on which they feed (Lillehammer et al. 1989; Clifford 1991). Plecoptera are very sensitive to changes in water quality and are intolerant of hypoxia (oxygen deficiency), pesticide use, as well as losses of in-stream and riparian habitat (Thorp and Covich 2010). Due to sensitivity to a lack of dissolved oxygen, the absence of Plecoptera is often an indication of organic pollution (Clifford 1991). Trichoptera are very adaptive, exhibiting the largest range of tolerance to pollution compared to Ephemeroptera and Plecoptera. Found in rocks or woody substratum of clear flowing water, Trichoptera live in ‘casings’ constructed from plant material and/or mineral matter (Thorp and Covich 2010; Clifford 1991). Trichoptera are found in a range of cool to warm streams, and although they are sensitive to oxygen depletion, they use their gills and body undulations to increase flow of water and dissolved oxygen through their casings allowing them to adapt in oxygen depleted environments (Thorp and Covich 2010). Trichoptera are important for biological monitoring because they are abundant and diverse and exhibit a wide variability of species-specific pollution tolerance (Thorp and Covich 2010).

Macroinvertebrate abundances are used as biotic indices of stream health. For example, small percentages of sensitive orders (i.e., EPT) relative to total taxa are an indication of increased perturbation. EPT taxa richness, given as the total number of EPT, is a simple way to assess water quality and level of disturbance (Table 2.1) (Lenat 1988). The EPT richness index is calculated by adding the number of E, P, and T counted. It is then compared to values on the EPT richness rating by Lenat (1988) (Table 2.1). The method by Lenat (1988) is established somewhat arbitrarily based on collections at unstressed and highly polluted sites. The samples are collected with standardized methods; a collection of kick net, dip net, leaf-pack, fine-mesh and visual composite samples from which organisms are picked proportionally to abundance (Lenat 1988). The index intends to examine the general level of pollution and was modelled after the Hilsenhoff index of biotic integrity (HBI) (Lenat 1988). A more complicated HBI applies a ‘tolerance value’ to individual species, from 0 (very intolerant) to 10 (very tolerant) based on the ability of the taxon to inhabit streams of varying water quality (Wallace et al. 1996). The Hilsenhoff biotic index is calculated by taking the sum of the number of individuals in each species multiplied by its tolerance value and divide by the total number of individuals in the sample (Hilsenhoff 1977). The HBI value is ranked to assess water quality and level of disturbance (Table 2.1) (Hilsenhoff 1977). A review of several biotic indices is given by Diaz et al. (2004).

Table 2.1. Water quality rating and disturbance level based on the EPT richness (Lenat 1988) and the Hilsenhoff index of Biotic Integrity (Hilsenhoff 1977).

	EPT taxa richness* (Lenat 1988)	HBI (Hilsenhoff 1977)
Excellent Clean, undisturbed	>31	<1.75
Good Some disturbance	24-31	1.75-2.25
Fair Moderate disturbance	16-23	2.25-3.0
Poor Significant disturbance	8-15	3.0-3.75
Very Poor Gross disturbance	0-7	>3.75

*EPT taxa richness values are provided for piedmont ecoregions, between July and September

For the purposes of this study the total number of Ephemeroptera, Plecoptera, and/or Trichoptera that were found in samples are used to assess stream health. These numbers are compared to the EPT richness index by Lenat (1988) to classify water quality within the sub-reaches as ‘good’ or ‘poor’. The HBI index was not used in this study as it requires the collection of all macroinvertebrate species and not just EPT.

2.3.8. Macrophyte Density

Macrophytes are emergent, submergent, or floating aquatic plants (Golder Associates 2014). Macrophyte coverage is a measure of the quantity of aquatic plants and vegetation present in or next to a stream. Emergent types, such as watercress, bulrushes and reeds, are typically rooted to banks or slightly below water level. Floating types, such as water lilies and duck weed, are not attached to substrate. Submerged macrophytes, such as milfoil and pondweed, are attached to substrate and typically midstream (Allan and Castillo 2007; Ministry of Environment 2009).

Macrophyte abundance influences invertebrate communities as they increase habitat heterogeneity, offer surface area for habitat and spawning, provide food, shelter, and refuge from predation and hydrological disturbances (Allan and Castillo 2007). Macrophytes also slow current and water velocity, form a canopy (depending on type), can trap or filter fine sediments and particulate organic matter, take up nutrients and produce oxygen (Allan and Castillo 2007; Bell et al. 2013; Golder Associates 2014). Macrophyte abundance and distribution is affected by and has impacts on water quality, hydrology and river morphology (Golder Associates 2014). For instance, nutrient enrichment contributes to overgrowth of vegetation (Golder Associates 2014), which varies with respect to flow events and depends on loading sources (e.g., fertilized properties). A ranking system developed by Golder Associates (2014) qualitatively describes percent macrophyte density measured in a quadrat (Table 2.2). A quadrat is a grid outlining the area under which macrophyte density (%) is counted. With a quadrat split into 100 squares, for example, the percent density is simply the number of squares occupied by vegetation (percent density (%) = (number of squares occupied by vegetation/100) * 100). The system by Golder Associates (2014) ranks macrophyte density from no, occasional, or individual growth as <1% to very dense, extensive growth as 80-100%.

Table 2.2. Ranking system to assess sparsity or density of macrophytes according to the percent cover. Cover is a measure of the percent of macrophytes in a predefined area of space (a quadrat) (Golder Associates 2014).

Density (%)	Macrophyte Abundance Description
<1	No macrophyte beds observed, occasional, or individual
1-20	Very sparse growth
20-40	Sparse growth
40-60	Moderately dense growth
60-80	Dense growth
80-100	Very dense, extensive growth

Macrophytes grow in the spring as temperatures increase, and growth is accelerated during low flows (i.e., summer) and when there is a lack of shading from bank vegetation. Overgrowth of macrophytes leads to choking of the channel, which can lead to increased deposition of fine-grained silt and clay due to insufficient flow capacity, allowing for additional macrophytes to establish. Dense growth of macrophytes can also lead to severe diurnal variations of dissolved oxygen and contributes to the absorption of a great deal of radiant energy from the sun, warming the water (Golder Associates 2014). Reducing turbidity, increasing bank vegetation cover, and decreasing nutrient inputs can help to limit macrophyte overgrowth (Golder Associates 2014).

Chapter 3. Experimental Design

3.1. Field Methods

3.1.1. Sub-Reach Description and Sample Site Locations

The delineation of sub-reaches (referred to as R1, R2, R3, etc.) was influenced by the work of Walker (2016), who identified five sub-reaches based on visual cues and property divisions in the field (Figure 3.1). Sub-reaches were identified as R1 through R5 from downstream to upstream. Alderson Creek crosses Highway 97 at the north and flows through one additional property before joining Fortune Creek, but this property as not part of the study.



Figure 3.1. Alderson Creek, located northeast of Armstrong in British Columbia, flows north from a groundwater spring into Fortune Creek. Proposed sub-reaches are identified. Used with permission. Copyright © 2018 Esri, ArcGIS Online, DigitalGlobe, GeoEye, Earthstar Geographics, CNES/Airbus DS, USDA, USGS, AeroGRID, IGN, and the GIS User Community GIS User Community. All rights reserved.

Sub-reaches separate land-holdings with varying agricultural management practices. The property adjacent to R1 was fallow but was used for crop production prior to 2015, and the creek

was lined with a riparian system (trees and shrubs), but the property underwent recent development of a driveway approximately 5 metres from the creek. The property adjacent to R2 was mainly used for forage crop production, which was available to a small herd of cattle (typically less than 10) for a portion of the year when R3 became heavily grazed, typically in the fall. The property adjacent to R3 was exposed to cattle grazing year-round where cattle had direct access to the creek, and the cattle were regularly seen crossing or standing within the creek, visually observed degrading the banks. The property adjacent to R4 was used for crop production, primarily hay and alfalfa. The creek within R4 contained an exclusion of a thick, natural, riparian zone with a dense cover of large trees and shrubs but is followed by a stretch accessible to horses. The property adjacent to R5, grazed year-round, contained a greater number of cattle (approximately 30) and was particularly degraded wherein the property exhibited a mucky and rutted pasture. Livestock grazing, particularly cattle, damage riparian areas due to uncontrolled and season-long grazing (Miller 2015).

A culvert under McLeod Road separated R4 from R5, and the stream was further segmented by fences along property lines between R4 and R3, R3 and R2, and R2 and R1. Characteristics of each sub-reach differ by land-management type, substrate type, average stream width, canopy coverage in the riparian zone, vegetation type and density, stream bank condition, and drainage characteristics (Table 3.1 and Figure 3.2).

Table 3.1. Land-use type and land characteristics observed in each sub-reach along Alderson Creek. Assessments are based on visual examination during field work.

		R1	R2	R3	R4	R5
Conditions on land adjacent to stream	Land management	Fallow, prior crop production (hay and alfalfa)	Forage crop production, fall cattle grazing (3 months/year)	Cattle and horse grazing year-round	Crop production (hay and alfalfa)	Cattle grazing year-round
	Riparian, stream bank and drainage conditions	Most of creek length protected by riparian buffer	Property was not waterlogged, no riparian buffer, dense grasses on banks	Livestock access to stream leads to erosion of stream banks	Natural riparian buffer, little disturbance to creek, property waterlogged during wet season	Muck within and adjacent to creek, property wet year-round, livestock access to creek creates mucky and eroded stream banks
Stream conditions	Percent of stream with vegetation canopy; type of vegetation	>50%, variety of trees and shrubs	None	<20%, six large cottonwoods	50%, variety of trees, shrubs, and aquatic species (skunk cabbage, horsetail)	None
	Average substrate type	Gravel, interbedded with clay-sand	Gravel, interbedded with clay-sand	Gravel, interbedded with clay-sand	Gravel and sand with a veneer of fine clay-silt in most places	Thick veneer of muck and fine-grained clay-silt over sand-gravel
	Average stream width (m)	1.45	1	1.2	0.7	2

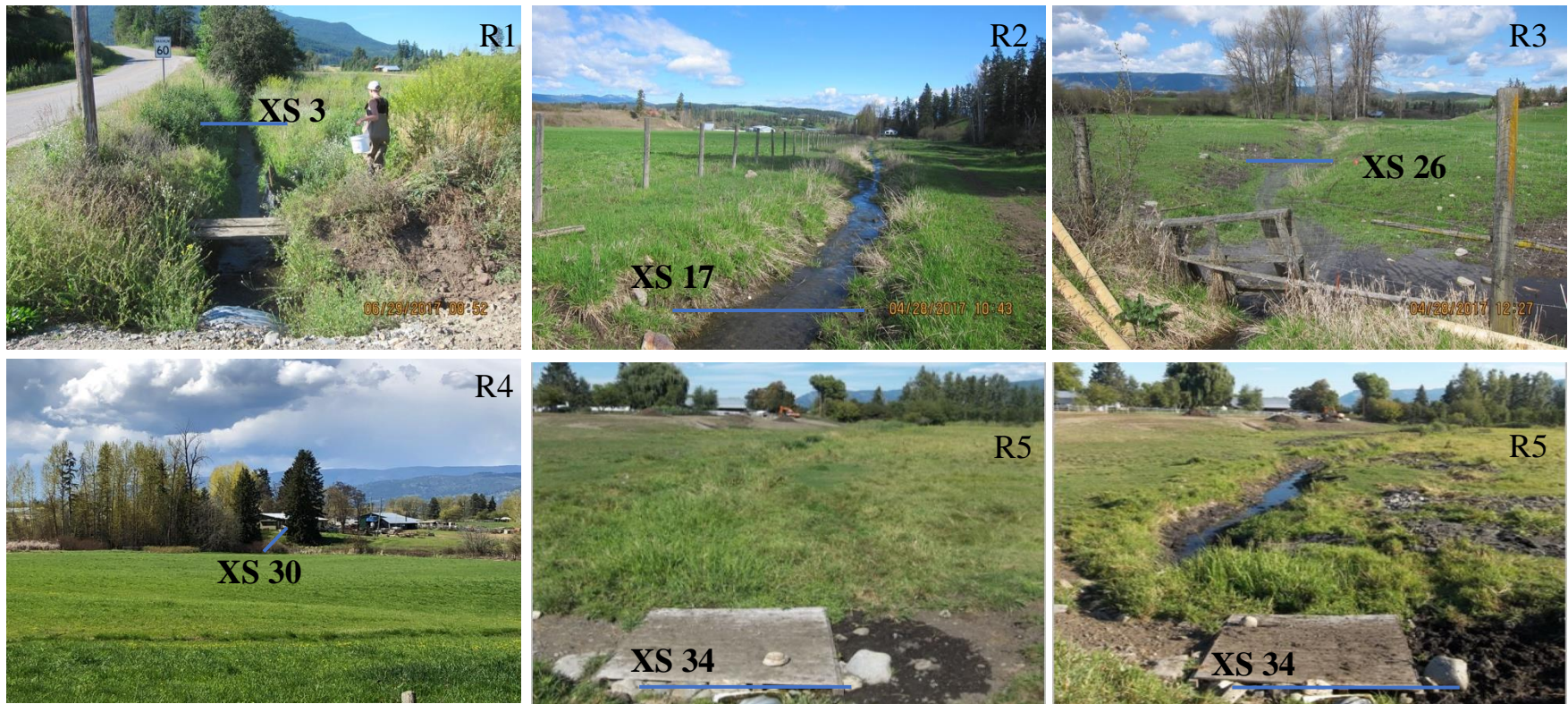


Figure 3.2. R1 through R5 of Alderson Creek. R1 is looking upstream, R2, R3 and R5 are looking downstream. Alderson Creek is in the background in the image of R4 (flowing through the stand of trees). Two images are shown for R5: the image on the left was taken prior to restoration in July of 2017, and overgrowth of vegetation in the creek bed hides the stream course. The image on the right was taken after excavation in August of 2017 but before replanting and fencing.

Monitoring the aquatic health of Alderson Creek involved measuring temperature, pH, conductivity, turbidity, dissolved oxygen (DO), and nitrogen, in addition to macroinvertebrate and macrophyte densities. These parameters were measured at several cross-sections (XS) that had been surveyed with engineer's levels and rods and labelled in the upstream direction from 1 to 35 (Figure 3.3). The parameters were measured at select sample sites, the locations of which chosen to obtain a representative spatial distribution while also capturing unique hydrologic or geomorphologic properties. Two additional sampling sites were monitored but not surveyed. One site was between XS 30 and XS 31 and the second site was at the outflow of a culvert that passes beneath McLeod Road (Figure 3.3). The first site had a seasonal contribution from a road-side ditch that augments the flow in Alderson Creek during the wet season. Both sites couldn't be surveyed because they were not reflective of the natural channel. The sampling site at XS 34 was also unique in that it is placed where Alderson Creek flowed out of a pond through a culvert, dropping into a small catch basin (industrial ceramic sink). Each of the proposed sub-reaches included three to six sampling sites (Table 3.2) that were monitored between June-December 2015, May-December 2016, and April-December 2017.



Figure 3.3. Locations of temperature pendant sampling sites in Alderson Creek. Symbols designate cross-section number. Copyright © 2018 Esri, ArcGIS Online, DigitalGlobe, GeoEye, Earthstar Geographics, CNES/Airbus DS, USDA, USGS, AeroGRID, IGN, and the GIS User Community. All rights reserved.

Table 3.2. Cross-sections that were monitored within the proposed sub-reaches (R1 to R5) along Alderson Creek.

R1	R2	R3	R4	R5
XS 1	XS 13	XS 19	XS 27	XS 32
XS 3	XS 15	XS 22	XS 28	XS 34
XS 4	XS 17	XS 25	XS 30	XS 35
XS 9		XS 26	Between XS 30 and XS 31*	
XS 12			XS 31	
			McLeod Rd*	

*Sample sites were not surveyed and were not labelled as a cross-section.

3.1.2. Temperature

Temperature was measured manually at all sampling sites illustrated in Figure 3.3 during every site visit (typically 1-2-week intervals). In-situ continuously recording temperature data loggers were also deployed at cross-sections 1, 4, 9, 13, 15, 17, 19, 27, 30, 34, and 35, as well as at the McLeod Road sampling site. Spatial gaps are due to the need to avoid locations where livestock had easy access to the creek (R3 and R5) so as to mitigate the risk of damage to instrumentation and to the adverse health effects to the cattle in case of ingestion. Onset Corporation HOBO (Bourne, MA, USA) temperature pendants were used to record water temperature at 10-15-minute intervals. Four different models were deployed (UA-001-64, UA-001-08, UA-002-64, AND UA-002-08). The ‘001’ series measures temperature only whereas the ‘002’ series also measures light intensity using a photo-diode. The ‘64’ and ‘08’ refer to the memory capacity in kilobytes (KB). The technical specifications are summarized in Table 3.3 based on the user manuals from the manufacturer.

Table 3.3. Onset HOBO temperature pendant specifications (Onset Computer Corporation 2011-2017).

	UA-001-	UA-002-
Range (Temp)	-20 to 70 °C	-20 to 70 °C
Range (Light)	n/a	0 to 320,000 lux
Accuracy	+/- 0.53 °C (from 0-50°C)	+/- 0.53 °C (from 0-50°C)
Resolution	0.14 °C at 25 °C	0.14 °C at 25 °C
Response time	5 minutes to 90%	5 minutes to 90%
Operating Range	-20 to 50°C	-20 to 50°C
Depth Range	30 m	30 m
Memory (Kilobytes)	8 or 64	8 or 64

Twelve pendants were placed in the creek and programmed to record stream temperature at 10-minute intervals. The pendants were tied to large spikes that were nailed in the creek, and the positive buoyancy of the pendants left them suspended into the middle of the water column. Every 7-10 days, the temperature recordings were downloaded using an Onset HOBOWare waterproof shuttle (Figure 3.4). The shuttle was subsequently connected to a computer, and the data files were downloaded using HOBOWare Pro software.



Figure 3.4. HOBOWare shuttle attached to the temperature pendants in the creek to download data stored on the pendants.

3.1.3. Conductivity, Turbidity, pH, Dissolved Oxygen

Conductivity, turbidity, pH and dissolved oxygen were measured at all sample sites in Figure 3.3. Conductivity and pH, in addition to manual temperature measurements, were measured with single handheld sensors (Oakton PCTestr 35). The pH range is 0.0-14.0 with a resolution and accuracy of ± 0.1 , and the conductivity range is 0-20,000 μS with a resolution of 10 μS and accuracy of $\pm 1\%$ full-scale. Measurements are automatically temperature compensated and sensors display temperature with a range of 0-50°C, resolution of 0.1°C and accuracy of $\pm 0.5^\circ\text{C}$. Turbidity was measured with a HACH 2100Q Portable Turbidimeter, which is based on a nephelometric light scattering principle. The range is 0-1000 NTUs, with $\pm 0.2\%$ accuracy and a 0.01 NTU resolution. DO was measured with a HACH HQ40d Portable Multi-parameter meter

and the Intellical™ LDO101 Field Luminescent/Optical Dissolved Oxygen Sensor. The DO-meter range is 0.1-20.0 mg/L (or 1-200% saturation), with a resolution of ± 0.01 mg/L and accuracy of ± 0.1 mg/L in solutions with DO between 0-8 mg/L and ± 0.2 mg/L for solutions with DO greater than 8 mg/L.

Conductivity, pH, turbidity, and DO data were collected every 7-10 days, the observations recorded in a field book and later transcribed. Sampling began at the lower end of the creek (XS 1) working upstream (XS 35). A water sample was taken using a 600 mL beaker, and two PCTestr 35 handheld probes were placed into the beaker. One of the probes was set to measure pH while the other was set to measure conductivity so that simultaneous readings could be acquired while using the same probe for consistency. Water temperature was averaged between both probes. Three small vials made of optical grade glass were filled with creek water to measure turbidity. Each vial was read in sequence by the portable turbidimeter and then read over three times, resulting in nine turbidity replicates per sample site (3 samples times 3 measurements each). The average of the 9 samples was transcribed. The DO probe was held in place in the water column while the meter stabilized and DO was recorded in mg/L and as a percent saturation, in addition to the temperature and the pressure. Between 1:49 pm October 1st, 2017 and 12:20 pm October 2nd, 2017, the DO meter was attached to a rebar in the centre of the creek, suspended into the water column and set to record DO every 30 minutes. This was to assess the minimum dissolved oxygen values, which are expected overnight. This was done at XS 9 because it was the farthest downstream site that was sheltered by a tree canopy and away from street traffic.

The duration of a full sample run at all sites with all parameters (conductivity, pH, turbidity, DO and temperature) was approximately 3 hours. This length of time may have introduced some bias into the measurements because conditions in the morning (downstream sites) were cooler than those later in the day (upstream sites). The potential bias was not examined in detail or corrected for because: (a) turbidity is not temperature dependent; (b) the pH and conductivity probes are temperature compensated; (c) the dissolved oxygen probe is temperature compensated; and (d) all temperature measurements from the pendants are time-stamped. Moreover, all sampling runs were conducted with similar start and end times so the bias, if present, is consistent.

3.1.4. Nitrogen

Nitrogen was sampled at five locations (Figure 3.5) corresponding to each of the proposed sub-reaches. The samples were taken at the downstream end of each sub-reach to account for changes that may have occurred within the creek as it flowed through the sub-reach. Samples at XS 1 represented R1, XS 13 represented R2, directly upstream from XS 17 represented R3, XS 27 represented R4, and XS 32 represented R5.

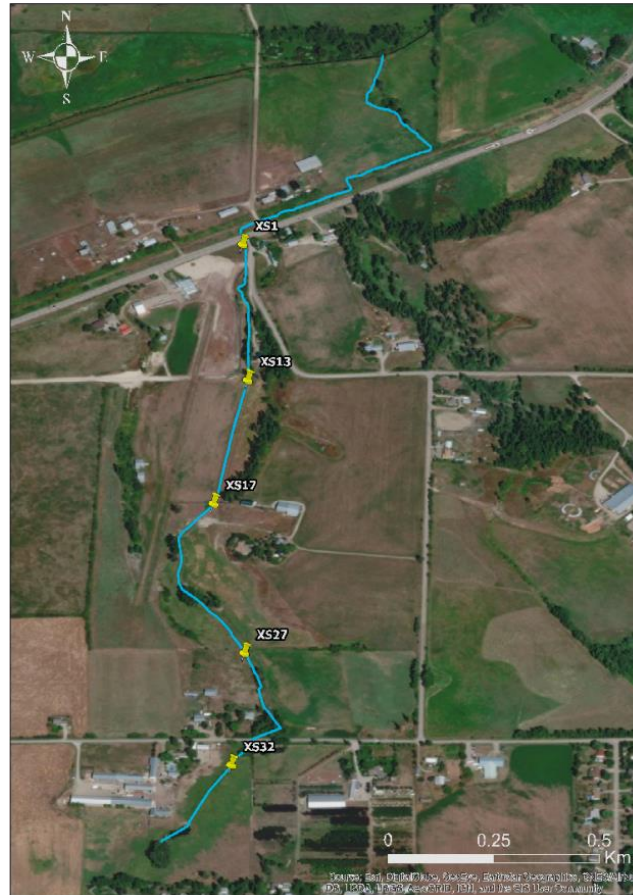


Figure 3.5. Locations of nitrogen sampling along Alderson Creek. Used with permission. Copyright © 2018 Esri, ArcGIS Online, DigitalGlobe, GeoEye, Earthstar Geographics, CNES/Airbus DS, USDA, USGS, AeroGRID, IGN, and the GIS User Community GIS User Community. All rights reserved.

Nitrogen samples were collected on the same 7-10-day schedule as the other water quality parameters, except with a later starting date of May 12th, 2017. Acid-washed vials were used to collect creek water samples. At each of the five sampling locations, a vial was placed into the water column upside down, tipped right side up and closed under water to prevent air bubbles

and contamination. The vials were labelled and brought back to the lab where they were refrigerated for less than 48 hours before analysis.

3.1.5. Macrophytes and Macroinvertebrates

Macrophyte density and macroinvertebrates were sampled at five locations, representative of each of the sub-reaches (Figure 3.6). These sample locations were chosen at sites that visually represented the sub-reach from field surveys and to minimize disturbances from livestock. In addition to macrophyte surveys, two methods were used to determine the number of macroinvertebrates in the creek: artificial substrate baskets and kick net sampling.



Figure 3.6. Locations of macroinvertebrate sampling and macrophyte density analysis along Alderson Creek. Used with permission. Copyright © 2018 Esri, ArcGIS Online, DigitalGlobe, GeoEye, Earthstar Geographics, CNES/Airbus DS, USDA, USGS, AeroGRID, IGN, and the GIS User Community. All rights reserved.

3.1.5.1. Macrophyte Density

Macrophyte density was measured monthly at each of the five sample locations using a square quadrat made of PVC tubing, connected with PVC elbows. The quadrat was split into one-hundred 10 cm squares using string (Figure 3.7). The quadrat was centered on the middle of the creek. Four blue flags were placed at the corners of the frame to allow for consistent relocation of the quadrat during subsequent visits. Macrophyte density was evaluated by estimating the number of squares in the creek that were fully or predominantly occupied by vegetation. Since the quadrat was split into 100 squares, the density could be expressed as a percent vegetation density per square metre.



Figure 3.7. A quadrat, placed onto the center of the creek, defines the 1 m² area used to count the percent of squares occupied by vegetation.

3.1.5.2. Macroinvertebrates: Artificial Substrate Sampling

Artificial substrate baskets were styled after gabions, or cages, typically used for erosion control or landscaping. Nine-centimetre cube baskets were made from a ½ inch by ½ inch hardware mesh secured by zip ties (Figure 3.8).



Figure 3.8. Artificial substrate basket consisting of river stone. Wire baskets were secured into the creek bed with a nail and left to collect macroinvertebrates.

The baskets were filled with 1 to 2 inch beach/river stone to provide a rocky substrate for invertebrate occupation. Sampling sites had different substrate material, most with exposed gravel like the beach/river stone, R4 veneered with a clay-silt material, and R5 veneered with muck. Studies have shown that macroinvertebrate compositions differ between substrata with different grain sizes -- fine sand is not preferred by macroinvertebrates (Duan et al. 2008). Coarse-grained material was chosen for the gabion baskets so that macroinvertebrates would occupy the baskets preferentially, if in the system, and also to avoid bias between sites that would arise from using locally derived substrate material.

Seven baskets were placed along the bank of each of the 5 sampling sites and secured in place with a 10" nail tied to the base of each basket. When installing the baskets, the bed of the creek was dug out slightly to ensure that the baskets were in intimate contact with the substrate and remained fully submerged even if the water levels decreased. At each site, the downstream basket was placed upstream from the upstream vegetation quadrat flag. Each of the remaining baskets were placed two centimeters upstream from the last one. The downstream basket remained in-stream for 6-months. The most upstream basket was the 'control' basket, which was retrieved and replaced each month. The remaining baskets were the 'cumulative' baskets, which

were left in place until their assigned month. For instance, the second-most upstream basket (below the control basket) was retrieved after 1-month (July) along with the control basket, which was replaced; the third-most upstream basket was retrieved after 2-months (August) along with the control basket, which was replaced; and so on until only the downstream and control baskets were retrieved after 6-months (December) and not replaced. Figure 3.9 illustrates the arrangements of the baskets along the right bank of the second site at XS 15.

The control baskets were handled on-site by placing the rocks into a Ziploc container with water, gently detaching insects from the substrate and retaining them in the container, placing the clean rocks back into the basket, and returning the basket to the creek, as illustrated in Figure 3.10. The cumulative baskets were collected at monthly intervals, removed from the creek and placed into a Ziploc container in its entirety and brought back to the lab to be analyzed, Figure 3.10.



Figure 3.9. Artificial substrate baskets placed along the right bank at site 2, XS 15, relative to the encircled blue quadrat flag on the lower left-hand side of the image. The red and white bobble was used to mark the downstream basket.



Figure 3.10. Collection of artificial substrate baskets. Stone in the control baskets were gently wiped and reinstalled into the Creek while cumulative baskets were completely removed.

3.1.5.3. Macroinvertebrates: Kick Net Sampling

Kick net methods followed the Canadian Aquatic Biomonitoring Network (CABIN) protocols (Environment Canada 2012). A kick net sampler is a net attached to a rod that is placed perpendicular to downstream flow along the creek bed, an example of which is shown in Figure 3.11. The substrate directly upstream from the kick net was kicked by foot to disturb it up to a depth of 5-10 centimeters. This was done in a zig zag pattern over the stream bottom for a period of 3 minutes. The kick net was emptied and rinsed with deionized water into a Ziploc container and brought back to the lab.



Figure 3.11. Kick net method to collect macroinvertebrate samples in Alderson Creek.

3.2. Laboratory Methods

Refer to Appendix A for details of the calibration of temperature, pH, conductivity, turbidity, and dissolved oxygen instruments.

3.2.1. Nitrogen

Spectrophotometric methods were used to measure nitrogen concentrations consistent with the methods described by Miranda et al. (2001). Nitrogen concentrations in Alderson Creek were reported as the concentration of Nitrate (NO_3) as it is the more dominant form of nitrogen in natural waters. Nitrate ions in a solution react with VCl_3 and Griess reagents to produce a range of color intensities proportional to the amount of nitrate (Miranda et al. 2001). Spectrophotometers measure the absorption of light in the solution at 540 nm by colorimetric detection, which can be converted to concentration in mg/L (Robledo et al. 2014; Miranda et al. 2001). To prepare the samples, vanadium (III) chloride (VCl_3) must be used to reduce the nitrates to nitric oxides which then react with the second reagent, Greiss, to form the color (Miranda et al. 2001). Vanadium (III) chloride (VCl_3) consists of 50 mL of 6 N HCl and 50 mL deionized water mixed with 2.0 g VCl_3 . The color produced by a Griess reagent, comprised of mixture of a *N*-(1-Naphthyl)ethylenediamine (NEDD) solution and a sulphanilamide solution. The NEDD solution contained 0.5 g *N*-(1-Naphthyl)ethylenediamine in 500 mL of deionized water. The sulphanilamide solution contained 5.0 g of sulphanilamide in a solution made up of 50 mL concentrated hydrochloric acid in 300 mL of deionized water. The NEDD and sulphanilamide solutions were stored in dark glass bottles and mixed in equal amounts to create the Griess reagent just prior to analysis.

Creek samples were filtered through a 0.7 μm glass fiber filter, from which 10 mL was placed into spectrophotometer vials. Six 10 mL samples were made, one for each sub-reach plus one for the groundwater input at the upstream terminus of the creek. The sulphanilamide solution and NEDD solution were mixed in equal portions to create the Greiss reagent. Half of a millilitre of the Griess reagent and 1 mL of the vanadium (III) chloride reagent were added to each 10 mL creek sample and left to incubate at room temperature for at least 6 hours.

In addition to the creek samples, standards were prepared with a 10-mM potassium nitrate (KNO_3) stock solution. The standards were made by adding 0 μL , 10 μL , 20 μL , 50 μL , 100 μL , 500 μL , 1000 μL and 1500 μL of KNO_3 stock standard into 100 mL of e-pure water. The standards were prepared using the same proportions of Greiss and VCl_3 reagents as the creek samples (Figure 3.12). Once incubated for at least six hours, the standards and the creek samples were placed into a Varian Cary® UV-Visible Spectrophotometer. The spectrophotometer output gave the absorbance of each sample, which was larger for darker colors, indicating larger nitrogen concentrations.

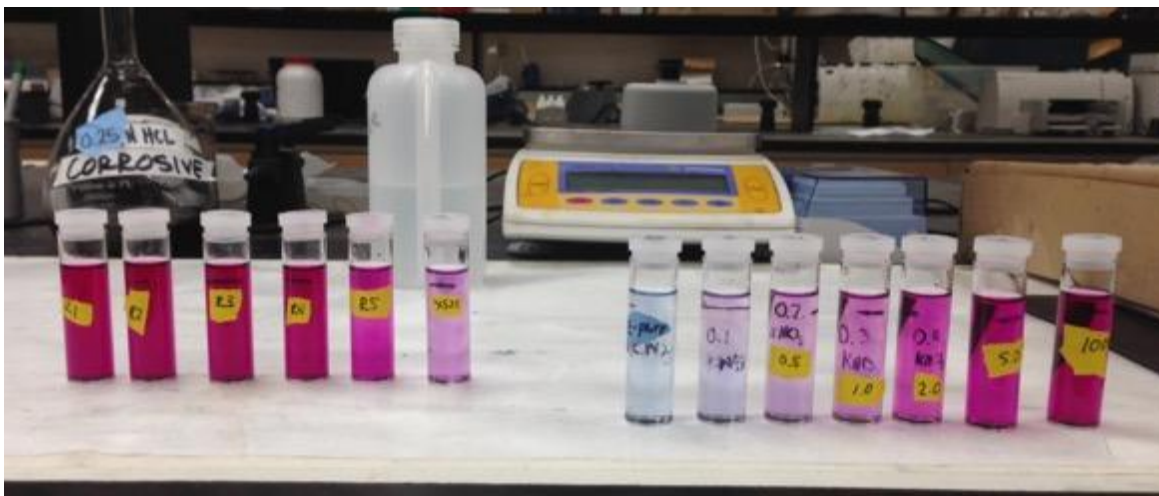


Figure 3.12. Samples prepared for nitrogen analysis of the five proposed sub-reaches and the sample upstream from XS 35 (left) as well as the KNO_3 standard solutions (right). The solutions have been prepared with Greiss and sulphanilamide reagents and incubated for over 6 hours. Darker colors indicate increased nitrogen concentration.

Refer to Appendix B for the calculation used to determine nitrogen concentrations.

3.2.2. Macrophytes and Macroinvertebrates

Macroinvertebrate samples were collected, transferred and preserved based on CABIN protocol (Environment Canada 2012). Entire artificial substrate baskets (cumulative baskets), rocks from control baskets, and kick net samples were rinsed and gently wiped off over a 400 μm sieve. The invertebrates retained on the sieve were placed into sample jars and preserved with 95% ethanol (Figure 3.13). The sample jars were labelled with site location, sampling method and date. Stereo-zoom microscope and fine forceps were used to identify and count Ephemeroptera, Plecoptera, and Trichoptera (EPT) macroinvertebrates for each sampling method (Figure 3.13).



Figure 3.13 Left: macroinvertebrates samples preserved in 95% ethanol. Each jar represents various locations and dates of collection. Right: sample in a petri dish under a stereo zoom microscope to count Ephemeroptera, Plecoptera, and Trichoptera occurrences.

Morphological features to identify aquatic insects vary by order but three body regions, the head, the thorax, and abdomen, are common among all insects (Thorp and Covich 2010):

- The head have a pair of antennae, eyes, and several mouthparts;
- The thorax is posterior to the head and consists of three segments, the prothorax, mesothorax and metathorax, each of which has a pair of legs; and
- The abdomen is the posterior region containing up to 10 visible segments.

EPT were identified at the order taxonomic level using guides from Hugh (1991) and Thorp and Covich (2010). Body shape, wings, antennae, and cerci (tails) differentiate between EPT, illustrated in Figure 3.14, Figure 3.15, and Figure 3.16.

Ephemeroptera larvae, ranging from 3-25 mm are readily distinguished from other aquatic insects by their three long tails, lateral gills on the first seven abdominal segments, segmented tarsus (part of arm, see Figure 3.14) and single claw (Thorp and Covich 2010; Hugh 1991). Plecoptera, ranging from 6-35 mm, closely resemble Ephemeroptera, but always have two tails, lack gills in their middle abdomen, and have two tarsal claws (Thorp and Covich 2010; Hugh 1991). The shape of Plecoptera thorax segments, wing pads, and abdomen are distinct from Ephemeroptera, and are typically distinguished from other insects by the presence of two long antennae and three-segmented tarsi (arms) (Figure 3.15) (Hugh 1991). Trichoptera are distinct in that their thoraxes are a much smaller proportion of their body size compared to their abdomen,

resulting in three legs crowding near their head. Other morphological distinctions of Trichoptera include a singular tarsal segment and tarsal claw on their legs, they have caterpillar-like abdomens with single or branched gills, short antennae, and instead of cerci they have an anal pro-leg that can contain claws or a brush of hairs (Figure 3.16) (Thorp and Covich 2010). Trichoptera are typically larger in diameter compared to Ephemeroptera and Plecoptera but are similar in length between 2-25 mm (Hugh 1991). Unique to Trichoptera larvae is that they build and live in cases made up of plant material or mineral matter (Figure 3.16) (Hugh 1991).

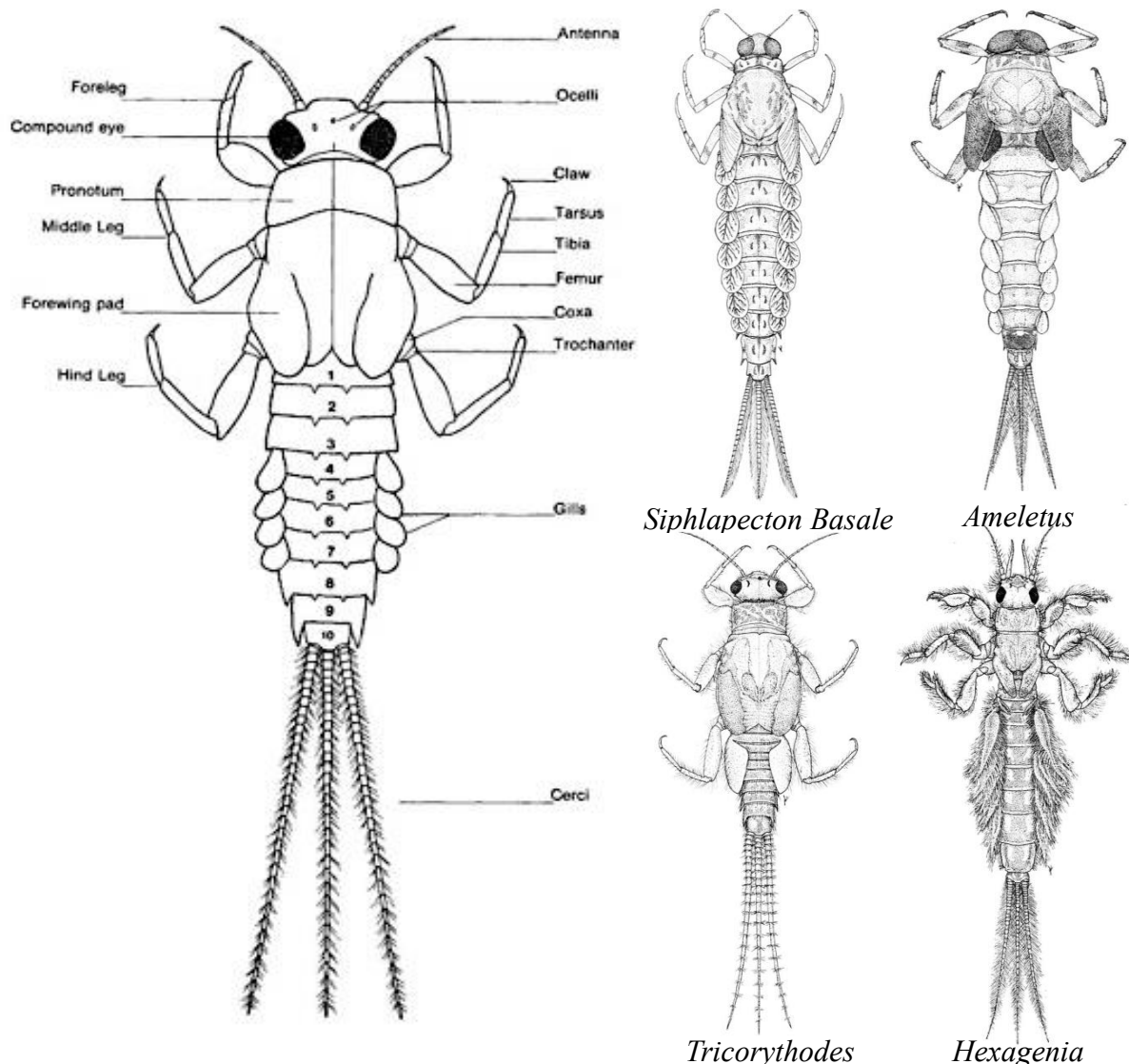


Figure 3.14. Features of an Ephemeroptera (left) and four examples of Ephemeroptera genera (right). A consistent and identifiable feature of Ephemeroptera are its three cerci, or tails. Figure from Hugh (© 1991 University of Alberta Press, by permission).

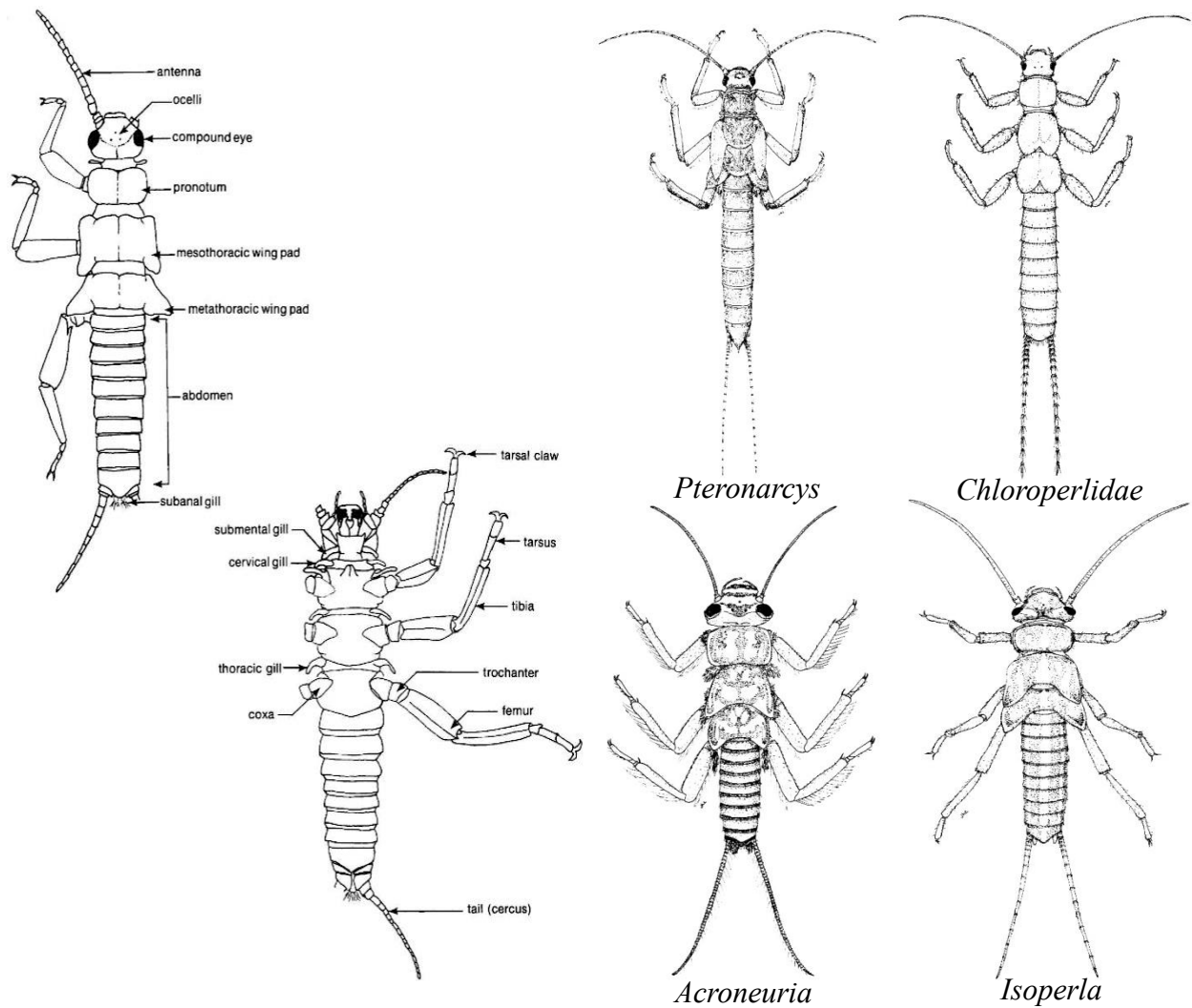


Figure 3.15. Features of the top and bottom view of a Plecoptera (left) and four examples of Plecoptera genera (right). A distinguishable feature of Plecoptera is its two cerci. Figure from Hugh (© 1991 University of Alberta Press, by permission).

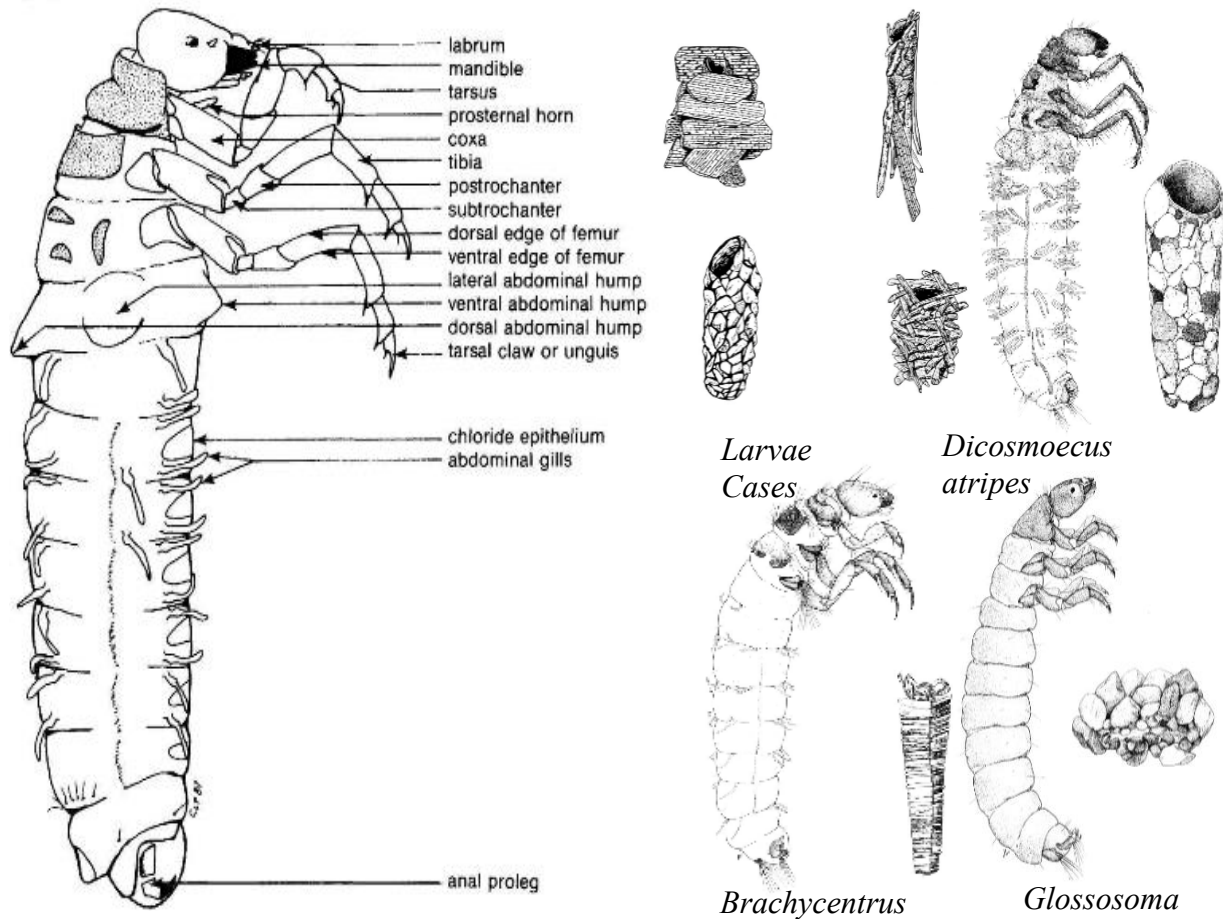


Figure 3.16. Features of a Trichoptera (left), examples of larvae cases, and three examples of Trichoptera genera with their respective cases (right). Figure from Hugh (© 1991 University of Alberta Press, by permission).

3.3. Data Analysis Methods

3.3.1. Temperature

As temperature data were downloaded, irregularities were eliminated from the time series, such as when a pendant was out of the water column due to low flow. Two approaches were used to derive statistical parameters: (1) temporal trends; and (2) spatial differentiation.

The data were separated temporally according to seasons based on equinoxes and solstices and diurnally according to the time of sunrise, time of sunset, and hours of sunlight, which were obtained from the National Research Council of Canada. Hourly air temperatures were used as a comparator, which were obtained from the Environment Canada historical database for the

nearest station in Vernon (Government of Canada 2017; NRCan 2017). Hourly air temperatures were re-worked into a 7-day moving average, which was used to define seasonal divisions observed in the data. Equinoxes occur on or about March 21st and September 22nd for spring and fall, and solstices occur on or about June 21st and December 21st for summer and winter. The maximum hours of sunlight, earliest sunrise, and latest sunset occur on summer solstice whereas the minimum air temperatures, minimum hours of sunlight, latest sunrise, and earliest sunset occur on winter solstice. For the purposes of this study, season starts and finishes were defined after the solar maximum and minimum to reflect the seasonal lag in temperature response. Four seasonal divisions were made (Figure 3.17): June to August for summer months, September to November for fall months, December to January for winter months, and February to March for spring months.

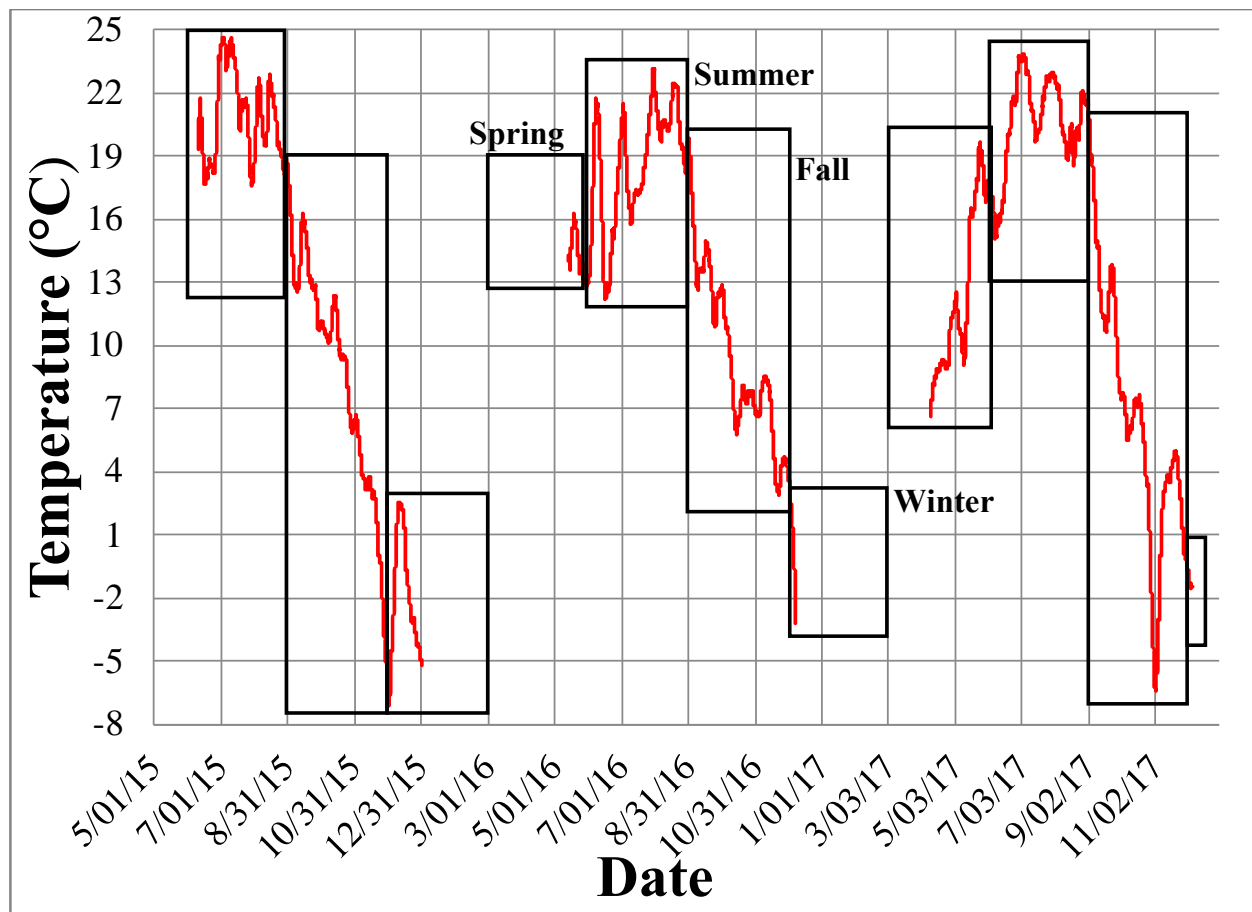


Figure 3.17. Seven-day moving averages of air temperature between April and December 2015, 2016 and 2017. The black boxes on the plot outline seasons, wherein summer is the peak

temperatures June-August, fall us the transition between September-November, winter is the minimum temperatures December-February, and spring is the transition from March-May.

The data were further divided using daily trends. From the original data, the time of maximum and minimum temperature were extracted for each day. Time of minimum and maximum temperatures were used to split the days into four increments: minimum temperatures between 12 am and 6 am; maximum temperatures between 12 pm and 6 pm; and two 6-hour transition periods between. The temperature data were grouped so that the average temperature could be taken for each time-period and split into season, reducing the data to a manageable form for statistical analyses.

3.3.2. Conductivity, Turbidity, pH, Dissolved Oxygen, Nitrogen, Macrophyte Density and Macroinvertebrate Abundance

Conductivity, turbidity, pH, dissolved oxygen, nitrogen, macrophyte, and macroinvertebrate data were not collected frequently enough to identify daily trends. Only long-term temporal patterns and spatial trends could be determined using the data set. The entire data set was organized in a master spreadsheet according to parameter type and date, with additional ‘Cross-section’, and ‘Season’ columns to designate location and season (e.g., Table 3.4).

Table 3.4. An example of the spreadsheet used to analyze the measured parameters along Alderson Creek. The sample date, location (numbered cross-section), and season were classified for each observation.

Date	Parameter 1	Parameter 2	Cross-section	Season
6/12/2015			1	Spring

3.4. Statistical Analysis

Discriminant analysis (DA) is a tool for discriminating between groups (i.e., sample sites in this study) based on a set of characteristics, or for classification to be able to predict the group to which a case most closely resembles (Klecka 1980). DA is different from similar regression methods including multivariate analysis of variance (MANOVA), the multivariate version of ANOVA. Where MANOVA tests whether there are mean differences between numerous

continuous dependent variables, DA analyzes group membership of numerous *categorical* dependent variables (i.e., cross-sections in this study) based on a set of predictors variables (independent variables) (Denis 2019).

Discriminating characteristics, or predictor variables, are called discriminant variables and can be environmental parameters (e.g., pH) (Klecka 1980). Combinations of discriminant variables are used to establish discriminant functions, which are linear mathematical equations (discriminant function equations) that maximize variability between groups through combinations of group characteristics (Rencher and Christensen 2012). The discriminant analysis also identifies which variables are important to the differentiation between groups (Myatt and Johnson 2009; Klecka 1980).

A discriminant function equation is made up of a combination of the discriminant variable raw values (e.g., pH = 7.2) and that variables ‘weight’ or ‘loading’, called discriminant coefficients (β), to correct for relationships between variables and maximize scores between groups (Aljandali 2017). Scores (F) are calculated by the linear discriminant function:

$$F = \beta_0 + \beta_1X_1 + \beta_2X_2 + \dots + \beta_nX_n$$

where X are the n values of predictor variables, and β are the n discriminant coefficients (Aljandali 2017). A discriminant analysis will indicate whether one (or several) discriminant functions significantly differentiate between groups. Typically, two discriminant functions explain almost all of the variance between groups, and any additional non-significant discriminant function(s) can be ignored. A plot (using standard deviation units) displays the scores of the first discriminant function (x-axis) and the scores of the second discriminant function (y-axis) so that both maximize separation between group means but also so that the second is perpendicular (uncorrelated) to the first (Klecka 1980). A centroid, the position where the total set of data cases have its mean on each of the axes, is plotted as well as the scores to be able to visualize groupings. Large separation distances between centroids indicate distinct groups (Klecka 1980).

Linear discriminant analysis (LDA) was performed with the statistical software package IBM® SPSS Statistics version 24. The cross-section numbers along the stream were used as the group variable whereas the values of the environmental parameters (e.g., temperature, pH,

conductivity, turbidity, DO, nitrogen, macroinvertebrate abundance and macrophyte density) were input as the discriminant variables or predictor variables. Due to seasonal variability in the parameters, the data were divided into seasons prior to analyses and only summer data were analyzed because the summer conditions are critical for aquatic life (i.e., temperature threshold, lowered dissolved oxygen, etc.).

Two key assumptions of discriminant analysis are that variables are normally distributed and that the variables are independent of one another so that the value of one observation doesn't influence the value of another observation (Bataineh et al. 2006; Myatt and Johnson 2009). The latter is called pseudo-replication (Hurlburt 1984), in which treatments are not replicated or replicates are not statistically independent. This assumption of independence is often violated in inferential statistics due to spatial correlation, which occurs when there is a similarity between two observations due to spatial proximity (Bataineh et al. 2006; Bart 1998). Additionally, observations may not be independent due to repeated measures arising from temporal autocorrelation, the correlation between observations from sample sites measured repeatedly in time over short time intervals. With repeated measures, the magnitude of correlation changes with differences in time-lag between measurements (correlation decreases as time lag increases). If the assumption of independence is ignored, p-values will be artificially small, leading to the rejection of the null hypothesis more often than it should be, and variability between groups would be overestimated, although results might still be useful if interpreted with caution (Klecka 1980).

Assumptions of spatial correlation or temporal autocorrelation are often inherently violated when studying streams and rivers; numerous sites along a stream are spatially correlated as water flows downstream and temporal autocorrelation of numerous measurements at one sample site as a result of an interest in how conditions change through time. Values of a variable will be more alike at sample sites side-by-side compared to sample sites farther upstream or downstream. Similarly, the value measured on day 1 at sample site 1 will be more alike to the value measured on day 2 at the sample site 1 compared to the value measured on day 2 at a second sample site. To account for this, sampling sites should be carefully selected to ensure observations are truly independent, such as several sampling sites along a large number of streams, sampled at one point in time. This design is not only labour intensive and costly to accomplish, but it is nearly

impossible to perform replicates while keeping other influences constant (i.e., streams flowing through different types of substrate). This also does not allow for changes in a stream to be observed over time.

There is no statistical test to estimate the amount of variation that is explained by spatial and/or temporal autocorrelation. In this study, minimizing the effect of spatial correlation was done using linear models and residuals. Linear models were fit to each parameter to predict the expected value at x-distance downstream (i.e., successive cross-sections). The difference between what was actually measured at each cross-section and what was expected based on the linear model gave the residual. The residuals demonstrate if there are patterns in how the parameters differ at sample sites compared to what would be expected linearly, resulting in a data set that ignores downstream trends. For the analysis, data were normalized using standardized residuals, calculated by dividing the residual by the predicted value. Standardized residuals help to satisfy the assumptions of normal distributions and independence.

Temperature data were unique because it was measured by in-situ pendants as well as manually when other parameters were measured. The pendants produced considerably more observations than other parameters. A greater number of observations would benefit the discriminant analysis; however, a discriminant analysis could not be performed when data points were missing. Rows that had missing observations were deleted, such as the dates that temperature was recorded, and other parameters were not. Temperature data had to be reduced to align with the observations of other parameters, which could be done in two ways. The first method was to use the 6-hour average between 12-6 pm (maximum temperatures) and the 6-hour average between 12-6 am (minimum temperatures) for the dates that other parameters were measured. The second method was to use the manual temperature measurement on the date and time that the other parameters were collected. The average of stream temperature in 6-hour time blocks reduces temporal autocorrelation because autocorrelation decreases as time increases so that recordings 6-hours apart are less correlated than recordings 10-minutes apart. The problem with using pendant temperatures, however, is that there were fewer sample sites that had temperature pendants than sites that were manually measured. More sample sites in the analysis provides a better understanding of group differentiation. The length of time between manual measurements, 7-10 days, is sufficient to reduce the effect of temporal autocorrelation. The date and time stamp of

manual temperature measurements (from field notes) were aligned with temperature pendant measurements (digitally downloaded from pendants) to ensure that they recorded nearly the same temperature at the same time. The comparison of pendant and manual temperature measurements is described in Section 4.2 and an example shown in Figure 4.27.

In addition to temperature, all other variables were not recorded at the same dates, such as when there were instrument malfunctions or parameters measured at different time scales (biweekly versus monthly). As a result, summer data were input in several combinations rather than all at once, maximizing the number of observations in the analysis (Table 3.5). In the first analysis, for instance, DO, nitrogen, macrophyte density and macroinvertebrate abundance were excluded so that all observations were included in the analysis with discriminant variables pH, turbidity, conductivity, and temperature. Another analysis tested how well nitrogen discriminated between the groups but was input with only pH and turbidity because those variables were the only ones that were consistently measured on the same dates as nitrogen.

Table 3.5. Combinations of discriminant variables that were used in eight discriminant analysis tests are indicated by check marks.

Discriminant Variable	DA 1*	DA 2*	DA 3	DA 4	DA 5	DA 6	DA 7	DA 8	DA 9	DA 10	DA 11 *	DA 12	DA 13
Temperature	✓	✓	✓	✓	✓	✓	✓	✓	✓	✓	✓	✓	✓
pH	✓	✓	✓	✓	✓	✓	✓	✓	✓	✓	✓	✓	✓
Conductivity		✓		✓		✓		✓			✓		✓
Turbidity	✓	✓			✓	✓	✓	✓					
Macrophyte density			✓	✓									
Total EPT in Control Baskets					✓	✓							
Total EPT in Cumulative Baskets							✓	✓					
Total EPT in Kick Net Samples									✓				
Dissolved Oxygen										✓	✓		
Nitrogen												✓	✓

*Analyses were done twice, once with all cross-sections and once without cross-sections in R5.

Chapter 4. Results

4.1. General Observations and Data Trends

4.1.1. Temperature

Several years of data collection using self-recording temperature pendants revealed complex spatial and temporal trends in the water temperature that make sub-reach assessment difficult. For example, there was considerable variability in temperature response to atmospheric forcing at daily, seasonal, and annual time scales, which implies that the use of mean statistics (e.g., daily, annual) for sub-reach comparisons becomes problematic because the averages reflect the extremes (maxima and minima) as well as the central tendency. Moreover, diurnal fluctuations differ according to seasons, especially summer versus winter, in terms of how the radiation balance influences temperature changes at different sampling sites. It is not immediately apparent how to best generate the statistics (maximum versus minimum; mean versus median; averaging intervals) that yield the greatest insights into sub-reach delineation.

Annual stream temperature trends were similar from year-to-year with progressive warming during the spring leading to a summer-time high in late August, followed by a gradual decline toward December (Figure 4.1). All temperature pendants measured approximately the same trends with the exception of the pendants at XS 35 and XS 34, which typically measured the coolest and hottest conditions, respectively, during the summer and early fall. This is due to XS 35 being closest to the groundwater source for Alderson Creek (with relatively constant temperature all year in comparison to other sites along the stream), whereas XS 34 is immediately downstream of a large pond that serves as a radiative heat sink during the summer. Diurnal fluctuations were very apparent at all pendant locations, with day-time temperatures rising quickly and peaking in early afternoon, whereas night-time temperatures decreasing gradually to a minimum just before sunrise. Daily stream temperatures often have a range of 5-10°C, which is surprising given that Alderson Creek is a spring-fed stream with rapidly flowing water due to the relatively steep gradient.

The 24-hour averages were quite stable from day to day despite diurnal fluctuations of almost 10°C (Figure 4.2). Additionally, daily temperature averages show that stream temperatures follow the same seasonal trends evident in the air temperature data (Figure 3.17).

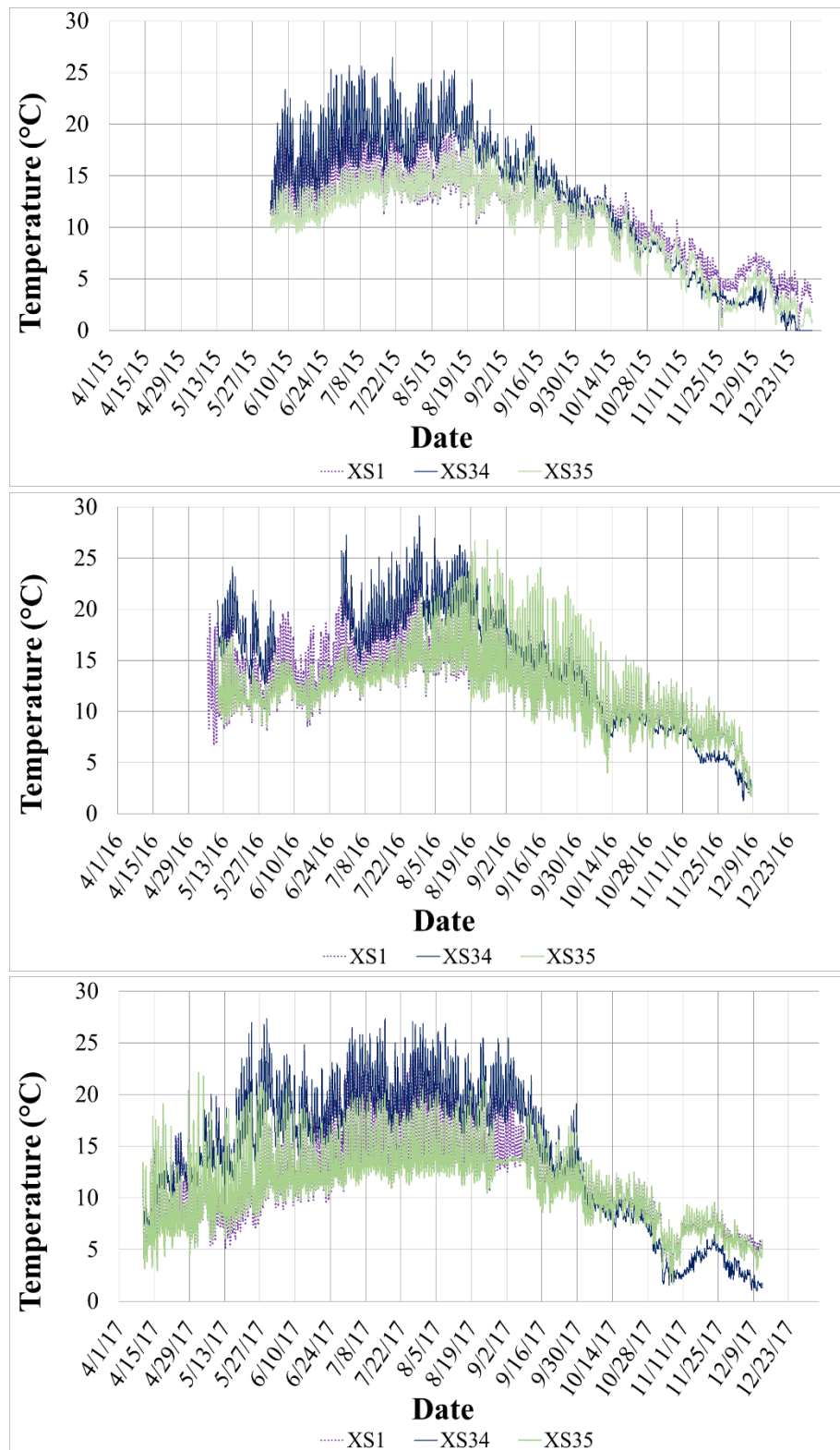


Figure 4.1. Temperature measurements at 10-minute intervals recorded at cross-XS 1, 34, and 35 along Alderson Creek. Trends for 2015 (top), 2016 (middle), and 2017 (bottom) field seasons are plotted in separate panels.

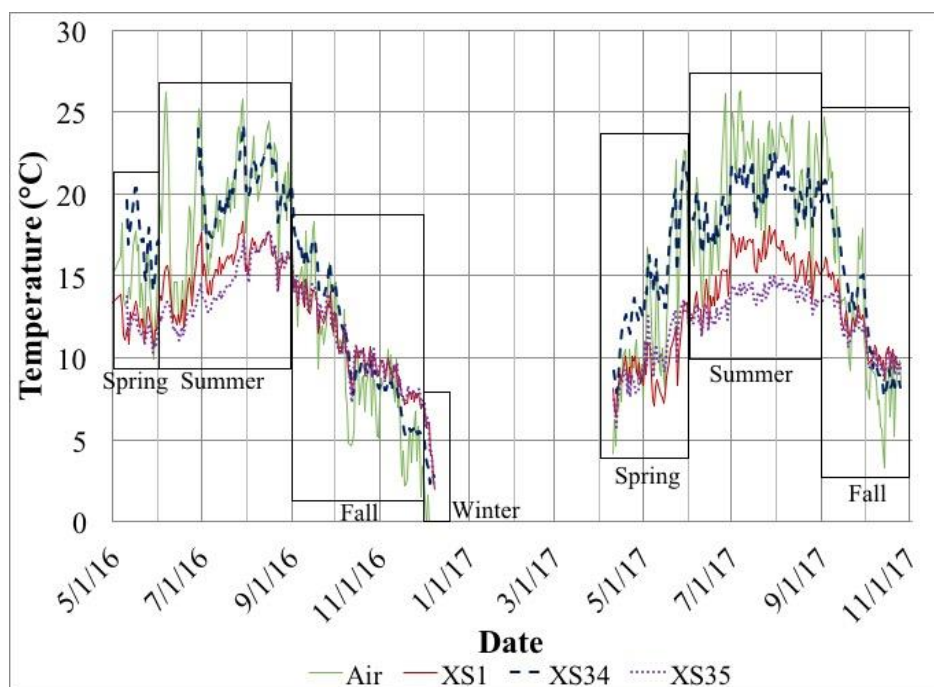


Figure 4.2. Daily average temperature at XS 1, 34, and 35 as well as air temperature throughout 2016 and 2017 field seasons. The boxes outline changes of seasons: the summer box is associated with the peak temperatures in June-August, the fall box delineates the transition in September-November from the warm to the cold seasons, the winter box delineates the minimum temperatures in December-February, and the spring box shows the transition months March-May.

In both Figure 4.1 and Figure 4.2, temperature trends at XS 35 (farthest upstream), XS 34 (at the pond outlet), and XS 1 (farthest downstream) illustrate how much variation there is temporally and spatially. The contrast between XS 34 and XS 35 is striking given their proximity. This is also evident in box-plots, which were based on 63,000 to 87,000 data points collected at 10-minute intervals at each sample site over the three-field seasons (Figure 4.3). Average water temperatures for most sites below XS 34 were fairly similar, although there was a slight increasing trend in the downstream direction. Cross-section 34 (at the outlet of the pond) was noticeably warmer, on average, than all other locations. In the box-plots, the average is displayed as a black dot, the middle line separating the box indicates the median, the top of the box indicates the 3rd quartile (75% of data are less than that value), the bottom of the box indicates the 1st quartile (25% of data are less than that value), the entirety of the box makes up the interquartile range (IQR) which shows dispersion of the middle 50% of the data, and the whiskers show the spread of the data from the maximum (top) to minimum (bottom)

observations. The height of the boxes and lengths of the whiskers are an indication of how variable and skewed the temperature measurements are; summer measurements have longer whiskers into warmer temperatures, winter temperatures have longer whiskers into cooler temperatures, whereas spring and fall temperatures result in large interquartile ranges.

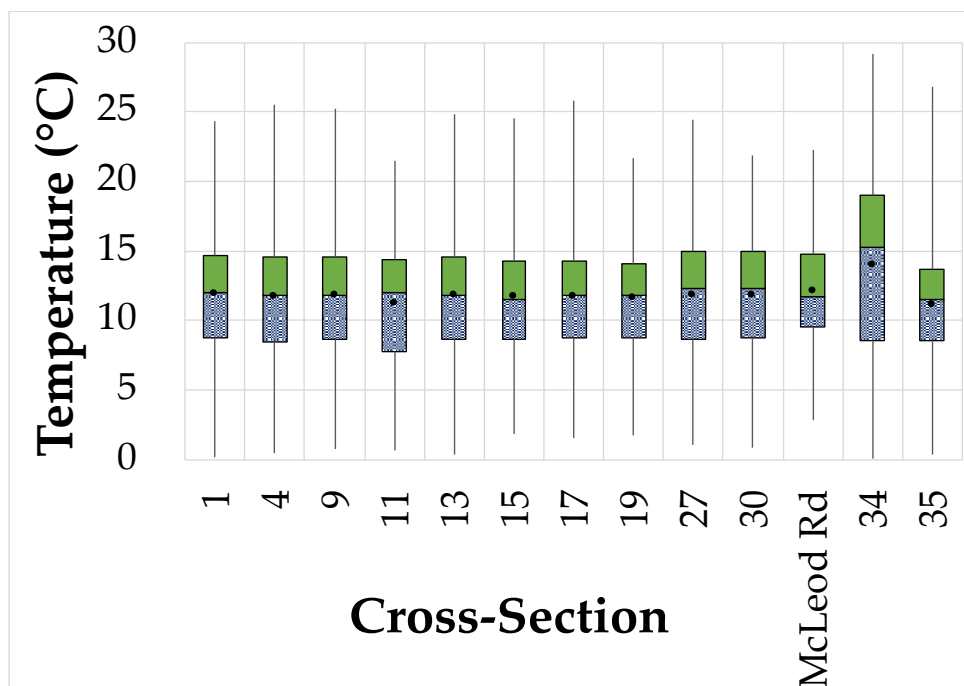


Figure 4.3. Box-plots of temperature data illustrate the mean, median, interquartile range, and dispersion of measurements as a function of location. These plots include all temperature measurements recorded by in-situ pendants between 2015 and 2017 at every cross-section.

4.1.2. Conductivity, pH, Turbidity, Dissolved Oxygen

Conductivity, turbidity, and pH were measured during site visits every 7-10 days over a three-year period, whereas dissolved oxygen was measured only during 2017. There were unique temporal and spatial patterns that emerged from these data. In the following section, conductivity, pH, turbidity, and dissolved oxygen are discussed individually with respect to the observed temporal and spatial trends. Temporal patterns are shown by raw measurements across three years at select sample sites and as the seasonal average at each sample site. Spatial patterns are evident from the box-plots, which characterise the variability in the data at every sampling point. Conductivity, pH, and turbidity box-plots contain approximately 35-45 data points

collected at each sample site over the three field seasons, whereas the plot for dissolved oxygen contains 13 data points for each sample site, collected in 2017.

4.1.2.1. Conductivity

Conductivity fluctuated on a day-to-day basis but exhibited an overall increasing trend from May to December, as demonstrated by individual sampling points (Figure 4.4) and when averaged across seasons (Figure 4.5). A decrease in conductivity at XS 1 and 4 in spring of 2017 was likely due to severe flooding causing dilution of conductive ions by rain and surface water at downstream sampling sites. Seasonally, conductivity increased by approximately 250 $\mu\text{S}/\text{cm}$ from spring to winter but ranged from 200-650 $\mu\text{S}/\text{cm}$ depending on the location. Conductivity increased in the downstream direction (Figure 4.6), although there is overlap between whiskers at adjacent sampling sites. Overlap between sample sites suggests conductivity is not unique between locations, although some cross-sections appear to ‘cluster’ about the same median value (i.e., XS 32, 34, and 35).

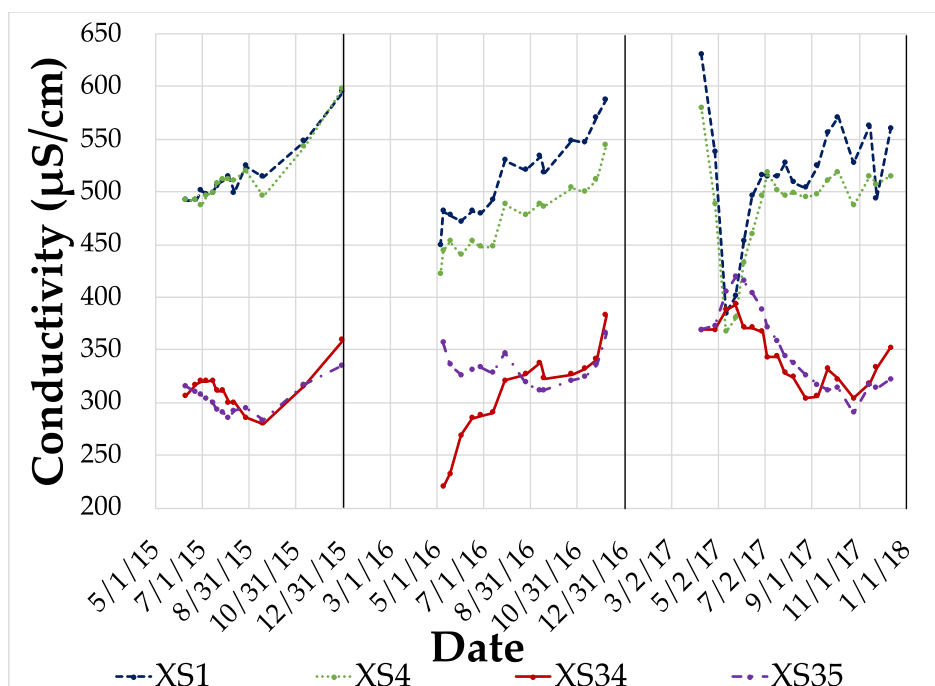


Figure 4.4. Raw data measurements of conductivity at XS 1, 4, 34, and 35 along Alderson Creek during 2015, 2016, and 2017 field seasons.

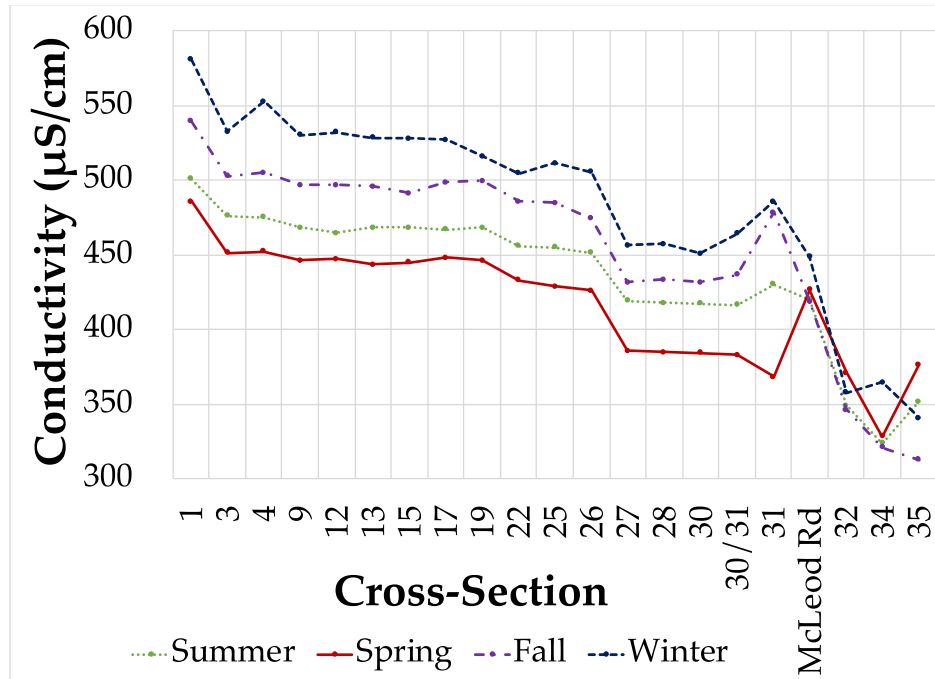


Figure 4.5. Conductivity measurements averaged across seasons. The average for summer, fall, winter, and spring are plotted at each cross-section.

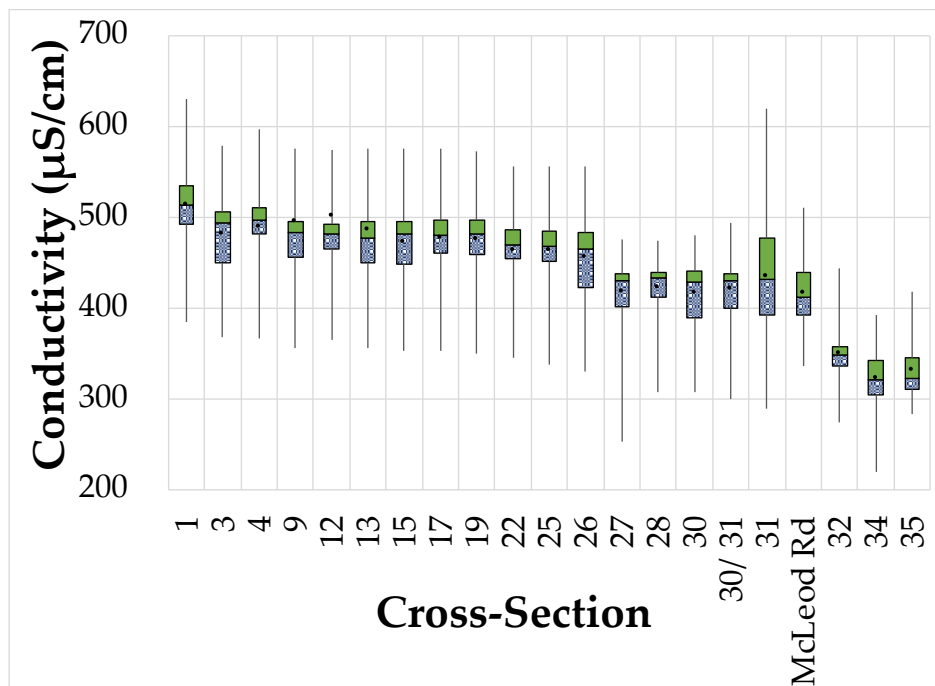


Figure 4.6. Box-plots of conductivity data illustrate the mean, median, interquartile range, and dispersion of measurements. Individual cross-section box-plots combine all data between 2015 and 2017. The range of values do not exceed the critical limits for aquatic life, livestock, and wildlife, thus are not likely a factor for fish survival.

4.1.2.2. pH

There was more variability in pH measurements between individual sample dates as compared to conductivity (Figure 4.7). There appeared to be an increasing trend in successive years, which is unexplained but may be due to changing source water conditions or altered land-use patterns. There was also an increasing trend in pH in the downstream direction, observed in plots of the raw measurements (Figure 4.7) and in plots of seasonal averages (Figure 4.8). Seasonal differences were not as evident as with conductivity, but the largest pH values were generally found in winter and spring with smaller values in summer and fall. Box-plots showed the increase of pH in the downstream direction and that the ranges of pH across sample dates was between 7 – 9.5 (Figure 4.9). In contrast to conductivity box-plots, the pH measurements had a large interquartile range relative to the whisker lengths, indicating that a large number of data were spread between the 25th and 75th percentile, meaning pH measurements didn't exhibit several outliers despite displaying large variability.

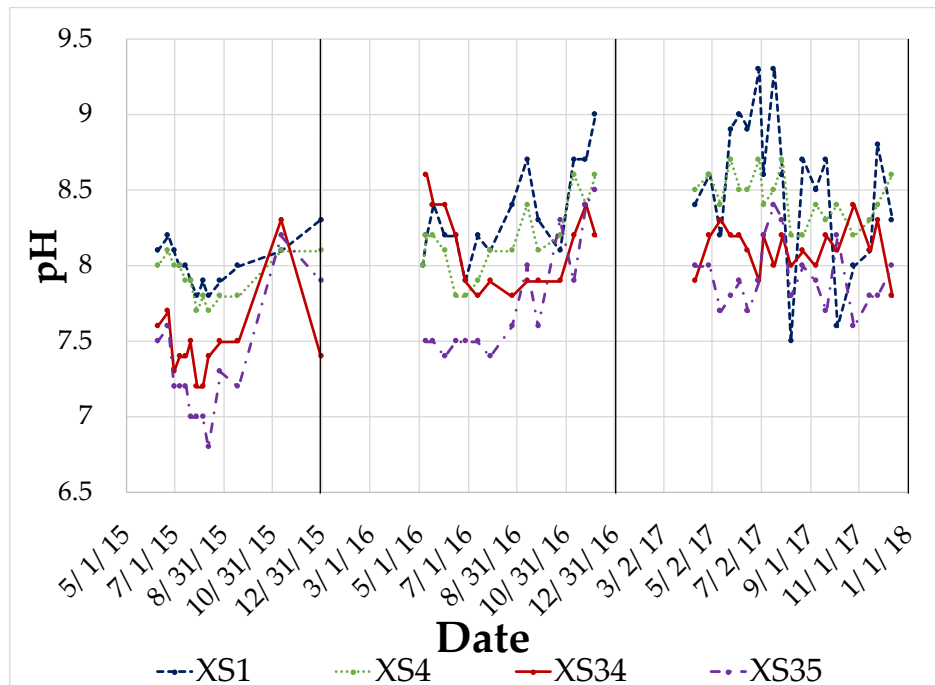


Figure 4.7. Raw data measurements of pH at XS 1, 4, 34, and 35 along Alderson Creek during 2015, 2016, and 2017 field seasons.

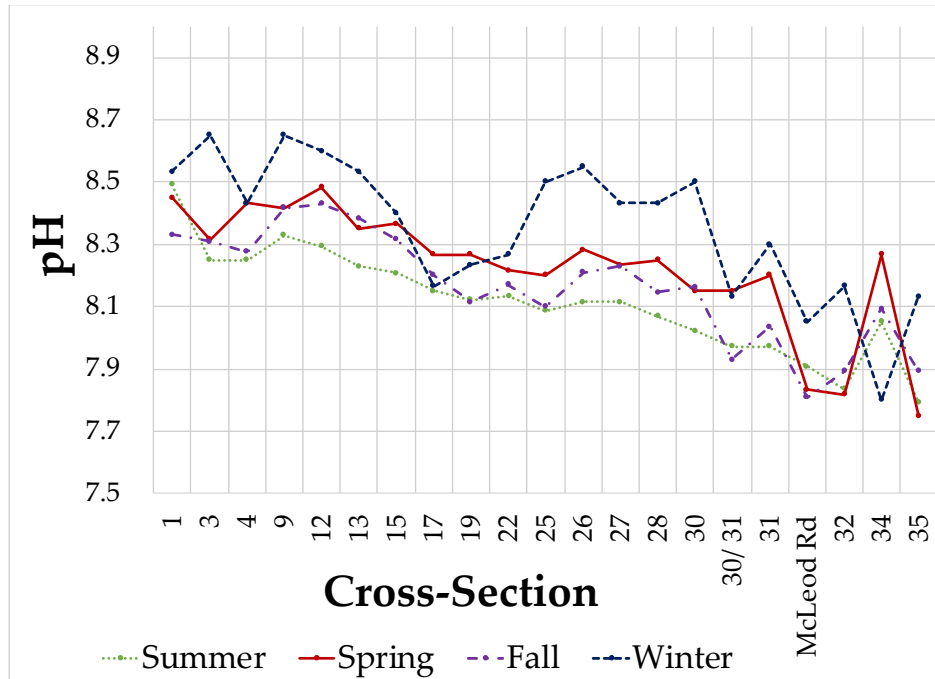


Figure 4.8. pH measurements averaged across seasons. The average for summer, fall, winter, and spring are plotted at each cross-section.

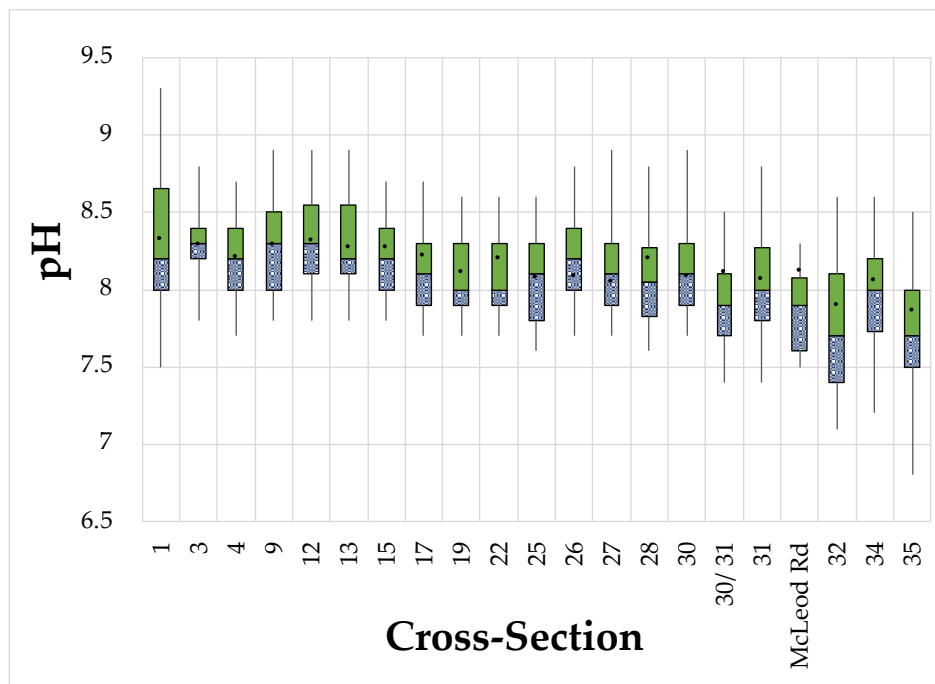


Figure 4.9. Box-plots of pH data illustrate the mean, median, interquartile range, and dispersion of measurements. Individual cross-section box-plots combine all data between 2015 and 2017. The range of pH values do not exceed the critical limits for aquatic life, livestock, and wildlife, thus are not likely a factor for fish survival.

4.1.2.3. Turbidity

Turbidity was highly variable across time without any consistent pattern throughout the year (Figure 4.10). When averaged across seasons, turbidity was largest in the spring and summer and smallest in the fall and winter (Figure 4.11). Spatial patterns are not evident in raw data (Figure 4.10) but there are some spatial differences when averaged seasonally (Figure 4.11). In general, turbidity increased downstream in the fall and summer but decreased downstream in the fall and winter. There is a spike in turbidity at XS 32 in spring, fall and winter. There are also spikes in the average turbidity at XS 15 is large in the winter and at XS 12 in the spring.

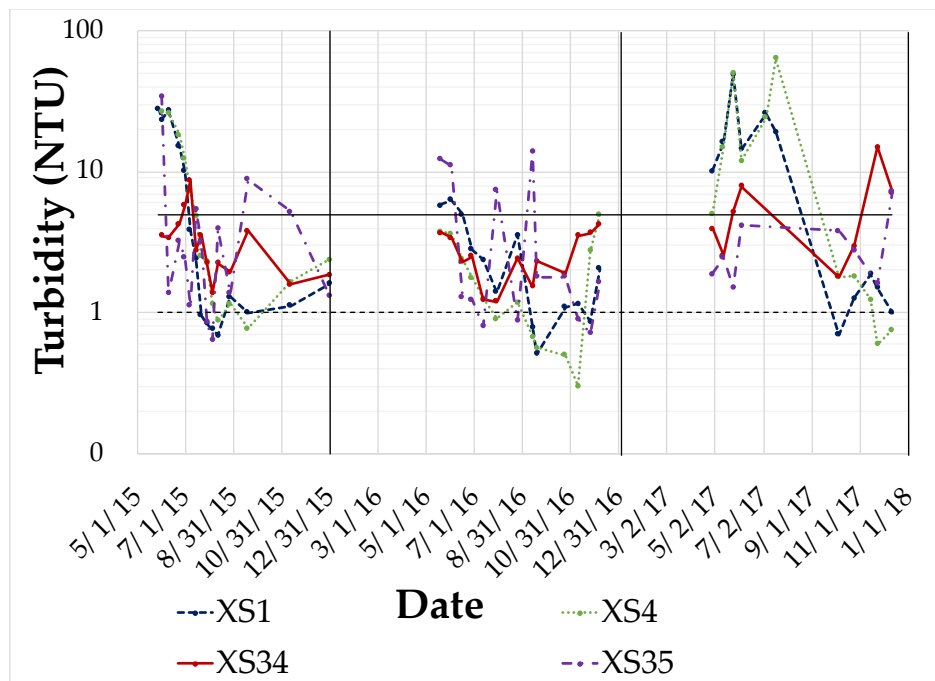


Figure 4.10. Raw data measurements of turbidity at XS 1, 4, 34, and 35 along Alderson Creek during 2015, 2016, and 2017 field seasons. The turbidity axis is logarithmic.

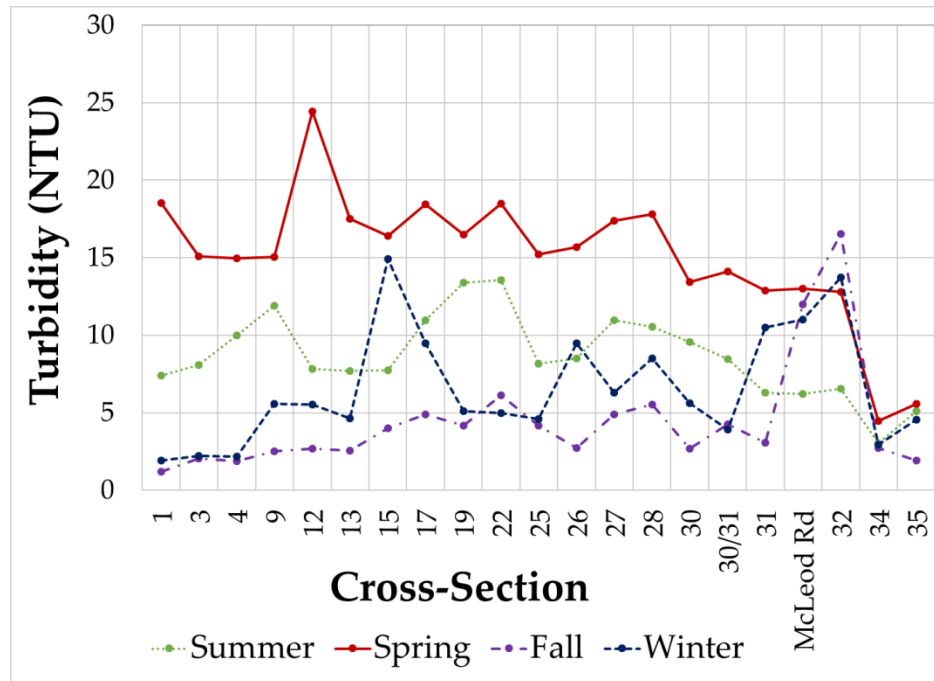


Figure 4.11. Turbidity measurements averaged across seasons. The average for summer, fall, winter, and spring are plotted at each cross-section.

Box-plots show that the turbidity ranges across time were similar at each sample site, with large dispersion (large whiskers) ranging from 0.3 – 88 NTU (Figure 4.12). Turbidity values were highly skewed with larger whiskers on the top of the boxes, demonstrating that the majority of turbidity measurements were generally quite small (0 – 4 NTU) despite being in excess of drinking water quality standards (see Figure 4.13). Histogram frequency distributions confirm that the data were noticeably positively skewed and that the most frequent turbidity measurement was between 2.5-3 NTU (above the boil water advisory of 1 NTU). A large number of measurements occurred between 1.5-4.5 NTU with decreasing frequency above 5 NTU (limitation for aquatic life) (Environment Canada 2008) (Figure 4.13). There were very few turbidity values above 30 NTU.

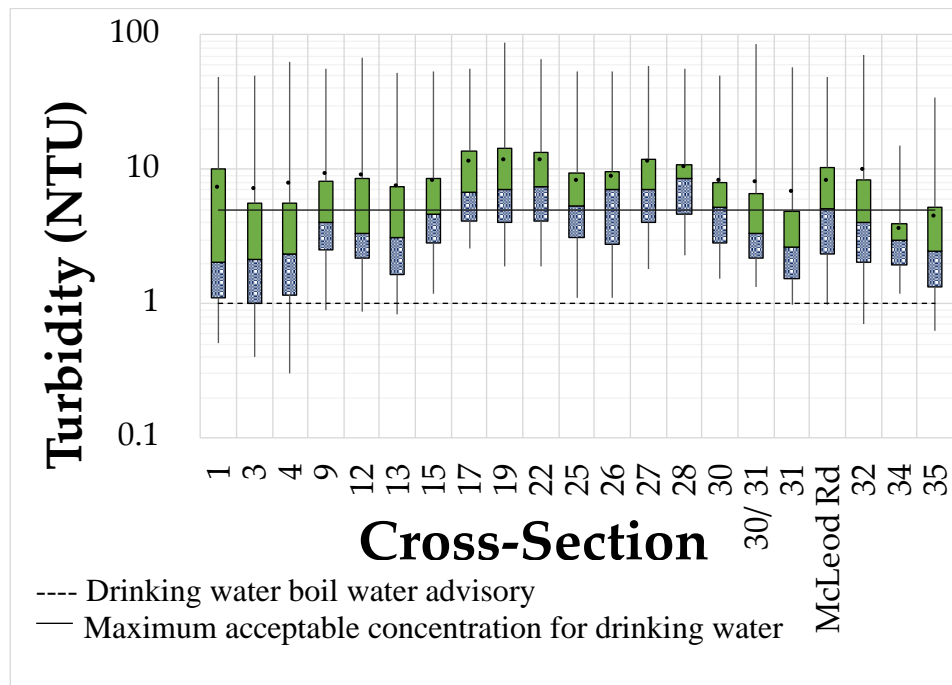


Figure 4.12. Box-plots of turbidity data illustrate the mean, median, interquartile range, and dispersion of measurements. Individual cross-section box-plots combine all data between 2015 and 2017. The limitation for drinking water of 5 NTU and boil water advisory of 1 NTU are shown as points of reference.

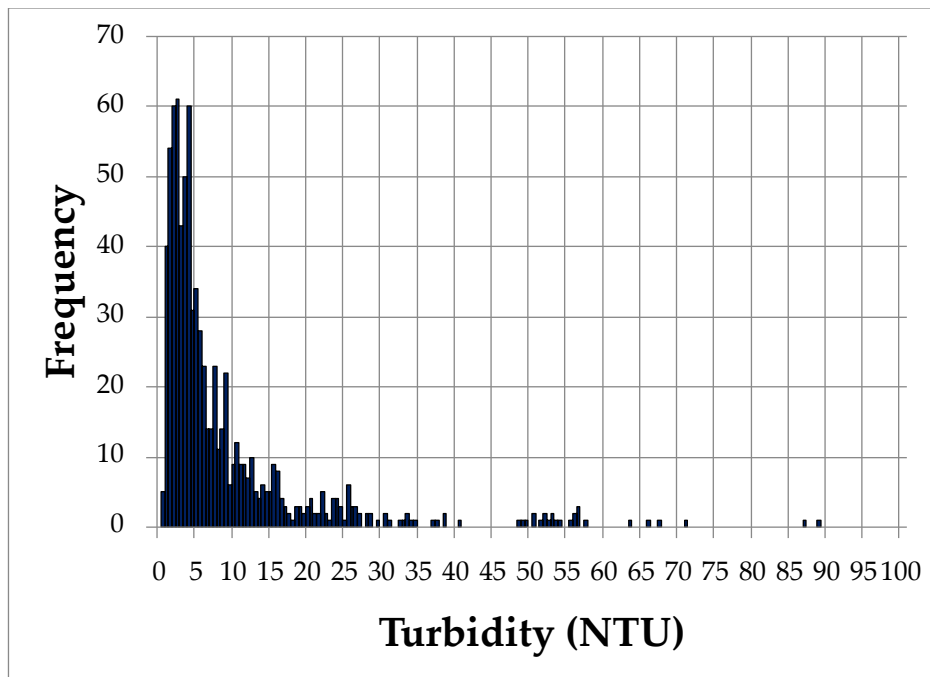


Figure 4.13. Frequency distribution of all turbidity measurements ($n = 799$) recorded between 2015 and 2017 along Alderson Creek. Bins are made up of a range of 0.5 NTU and labelled on the x-axis every five bins.

4.1.2.4. Dissolved Oxygen

At XS 1, 4, and 35, DO was relatively constant between May to December 2017 (Figure 4.14). This was similar for all cross-sections in most of the creek downstream of XS 31. Upstream, DO measurements became variable.

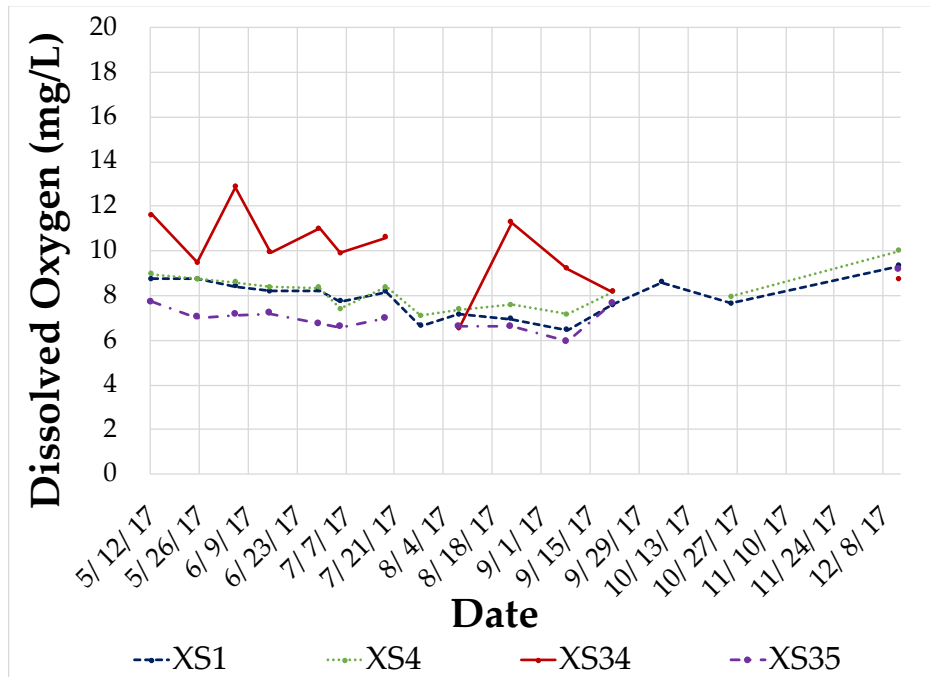


Figure 4.14. Raw data measurements of dissolved oxygen (mg/L) at XS 1, 4, 34, and 35 along Alderson Creek between May to December 2017.

The box-plots shown in Figure 4.15 showed the same spatial trend, with relatively constant DO values and ranges downstream of XS 31. Sample sites upstream from XS 31 were quite different from one another depending on stream morphology and land use. XS 31, for instance, had highly variable DO content with time because it was immediately below a location where a drainage ditch running alongside McLeod Road joins Alderson Creek. Alderson Creek receives most of its water from a groundwater source upstream of the road, but the ditch contributes water during the wet season. So XS 31 was influenced by the variable mixing proportions from the ditch water with Alderson Creek water. The water in the ditch comes from a small neighbourhood to the south-east of XS 31, and it loses flow in the summer and often dries up completely. The variable DO at McLeod Road sample site was also influenced by the flow cascading out of a corrugated culvert beneath McLeod Road, which leads to aeration. However, the culvert occasionally clogs,

limiting flow and oxygenation. XS 32 and XS 35, which are upstream of McLeod Road, had low DO content because of dense stands of watercress that extract oxygen from the stream during respiration (Goodwin et al. 2008). XS 34 had large DO because the water flowing out of the pond was aerated after cascading down and out of the culvert from the pond.

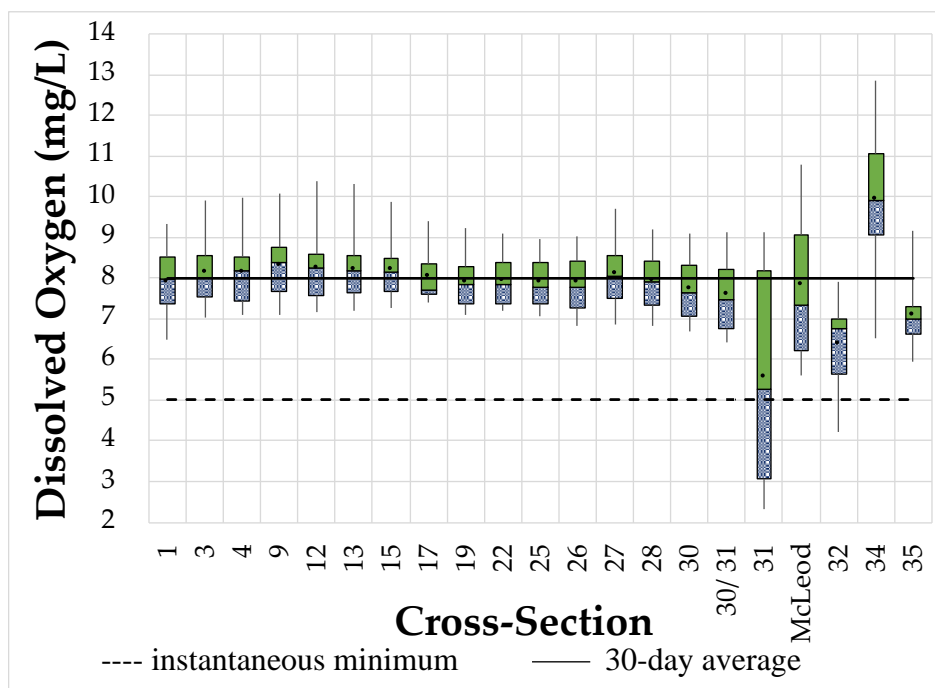


Figure 4.15. Dissolved oxygen measured in mg/L at each cross-section along Alderson Creek. All observations between May and December 2017 are included in individual box-plots. The instantaneous minimum of 5 mg/L and 30-day average of 8 mg/L required for aquatic life are shown as points of reference.

DO concentrations demonstrate that Alderson Creek did not contain a large amount of dissolved oxygen (Figure 4.15). XS 31, 32, and 34 experienced an average DO below the recommendation for aquatic life; XS 32 was particularly low with a maximum concentration below 8 mg/L even with the increase in DO concentration directly upstream at XS 34. This is likely due to the overgrowth of vegetation at XS 32 reducing DO in the water. Additionally, XS 31 and 32 experienced DO concentrations below the guideline for an instantaneous minimum of 5 mg/L. The small DO measurements are concerning for aquatic health.

DO is expected to maximize in late-afternoon and reach minimum before dawn when there is a switch in plant metabolism from photosynthesis to respiration. These trends were not confirmed

when DO was measured overnight at XS 9 (Figure 4.16), which saw minimum concentrations near sunset and maximum concentrations just after sunrise. A possible explanation is that the changes in DO concentration in Alderson Creek were simply an effect of temperature changes (DO increases with decreasing temperature), which is supported by the fact that DO saturation in Alderson Creek was nearly 100% for the 24 hours it was recorded. In Alderson creek, the diurnal range in DO at XS 9 was between 8-9 mg/L which meets the standard suitable for aquatic life (8 mg/L). However, a 1 mg/L diurnal fluctuation is likely modest as diurnal fluctuations in DO have reportedly ranged from 1 – 3 mg/L in other stream studies (Moraetis et al. 2010; Viswanathan et al. 2015).

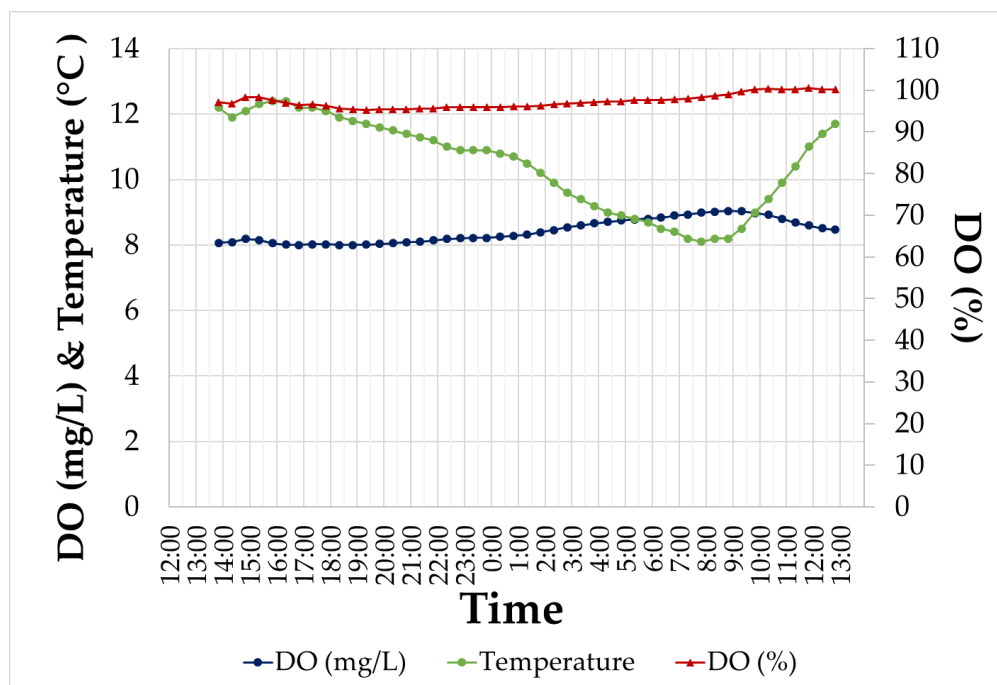


Figure 4.16. Dissolved oxygen and temperature recorded at 30-minute intervals using the HACH HQ40d DO probe, between 1:50 pm October 1st, 2017 and 12:20 pm October 2nd, 2017. DO meter was set up at XS9 along Alderson Creek. DO is shown as concentration (mg/L) and as percent saturation (%).

4.1.3. Nitrogen, Macrophytes, Macroinvertebrates

4.1.3.1. Nitrogen

Nitrogen concentrations at most sample sites increased from spring through the summer but leveled out in early fall through December (Figure 4.18). This seasonal dependency was evident

for XS 1, 13, 17, and 27 as shown by the seasonal averages (Figure 4.17) and by the raw data (Figure 4.18). Spring measurements were noticeably different from the other seasons, which were all basically the same (Figure 4.17). There may be nitrogen accumulating during the summer and fall, which carries into winter. The concentration of nitrogen in the creek becomes larger in the summer due to animal husbandry, fertilization practices, and reduced rainfall. When freshet happens, the nitrogen is largely flushed out of the creek when increased discharge causes dilution. It is of concern, however, that the nitrate concentrations were often above the guideline of 3 mg/L as a long-term average (Ministry of Environment 2018).

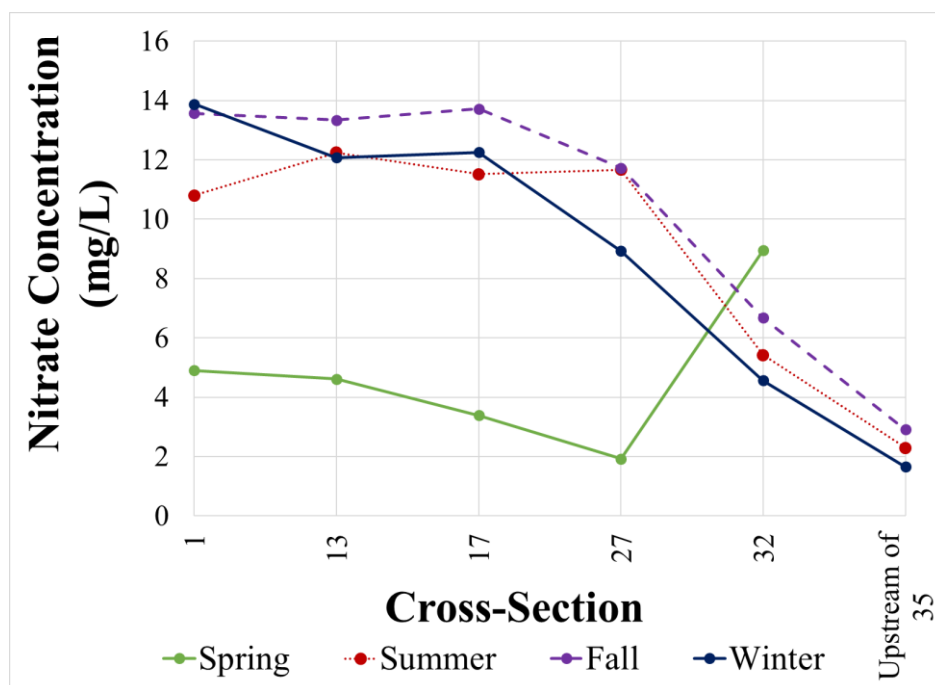


Figure 4.17. Nitrate concentration averaged across seasons. The average nitrate concentration in the summer, fall, winter, and spring is plotted for every cross-section that was sampled.

Nitrogen accumulation also occurs in the downstream direction (Figure 4.18). Nitrogen concentration at XS 32 and at the groundwater source upstream from XS 35 did not follow seasonal trends (Figure 4.18). The concentration at these two upstream sites was also typically less than at the other cross-sections, perhaps because contamination from livestock and fertilization had less of a cumulative impact relative to downstream sampling sites. Overall, then, nitrogen concentration increased downstream from the groundwater source at XS 35 to the mid-section of the creek (about XS 27 to XS 17) and then stabilized in the lower reaches between XS 13 and XS 1.

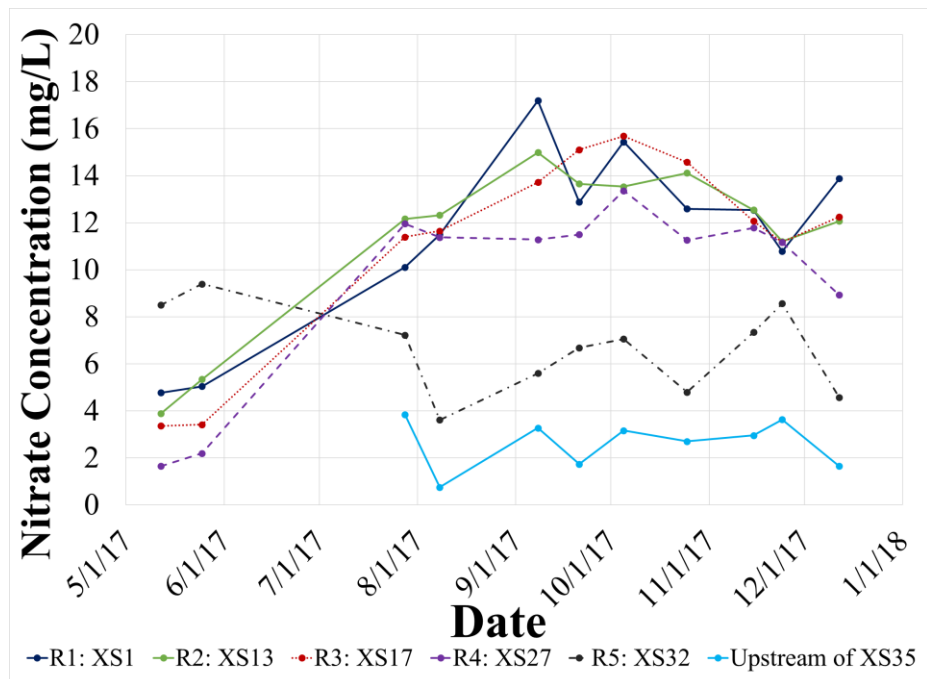


Figure 4.18. Raw nitrate concentrations between May and December 2017 at the cross-sections representing each sub-reach (R1-R5). XS 1, 13, 17, 27, and 32 were sampled to represent the flow out of R1, R2, R3, R4, and R5, respectively. The water upstream from XS 35 was sampled to represent the groundwater source.

4.1.3.2. Macrophyte Density

Macrophyte density increased from spring to late summer and decreased into winter. This was true for all sub-reaches (R1-R5), except R3 where macrophyte density decreased in July and August (Figure 4.19). Field notes refer to the banks at R3 as having been intensely degraded by cattle as they crossed the creek directly through the sample site. The sample site in R5 was often 100% overgrown by mid-summer, typically with watercress (*Nasturtium officinale*), resulting in large macrophyte density values compared to other sub-reaches. There was also an uncharacteristic reduction in macrophyte density in September at R5 due to excavation work in the creek at the end of August 2016. The R4 sample site was consistently less densely vegetated than all other sample sites. The vegetation cover at R4 consisted of tall scouring-rush (of the horsetail family, *Equisetum hyemale*), skunk cabbage (*Lysichiton americanus*), and jewelweed (*Impatiens capensis*), all of which are typical of mesic to hydric soils and found in moist forests or river banks (Crow 2000). The R4 site was considerably different than the others because it had

a closed canopy provided by large cottonwood trees. Very little sunshine makes it to the creek bed, so plants like watercress do not compete very well. In contrast, skunk cabbage and other broad-leaved plants can absorb enough sunlight to thrive because of their adaptive strategies (i.e., big leaf surface area).

Macrophyte densities in May, June, and July were quite variable (large interquartile ranges shown in Figure 4.19), indicating that macrophyte density can vary from year-to-year during these months. Small interquartile ranges and short whiskers in September, October and November indicate that macrophyte density was consistent year-to-year in these months presumably because most of the vegetation is dying through fall into winter.

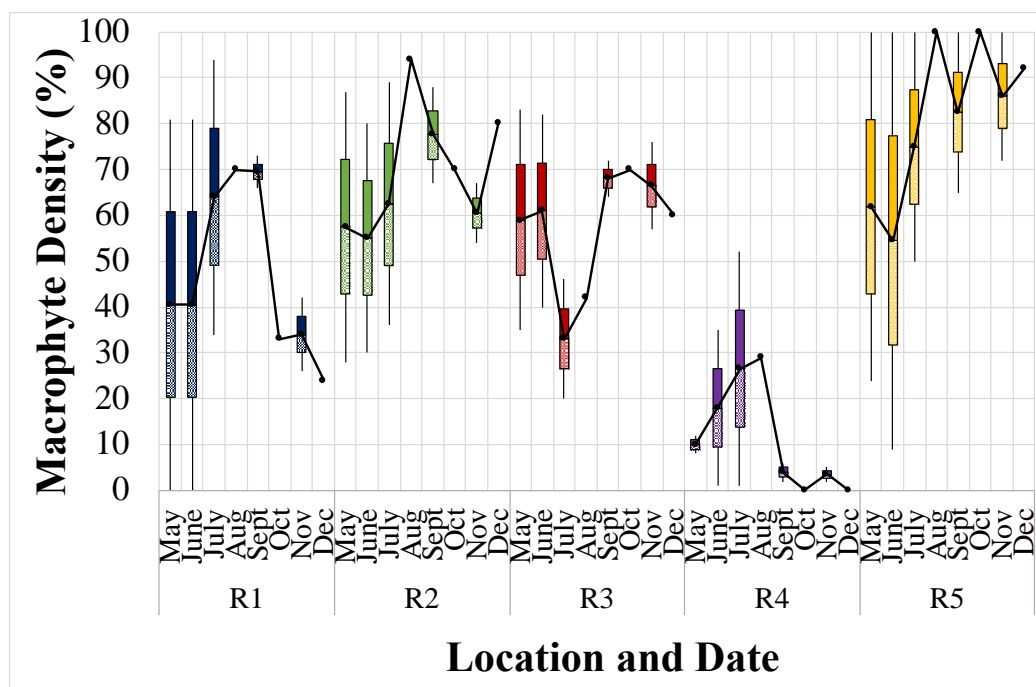


Figure 4.19. Maximum, minimum, mean, median and interquartile range of in-stream macrophyte density. Box-plots include measurements from 2015 to 2017 and demonstrate temporal trends from May to December as well as spatial trends (sub-reaches).

4.1.3.3. Macroinvertebrate Density

The abundance of total Ephemeroptera, Plecoptera, and Trichoptera in control baskets (Figure 4.20), in cumulative baskets (Figure 4.21), and in kick net samples (Figure 4.22) are shown in the form of box-plots. Note that individual box-plots for every month contain only three data points (i.e., total count for each of three years), and therefore the statistics were not reliable due

to the small sample number. However, the plots were revealing of spatial and temporal patterns. For example, the total number of EPT on almost all sample dates (and in most sub-reaches) were below 35 and typically in the 5-20 range. According to the EPT taxa richness index by Lenat (1988), these sites would be classified as 'poor' with several in the 'very poor' or 'gross disturbance' category.

Counts in the control and cumulative baskets demonstrate that R4 had the largest number of macroinvertebrates in every month. R1 contained more invertebrates than R2 whereas R3 had the second least abundance. R5 had no macroinvertebrates whatsoever in the baskets during the three years of data collection. Counts in the kick net samples were different from baskets. The most notable difference was how few invertebrates were found in R4 using kick net methods, and that the number of macroinvertebrates progressively decreased upstream. A veneer of fine-grained sand in R4 was not the favoured substrate type for macroinvertebrates, which was why the kick net approach yielded very few counts. In contrast, the artificial substrate baskets more closely mimic the 'preferred' substrate, and therefore served as 'attractors'. Macroinvertebrates occupied the baskets at R4 but did not reside in the sandy substrate at that site. Macroinvertebrates in a sub-reach, whether resident or transient, may therefore favor the substrate character in the baskets over the local stream substrate. The baskets at R5 were never occupied by invertebrates, despite having the same substrate material as other baskets placed at other sites. This suggests that there were no invertebrates resident in the stream at this location. A small number of macroinvertebrates were found in the kick net samples at R5, however, these were only found after an in-stream excavation and fencing project was conducted along the banks in 2017 which disturbed the entire reach. It is possible that macroinvertebrates were seeking refuge wherever possible at that time.

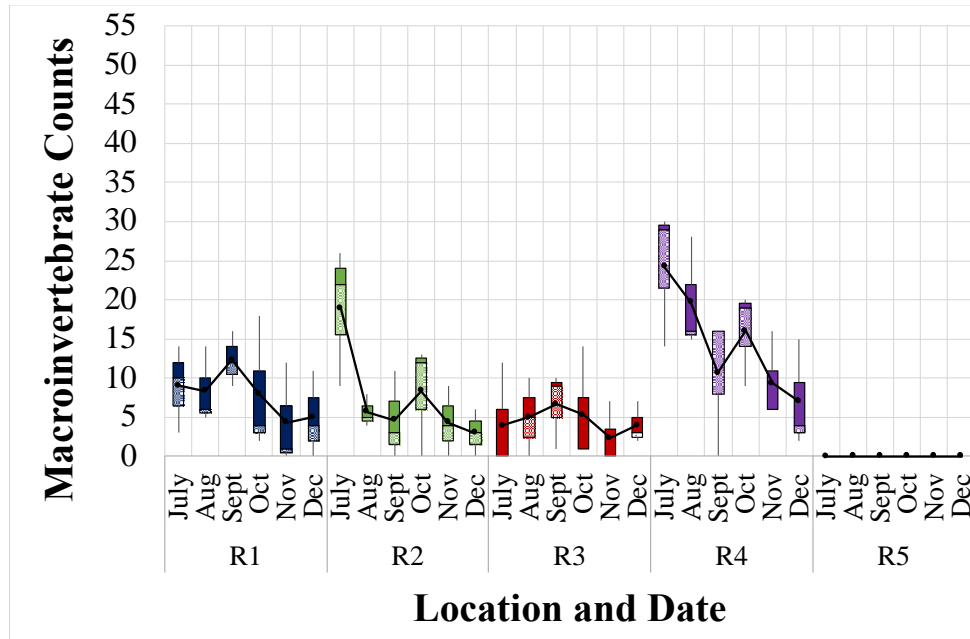


Figure 4.20. Maximum, minimum, mean, median and interquartile range of the total EPT counted in the **control** baskets from 2015-2017. Individual box-plots represent the counts each month at the five sub-reach sample sites (R1-R5).

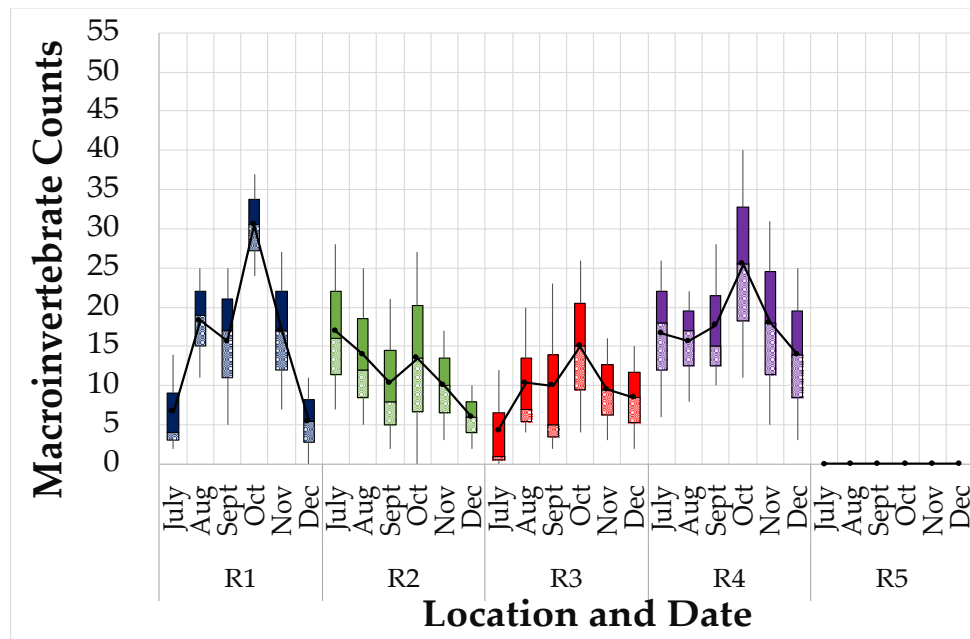


Figure 4.21. Maximum, minimum, mean, median and interquartile range of the total EPT counted in the **cumulative** baskets from 2015-2017. Baskets collected samples for 1 month (July) progressively up to 6 months (December). Individual box-plots represent the counts each month at the five sub-reach sample sites (R1-R5).

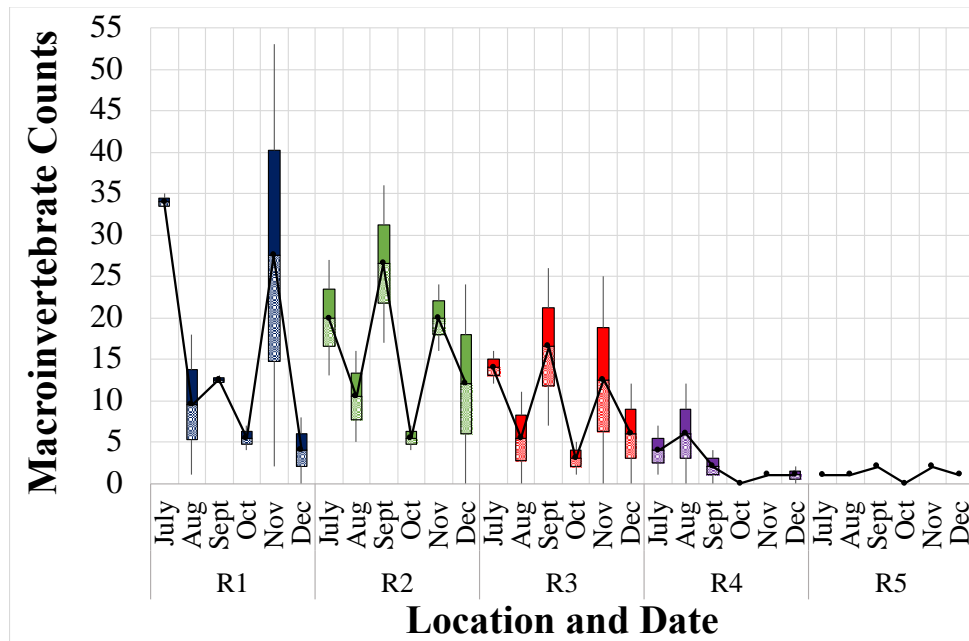


Figure 4.22. Maximum, minimum, mean, median and interquartile range of the total EPT counted in the **kick net** samples from 2015-2017. Individual box-plots represent the counts each month at the five sub-reach sample sites (R1-R5).

Macroinvertebrate abundance from month-to-month is affected by the life cycle of each of the different orders of macroinvertebrate (Ephemeroptera, Plecoptera, and Trichoptera) as well as by the influence of environmental factors (e.g., sensitivity to pH or dissolved oxygen) and habitat characteristics (e.g., substrate type). Two main conclusions can be drawn from a comparison of the number of each type of macroinvertebrate found in the cumulative baskets (Figure 4.23). The first is that the conditions of Alderson Creek, overall, are not favourable for aquatic life in terms of water quality, and as a consequence there were very small numbers of macroinvertebrates recovered in each sample. The second is that there is a self-selection of the more tolerant species and there are some order-specific spatial trends in the system. Typically, Ephemeroptera are less tolerant to degraded water quality and prefer cleaner water (Lenat 1988). They have been found to be less prevalent than Plecoptera and Trichoptera in agricultural sites (Lenat 1988). The largest number of these sensitive species were found in R4, which tends to have the best water quality of all sub-reaches on Alderson Creek. Trichoptera, although classified as intolerant to toxicity, have a larger tolerance range than Ephemeroptera and Plecoptera (Lenat 1988). Trichoptera were more abundant than Ephemeroptera and Plecoptera in most sub-reaches, except for R3 and R5, which are arguably the two sub-reaches that exhibit the poorest water quality.

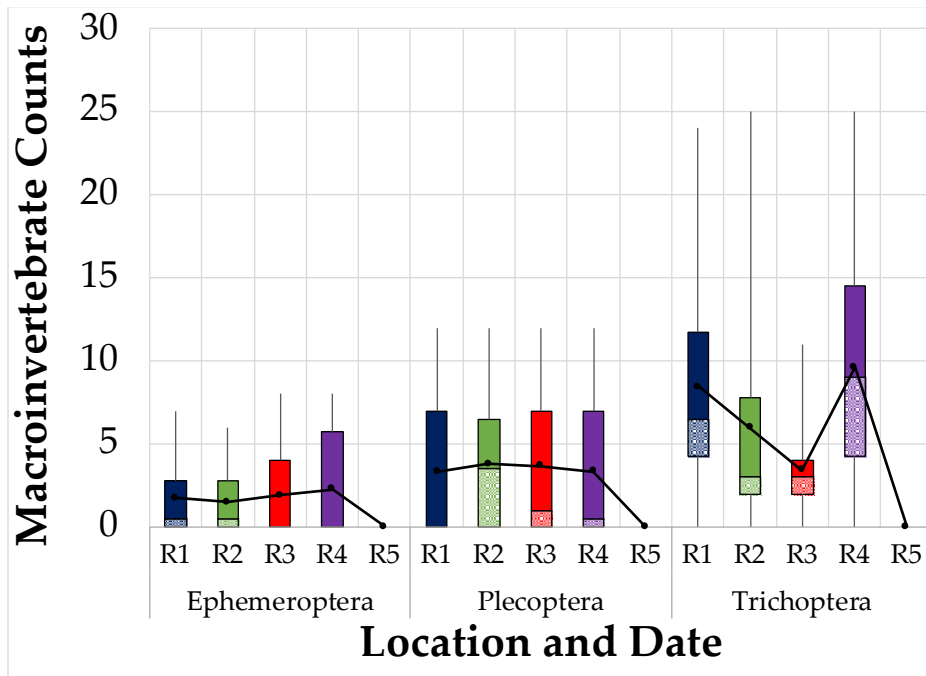


Figure 4.23. Range of total individual invertebrate species, Ephemeroptera, Plecoptera, and Trichoptera counted at each sample site, in cumulative baskets, from 2015-2017.

4.2. Sub-Reach Differentiation

In order to determine whether there was spatial variability in the water quality parameters, to support the notion that sub-reaches could be identified in Alderson Creek, a series of box-plots were constructed that lumped together observations from adjacent cross-sections that are within individual sub-reaches (Figure 4.24). For example, all observations of one parameter such as pH from XS 1 to XS 12 between 2015-2017 were aggregated as being representative of R1 (Table 3.2). In this way, the distinctions between sub-reaches rather than individual cross-sections or sampling sites might become evident.

Conductivity increased in the downstream direction, which was most pronounced in the upper three sub-reaches. The interquartile ranges did not overlap between R5, R4, and R3, suggesting that they were distinctly different. Differences between R3, R2, and R1 were not as distinct. With regard to pH, there appears to be a slightly increasing trend in the downstream direction that was, again, most evident in the upper reaches. But the interquartile ranges overlap, suggesting that neighbouring sub-reaches were not different as regards pH. Turbidity increased downstream from R5 to R3, at which point it decreased towards R1. Large interquartile ranges

and extended whiskers overlapped at each sub-reach suggesting turbidity is not a good differentiator. The same was true of the temperature data, where interquartile ranges and long whiskers were very similar for each sub-reach. Thus, the variability within each sub-reach exceeds the differences among sub-reaches. R5 tended to be slightly warmer than other sub-reaches likely due to XS 34 being at the outlet of a large pond and influencing the results for this sub-reach. Temperatures within R5 were highly variable, whereas R3 temperatures were steadier. Dissolved oxygen was relatively consistent between R1, R2, and R3. R4 and R5 had individual sample sites with very large DO and other sample sites with very small DO, which yielded large spread in the data for these two sub-reaches. Nevertheless, the averages and medians were similar to other sub-reaches. Nitrogen increased from a minimum at the groundwater source upstream (R5) to the middle sub-reach (R3) where it stabilized in the downstream direction. A large increase was observed from R5 to R4 (no overlap between boxes) but not as much of a difference can be seen between R4 to R3. The largest concentrations were observed in R3, though. Because there was little overlap between measurements in the upper reaches, nitrogen may be a useful parameter for discriminating sub-reaches.

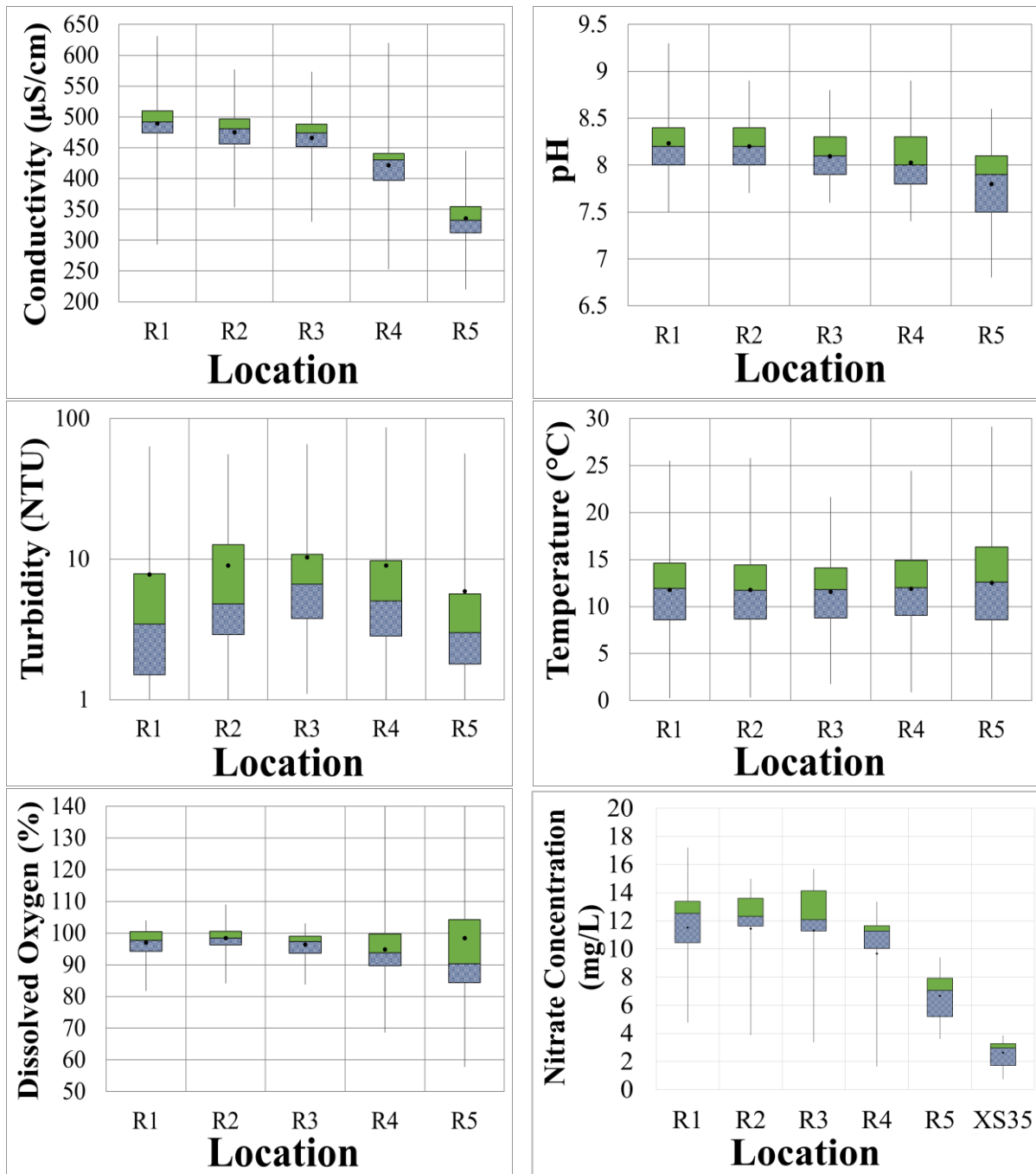


Figure 4.24. Maximum, minimum, mean, median and interquartile range of conductivity, pH, turbidity, temperature, dissolved oxygen, and nitrate concentration. All measurements taken between 2015 and 2017 at all cross-sections within each sub-reach are included.

The average and median macroinvertebrate counts for each sub-reach are shown in Figure 4.25 for control basket, cumulative basket, and kick net data. Macroinvertebrate counts may be useful to differentiate between sub-reaches; however, the ranges of macroinvertebrate abundances

overlap across several of the sub-reaches. This overlap was also seen in the in-stream macrophyte density box-plots (Figure 4.26). In both the macrophyte and macroinvertebrate sub-reach box-plots there were noticeable differences between R5 and R4. R5 exhibited very dense macrophyte growth and hardly any macroinvertebrates, whereas R4 exhibited very sparse macrophyte growth and the most macroinvertebrates. R4 had natural riparian cover in the form of a large cottonwood stand in the upper sections and was bounded by a field used for forage crop production in the lower section. Therefore, the creek was not modified by livestock trampling or bank reworking, and it showed natural riparian characteristics. R5 was intensely grazed by cattle and had no riparian cover. R3 was also used for cattle grazing but not to the same intensity. It had the second largest percentage of vegetation cover and second least macroinvertebrate abundances. R2 was not generally used for grazing, but cattle were put to pasture on this small stretch of property for short periods of time when the main pasture was depleted. R2 had macrophyte density and macroinvertebrate abundances between that of R1 and R3.

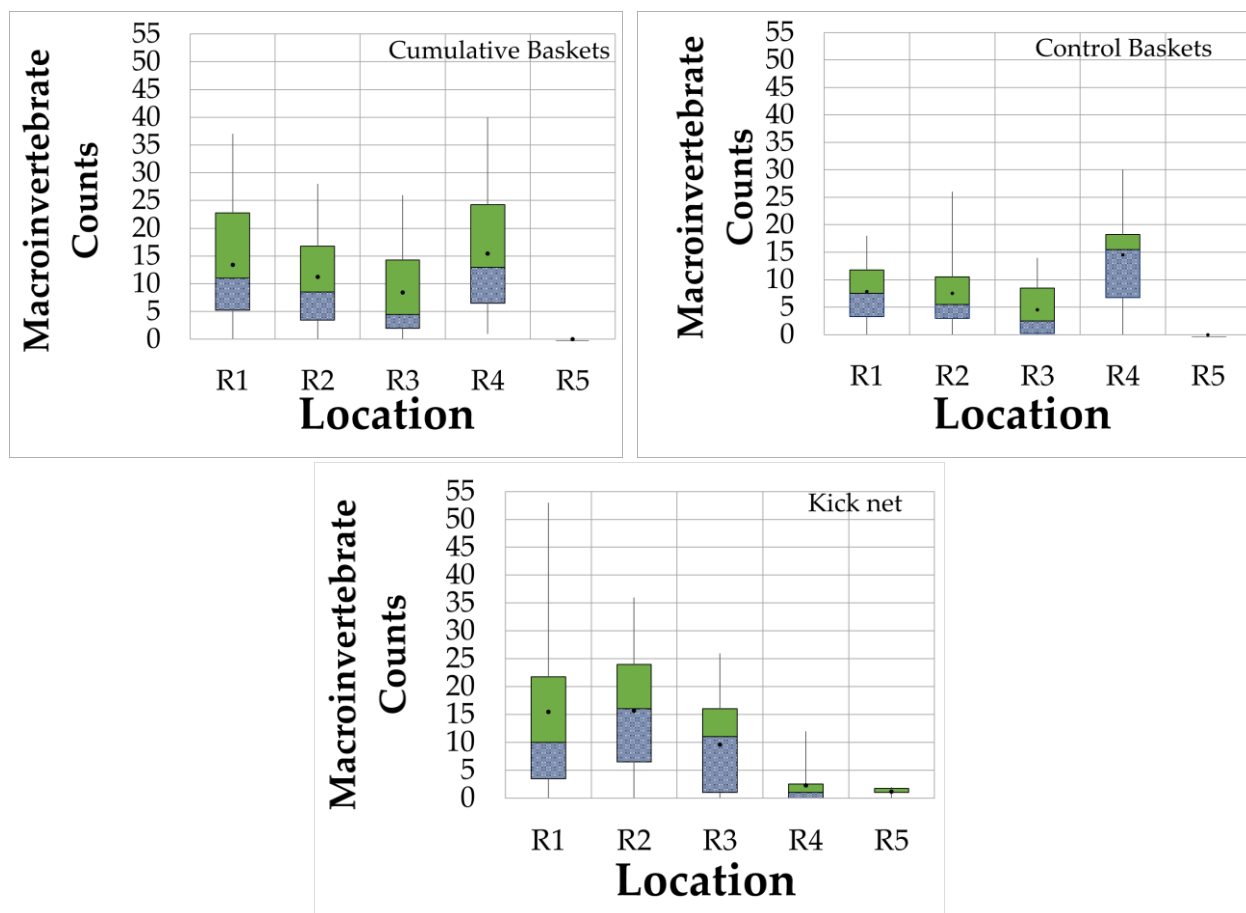


Figure 4.25. Maximum, minimum, mean, median and interquartile range of number of macroinvertebrates counted in each sub-reach. Macroinvertebrate counts are plotted for the cumulative basket and control basket methods and the kick net samples. Box-plots include the number of macroinvertebrates counted in each sample (once a month) for all three field seasons.

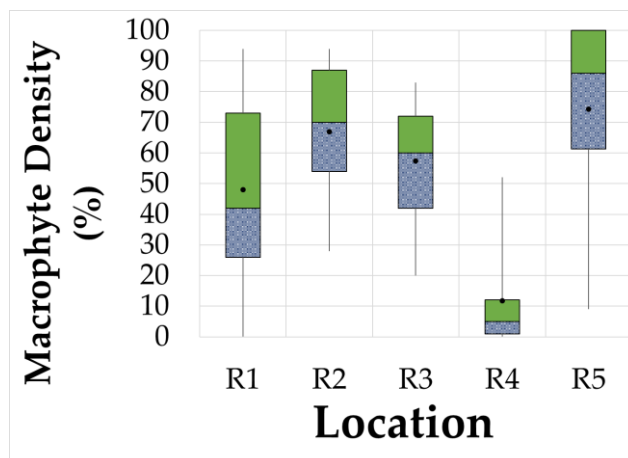


Figure 4.26. Maximum, minimum, mean, median, and interquartile range of number of macrophyte density observed in each sub-reach. Box-plots include the percent macrophyte density observed in a 1 m² quadrat for all three field seasons (measured once a month).

4.3. Discriminant Analysis

Overall, the data indicate that there is considerable spatial and temporal variability in stream characteristics and water quality parameters along Alderson Creek. There was some evidence in support of sub-reach clustering of the data, especially with regard to the differences between R5, R4, and the remainder of the sub-reaches (R3, R2, and R1) Linear discriminant analysis is used in this section to determine whether the sub-reaches can be differentiated in a statistically significant manner. In undertaking this analysis, no preconceptions of sub-reach delineation were assumed. The intent of the analysis was to identify sub-reach membership based on statistical similarities and differences using the many parameters collected during the study period.

Prior to undertaking the statistical analysis, a choice needed to be made as to whether the data from the temperature pendants or the handheld probes should be used. The pendants provided semi-continuous data, but they weren't positioned at the same locations as where the manual samples of turbidity, pH, conductivity, and DO were taken. Since discriminant analysis requires that the data be sampled at similar times and locations, there was the need to demonstrate that the two temperature data sets provided the same results. A comparison of stream temperatures measured by pendants (at 10 – 15 minute intervals) and by handheld probes (at 7-10 day intervals) was undertaken, and it demonstrated that both methods recorded similar temperatures at all sampling sites. Figure 4.27 shows examples from XS 4 and XS 30 because both methods were used simultaneously at these locations. Given that the temperatures recorded by the handheld probes were similar to temperatures recorded by pendants and noting that more sampling sites with the other water quality parameters could be included when using the handheld probe data, it was decided to use the handheld data for the DA.

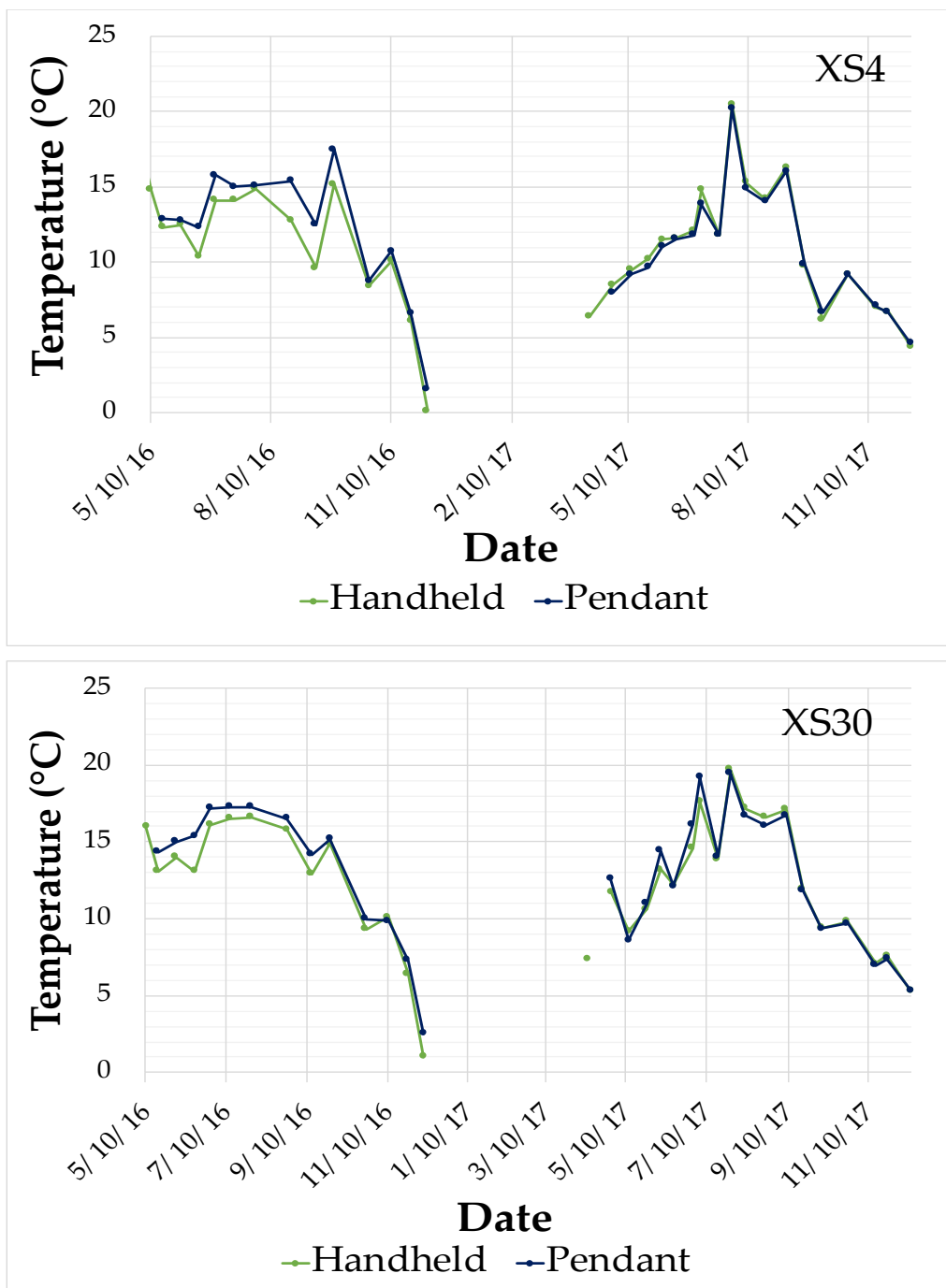


Figure 4.27. Comparison of stream temperature when manually measured with handheld probes (Oakton PCTestr35) and from in-stream temperature pendants at XS 4 (top) and XS 30 (bottom).

The first discriminant analysis was performed with pH, turbidity, temperature, and conductivity. This example serves only to demonstrate how the results from such an analysis can be interpreted for the purpose of identifying clustering in the data set. Additional analyses with

different variable combinations were performed to assess which variables were best at discriminating between stream sub-reaches, and these results will be discussed later. Prior to discriminant analysis, all data were normalized with standardized residuals, which is comparable to a z-score (Ware et al. 2013). Discriminant analysis results are given in the form of a significance level for the discriminant functions, the degree of association of the discriminator variables with the discriminant functions, and potential group identification based on group centroids. The quantitative results are summarized in two tables as well as a discriminant function plot. Note that the "groups" in this analysis (terminology that is specific to discriminant analysis) are the sampling sites where field measurements were taken. Thus, the intent is to discriminate among sampling sites (i.e., "groups") and to determine whether some of them cluster together based on similar data trends. Whether sample sites demonstrate clustering will be determined from the discriminant function plot and not be assumed a priori. And based on the nature of clustering, it may be possible to identify spatially contiguous sampling sites that represent distinct stream sub-reaches. Variables are deemed useful at differentiating between sub-reaches if there is little to no overlap in the scores.

The significance of the discriminant function must be determined from the summary of canonical discriminant functions (Table 4.1). There can be up to $n-1$ discriminant functions where n is the number of grouping variables (e.g., sample sites), with each discriminant function explaining progressively more of the variance in the data. The percent of variance (%) is a measure of the variation in the data that is explained by the discriminant function. Ideally, only the first two functions explain most of the variance (i.e., in excess of 70%), which simplifies the interpretation. Eigenvalues are used to calculate the percent of variance, and they are the ratio of between-group variability to within-group variability. A large eigenvalue means that the discriminator variables (i.e., real parameters) that 'load' on that function are better at accounting for group differences. Canonical correlation is the amount of group variability captured by the function, with a large canonical correlation indicating greater importance of that function. Wilks' lambda (between 0-1) is a ratio of within-group variability to total variability wherein a smaller Wilks' lambda indicates that variability in the discriminator variables is due to group differences. Finally, the significance indicates whether the function is statistically significant at the 0.05 level at differentiating between groups (Brown and Wicker 2000). In the example below, functions 1,

2 and 3 explain 99.5% of the variance between groups, and all three functions are significant ($p < 0.05$) at differentiating between groups (sample sites). Function 1 clearly dominates, and it explains 81.5% of the variance among groups. Function 2 adds another 13.1% of explanation, and the remaining functions are largely irrelevant because they offer little added statistical explanation (i.e., function 4 in this instance explains less than 1% of the variance).

Table 4.1. A summary of canonical discriminant functions based on variances in pH, turbidity, conductivity, and temperature to differentiate between sub-reaches along Alderson Creek.

	Eigenvalue	% of Variance (Cumulative %)	Canonical Correlation	Wilks' Lambda	Sig.
Function 1	2.879	81.5	0.862	0.148	0.000
Function 2	0.462	13.1 (94.6)	0.562	0.573	0.000
Function 3	0.171	4.8 (99.5)	0.382	0.838	0.039
Function 4	0.019	0.5 (100)	0.136	0.981	0.998

The association of discriminator variables with the functions are given in Table 4.2. The absolute magnitude of the standardized canonical discriminant function coefficients indicates the importance of and the degree to which each discriminator variable is associated with differences among the groups, and the sign indicates the direction of the relation (Brown and Wicker 2000). The larger the absolute value of the standardized canonical discriminant function coefficient, the better the discriminant variable is at differentiating between groups. In this example, conductivity played an important role in group discrimination within discriminant function 1, and pH played an important role within discriminant function 2 (because they have the largest standardized canonical discriminant function coefficients). Since these variables appeared strongly in one function but not the other, the implication is that conductivity and pH discriminate group membership in different ways (i.e., the two discriminant functions are orthogonal and therefore uncorrelated). Temperature was the next relevant variable, and it appeared in both discriminant functions but with negative values, which indicated that temperature explained variation among the group structures in an opposite direction as conductivity and pH.

Table 4.2. Standardized canonical discriminant function coefficients for pH, turbidity, conductivity, and temperature discriminant variables for each discriminant function. The sign (+/-) indicates the direction of the relationship and the asterisk indicates largest loading on that function.

	Function 1	Function 2	Function 3	Function 4
pH	-0.240	0.810*	0.670*	0.035
Conductivity	1.009*	0.053	0.412	-0.126
Turbidity	-0.183	0.334	0.059	1.034*
Temperature	-0.577	-0.610	0.648	0.054

Group differentiation is summarized by the group centroid scores and casewise results, which are visually represented in the discriminant function plot (Figure 4.28). The centroid is the mean discriminant function coefficient, plotted as large circles, calculated by inserting the mean of each discriminant variable into the discriminant function. Differences in the locations of group centroids show how well, and the dimensions along which, the groups differ. The casewise results are the scores for each observation in time, plotted as small circles (compared to group centroids as large circles). Casewise results are calculated by inserting the raw parameter values (in standardized form) into the linear discriminant function equations. For example, the standardized residuals of pH, temperature, conductivity, and turbidity at time 1 would be inserted into the discriminant function equations to obtain the x,y (F1₁, F2₁) coordinates for that sampling period. As with group centroids, clustering of the casewise results with little overlap would be indicative of sub-reach differentiation. The centroid and casewise results shown in Figure 4.28 demonstrate the raw output in a DA but for simplicity, remaining discriminant function plots will only show centroids.

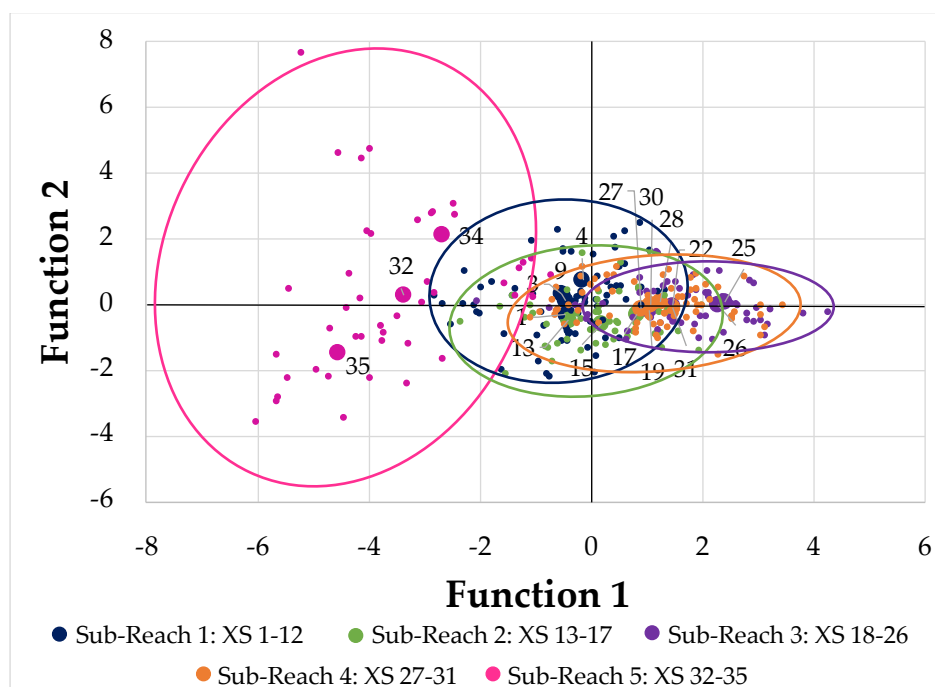


Figure 4.28. Centroids for each sampling site (i.e., cross section) on a combined-group plot. Discriminant functions maximize the variance between sampling sites based on the summer pH, turbidity, temperature, and conductivity observations along Alderson Creek.

Figure 4.28 shows that there was considerable spread between sample sites along function 1 with XS 32, 34, and 35 positioned to the far left. These three sites were quite separate from the other sampling sites. For the purposes of these diagrams, each of the sample sites has been colour-coded according to which sub-reach it is thought to be a member of, based on the qualitative assessment described earlier. This is simply a visual aid for purposes of assessing potential clustering, and it is not part of the formal discriminant analysis. The R5 sites (XS 32, 34, 35) are coded in pink, and they are distinctly different. The R3 sites (purple) and R4 sites (orange) are positioned on the far right of function 1, showing only minimal overlap with the R2 (green) and R1 (dark blue) sites, which are centrally located on the diagram. The horizontal spread along the function 1 axis suggests that conductivity, which was the dominant variable in function 1 (see Table 4.2), is a significant explanatory parameter for distinguishing among sites. A similar pattern was evident in the box-plots of conductivity for all the cross-sections along Alderson Creek (Figure 4.6) with a distinct increase in conductivity in the downstream direction.

A second discriminant analysis was performed without conductivity as a variable so as to determine whether the remaining variables (pH, turbidity, temperature) were effective for cluster

identification (Figure 4.29). The orientation of the resulting diagram differs from the first analysis because the new functions have different combinations of variables with different loadings (Table 4.3). Temperature and pH now have the largest loadings on function 1 and these are oriented in the positive direction.

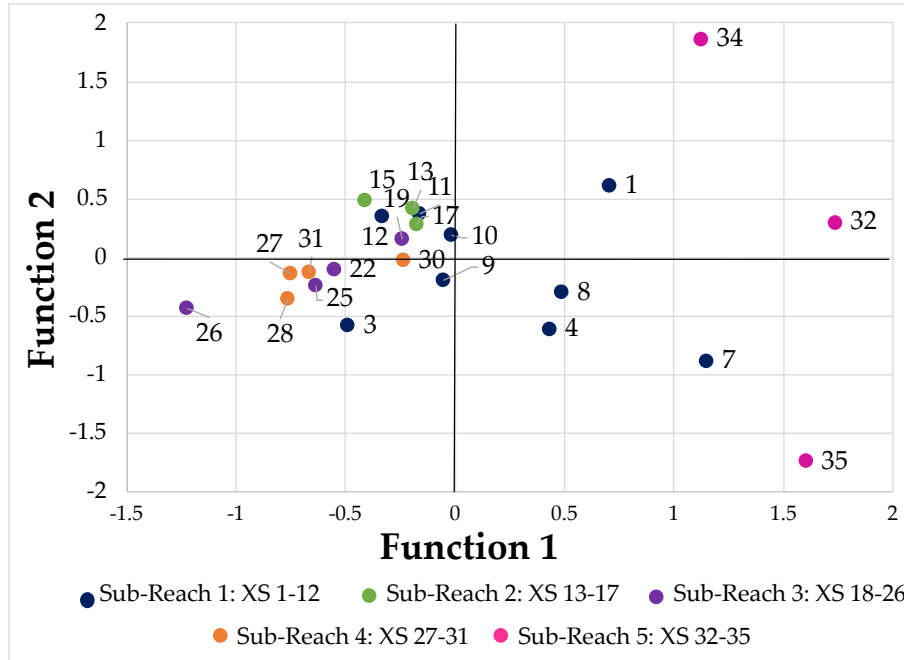


Figure 4.29. Centroids for each sampling site (i.e., cross section) on a combined-group plot. Discriminant functions maximize the variance between cross-sections based on the summer pH, turbidity, and temperature observations along Alderson Creek.

Table 4.3. Loadings of each parameter on the respective functions, shown for the analysis that included pH, temperature, and turbidity. The larger the loading, the stronger the correlation between the variable and the discriminant function. The sign (+/-) indicates the direction of the relationship and the * indicates largest loading on that function.

	Function 1	Function 2
pH	0.871*	-0.449
Temperature	0.38	0.881*
Turbidity	-0.231	-0.078

Once again, the sample sites in R5 stand out from the rest (according to function 1), and there continues to be a small degree of clustering of the other sites. For example, R2 (green) was different from R4 (orange), which were both different from R5 (pink). The sites in R1 (dark blue) and R3 (purple) did not cluster and were spread along the axis of function 1 and were

intermingled across function 2. Although XS 34 and 35 were both members of the R5 sub-reach, they were distinctly different in terms of function 2. As mentioned previously, XS 35 was positioned immediately below a groundwater spring at the most upstream location along Alderson Creek. XS 34 was the next sampling site downstream, so it was spatially contiguous, but it was below a large livestock watering pond which acted as a heat sink in the summertime. Thus, the water quality in XS 34 was different than in XS 35, and function 2 highlighted those differences (driven mostly by temperature). Overall, function 2 did not allow for effective sub-reach differentiation in this (or the previous) analysis. Thus, the dominant discriminating variables in this data set appear to be conductivity and pH, which is broadly consistent with the qualitative interpretation of the data represented in the box-plots.

The distinction between R5 and the other sub-reaches becomes readily apparent when dissolved oxygen was included as a discriminating variable (Figure 4.30). Here, the clustering of sub-reaches was noticeable, and there appears to be good alignment with the proposed sub-reaches, except for individual outliers. Sub-reach differentiation along Alderson Creek is therefore explained in terms of trends in conductivity, as loaded on function 1 and in dissolved oxygen as loaded on function 2 (R5 farthest from R3 and R4) (Table 4.4).

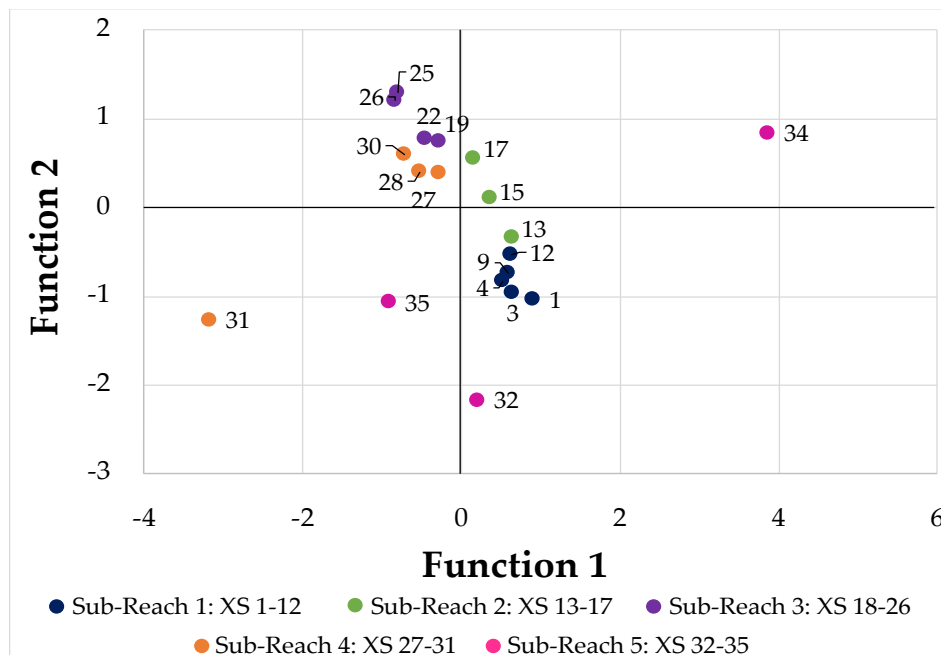


Figure 4.30. Centroids for each sampling site (i.e., cross section) on a combined-group plot. Discriminant functions maximize the variance between cross-sections based on the summer dissolved oxygen, pH, temperature, and conductivity observations along Alderson Creek.

Table 4.4. Loadings of each parameter on the respective functions, shown for the analysis that included pH, temperature, conductivity, and DO. The larger the loading, the stronger the correlation between the variable and the discriminant function. The sign (+/-) indicates the direction of the relationship and the asterisk indicates largest loading on that function.

	Function 1	Function 2
Conductivity	0.768*	-0.154
DO	0.204	0.905*
Temperature	-0.148	0.229
pH	-0.157	-0.027

The clustering of the proposed sub-reaches was also evident when analyses were performed that include macrophyte density (Figure 4.31) and total number of EPT (Figure 4.32) as discriminating variables. However, these analyses differ from those above because macrophyte density and macroinvertebrate samples were measured at only 5 cross-sections, but at multiple times throughout the year. Each of the five sub-reaches is represented by a series of points that represent the sampling periods rather than different geographic locations. This approach requires an a priori assumption to be made about sub-reach membership, and the analysis is intended to show whether the sub-reaches are distinctly different in terms of the data points appearing in different sections of the diagram. The casewise results are included in these plots to provide a better indication of sub-reach differentiation (i.e., clusters have little to no overlap).

Recall that macrophyte density box-plots indicated that R5 and R4 were different from each other and distinctly different from all other sites (Figure 4.25). Figure 4.31 and Table 4.5 indicate that R5 was farthest from R3 and R4, as before, and this was due to function 1, which was heavily loaded by conductivity. R1 and R2 were distinct from R3, R4, and R5 with respect to function 2, driven by pH. Although macrophyte density influences how observations cluster on the plot, it didn't have the largest loadings onto functions nor did it contribute to the functions discriminating ability.

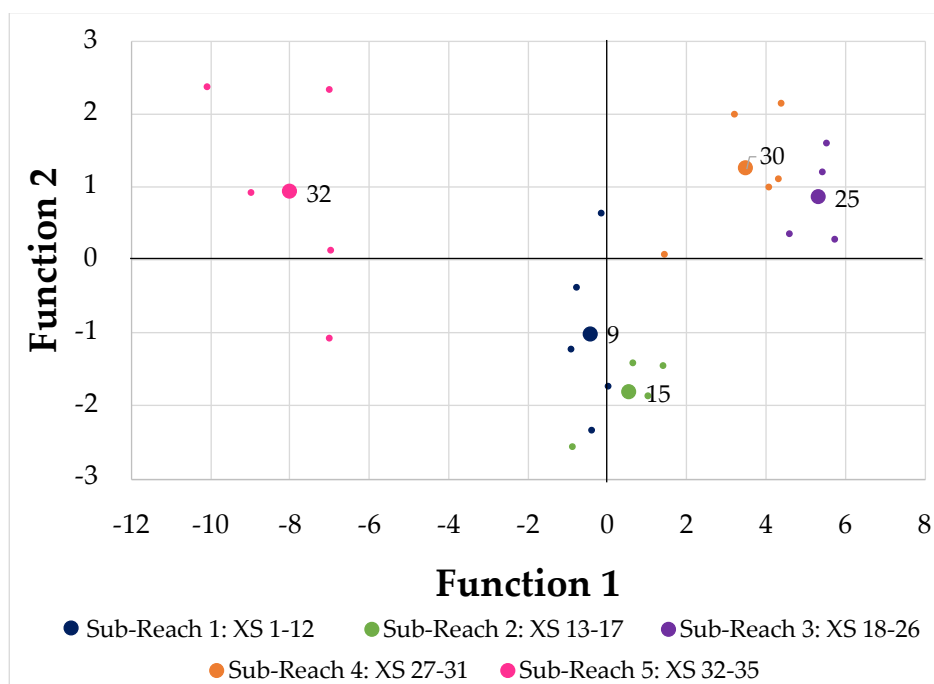


Figure 4.31. Centroids and casewise results for each sampling site (i.e., cross section) on a combined-group plot. Discriminant functions maximize the variance between cross-sections based on the summer macrophyte density, pH, temperature, and conductivity observations along Alderson Creek. Large circles represent XS centroids and small circles represent casewise results.

Table 4.5. Loadings of each parameter on the respective functions, shown for the analysis that included pH, temperature, conductivity, and macrophyte density. The larger the loading, the stronger the correlation between the variable and the discriminant function. The sign (+/-) indicates the direction of the relationship and the asterisk indicates largest loading on that function.

	Function 1	Function 2
Conductivity	0.737*	0.498
pH	-0.302	0.727*
Temperature	-0.155	-0.221
Macrophyte Density	0.115	0.15

In a similar analysis involving macroinvertebrate abundance in addition to pH, temperature, and turbidity, R5 was again distinct from all other sub-reaches. R4 was opposite to R5 along function 1, whereas R1, R2, and R3 were positioned in the middle of the plot (Figure 4.32). With the exception of turbidity, all parameters, including macroinvertebrate abundance, contributed to group differentiation. The variance explained by function 1 was driven by macroinvertebrate counts for both basket methods whereas the variance explained by function 2 was driven by temperature (Table 4.6).

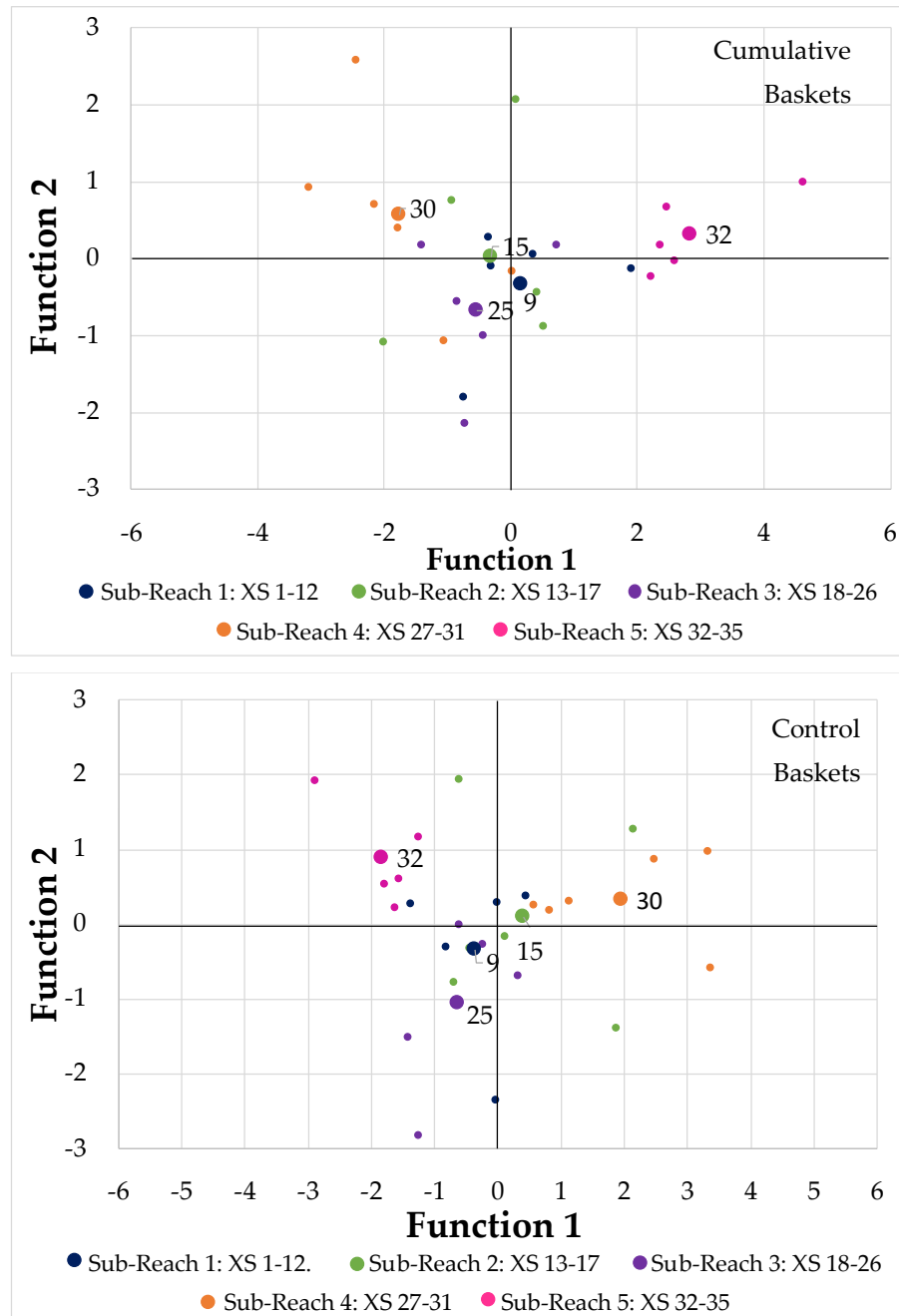


Figure 4.32. Centroids and casewise results for each sampling site (i.e., cross section) on a combined-group plot. Discriminant functions maximize the variance between cross-sections based on the total number of EPT, pH, turbidity and temperature observations along Alderson Creek. Results are given for the total number of EPT in cumulative baskets (top) and in control baskets (bottom). Large circles represent XS centroids and small circles represent casewise results.

Table 4.6. Loadings of each parameter on the respective functions, shown for the analysis that included macroinvertebrate abundance, pH, turbidity, and temperature, separated into results from control baskets and from cumulative baskets. The larger the loading, the stronger the correlation between the variable and the discriminant function. The sign (+/-) indicates the direction of the relationship and the asterisk indicates largest loading on that function.

	Control Baskets - Macroinvertebrate Abundance (bottom Figure 4.32)		Cumulative Baskets - Macroinvertebrate Abundance (top Figure 4.32)	
	Function 1	Function 2	Function 1	Function 2
pH	-0.220	0.404	0.244	0.263
Temperature	-0.083	0.635*	0.178	0.704*
Turbidity	0.225	0.033	-0.165	0.375
Macroinvertebrate Counts	0.942*	0.129	-0.569*	0.643

Thus far, the clustering analyses has shown that (a) conductivity was the most powerful discriminating variable; (b) there was group differentiation (i.e., clustering) even when conductivity was not included as a discriminant variable in the analysis; and (c) R5 stands out as unique in all the analyses. A summary of the DA results (Table 4.7) confirms that conductivity was the single best explanatory variable, and that temperature and pH frequently dominate the functions that significantly differentiate between sub-reaches. Nitrogen doesn't appear to contribute to sub-reach differentiation. The summary also confirms that R5 is considerably different from R4, but there is overlap between sample sites that make up the remaining sub-reaches (R1 – R3). Overlap among the clusters was greatest when only pH, temperature, turbidity, and conductivity were considered but the five proposed sub-reaches became more distinct when dissolved oxygen, macrophyte density, and macroinvertebrates counts were also considered. The most important observation is that the five sub-reaches were distinguished in the same way that the qualitative assessment suggested (i.e., spatially contiguous cross-section aligning with land-use practices on different properties).

Table 4.7. Results from a discriminant analysis performed with various combinations of environmental parameters as the discriminating variables.

Parameters included in DA	Significant discriminant function(s)	Parameter with largest loading on function	Observations from combined-group plot
Temperature Turbidity pH	Function 1	pH	R5 distinct from other sub-reaches; Sites in R1 moderately grouped near R5; Overlap with sample sites in R3, R2, and R4
	Function 2	Temperature	Distinction between sub-reaches unclear, sample sites generally cluster near zero
Temperature Turbidity pH Conductivity	Function 1	Conductivity	R5 distinct from other sub-reaches; Sites in R1 moderately grouped near R5; Overlap with sample sites in R3, R2, and R4
	Function 2	pH	Overlap between sample sites with the exception of select sample sites (from various sub-reaches)
Temperature (excluding R5) Turbidity (excluding R5) pH (excluding R5)	Function 1	pH	Overlap between sample sites with the exception of select sample sites (from various sub-reaches)
	Function 2	Temperature	
Temperature (excluding R5) Turbidity (excluding R5) pH (excluding R5) Conductivity (excluding R5)	Function 1	Conductivity	Sample sites group into predicted sub-reaches
Macrophyte Density Temperature pH	Function 1	pH	R5 distinct from other sub-reaches; Overlap of sample sites in R4, R3, R2, and R1; Distinction between R1, R2, R3 and R4 on Function 2 (dominated by temperature)
Macrophyte Density Temperature pH Conductivity	Function 1	Conductivity	Sample sites group into predicted sub-reaches
	Function 2	pH	
Total Macroinvertebrates in Control Baskets pH Temperature Turbidity	Function 1	Total Macroinvertebrates in Control Baskets	Overlap of sample sites in R3, R2, R1; Sample sites reasonably group into R4 and R5, which plot on opposite ends of the axis

Parameters included in DA	Significant discriminant function(s)	Parameter with largest loading on function	Observations from combined-group plot
Total Macroinvertebrates in Control Baskets pH Temperature Turbidity Conductivity	Function 1	Conductivity	Sample sites group into predicted sub-reaches
	Function 2	Total Macroinvertebrates in Control Baskets	
Total Macroinvertebrates in Cumulative Baskets pH Temperature Turbidity	Function 1	Total Macroinvertebrates in Cumulative Baskets	Overlap of sample sites in R3, R2, R1; Sample sites reasonably group into R4 and R5, which plot on opposite ends of the axis
Total Macroinvertebrates in Cumulative Baskets pH Temperature Turbidity Conductivity	Function 1	Conductivity	Sample sites group into predicted sub-reaches
	Function 2	Temperature	
Total Macroinvertebrates in Kick Net pH Temperature Turbidity	None	n/a	n/a
Dissolved Oxygen pH Temperature	Function 1	Dissolved oxygen	R1, R2, R3 and most of R4 clustering. XS 31 and sample sites in R5 outliers.
Dissolved Oxygen pH Temperature Conductivity	Function 1	Conductivity	Sample sites group into predicted sub-reaches
	Function 2	Dissolved oxygen	
Dissolved Oxygen (excluding R5) pH (excluding R5) Temperature (excluding R5) Conductivity (excluding R5)	Function 1	Conductivity	Sample sites group into predicted sub-reaches
Nitrogen pH Temperature	None	n/a	n/a
Nitrogen pH Temperature Conductivity	None	n/a	n/a

Chapter 5. Discussion

It was hypothesized that anthropogenic signatures imposed on streams due to land management decisions should be evident at the sub-reach scale. If true, then an otherwise natural stream should display evidence of sub-reach differentiation with respect to biotic and abiotic parameters, and the sub-reach boundaries should align roughly with fence lines, property markers, road crossings, or subdivision edges. Specifically, Alderson Creek is expected to show downstream changes that map onto land ownership patterns.

5.1. Sub-Reach Differentiation in Alderson Creek

Field and statistical methods were used to test the hypothesis, and the results indicate that there is some evidence for sub-reach differentiation. Clustering of cross-sections was evident in the raw data (i.e., box-plots) as well as in statistical tests (i.e., discriminant analysis), although sub-reaches weren't delineated exactly as expected. This leads to the rejection of the null-hypothesis that sample sites will not cluster into groups that align with land-management practices.

The most consistent observation was that XS 32, 34, and 35 (members of sub-reach 5) stood out in stark contrast to all other cross-sections. This was particularly evident with respect to conductivity (see Figure 4.6), with R5 sites having consistently smaller conductivity values than sites downstream. Dissolved oxygen values also differed, but mostly with respect to variance rather than the mean values (see Figure 4.15). Temperature (see Figure 4.3) and turbidity (see Figure 4.12) values in R5 were similar to other cross-sections downstream.

Despite being adjacent within the same sub-reach (R5) as well as being very different from the other cross-sections along Alderson Creek, XS 34 and 35 were also quite different from each other, as shown in the discriminant analysis (see Figure 4.29). A series of discriminant analyses were therefore conducted to determine how the differentiation of R5 might depend on the peculiar nature of XS 34 and 35 relative to all others. When XS 34 and 35 were eliminated from consideration, leaving only XS 32 to represent R5, the results were qualitatively unchanged in the sense that R5 was still distinguishable from the other sub-reaches (see Appendix C Figure A1 – see also Figure 4.6). When all of the R5 cross-sections were eliminated from the DA test (see Appendix C Figure A2 and A3), the results show that there wasn't much change in how the

cross-sections in R1 through R4 were represented relatively to each other. Specifically, there remained considerable overlap between cross-sections in sub-reaches R1, R2, and R3, with R4 standing out as somewhat different.

The cross-sections in R4 (XS 27 through 30) cluster together, often with XS 31 (located downstream of McLeod Road), and they are in some respects transitional between R5 and R3 (see Figure 4.24). The average conductivities in R4, for example, were around 430 $\mu\text{S}/\text{cm}$, relative to 330 $\mu\text{S}/\text{cm}$ in R5 and 475 $\mu\text{S}/\text{cm}$ in R3 (see Figure 4.6). Nitrogen and pH values were, on average, between those of R5 and R3, as shown in Figure 4.24. DO content was more variable in R4 than R3, but less variable than R5. Differences in temperature and turbidity were not revealing (see Figure 4.24). The most compelling evidence for R4 being different from other sub-reaches comes from macroinvertebrate counts (Figure 4.25) and macrophyte density (Figure 4.26). R4 consistently had the largest numbers of macroinvertebrates, whereas R5 had the fewest, and DA tests that included macroinvertebrate counts as a variable clearly showed that R4 differed from other sub-reaches (see Figure 4.32). Macrophyte densities were the least in R4 and the largest in R5. The macrophyte densities at R3, R2, and R1 were between those of R5 and R4.

The results for sub-reach differentiation were less persuasive with respect to cross-sections 1 through 26. There was a lot of overlap in the conductivity measurements (see Figure 4.6) as well as with respect to temperature (see Figure 4.3), pH (see Figure 4.9), turbidity (see Figure 4.12) and DO (see Figure 4.15). Thus, it was not possible to differentiate between R1, R2, and R3 on the basis of these parameters (see Figure 4.24). Macroinvertebrate counts and macrophyte densities were also quite similar in R1, R2, and R3 (see Figure 4.25 and Figure 4.26). The DA tests similarly were unable to show clustering among the cross-sections in R1, R2, and R3 (see Figure 4.32).

Overall, then, the DA tests indicate that: (1) R5 is different than R4; (2) R5 and R4 are different than R3, R2, and R1; and (3) R3, R2, and R1 are largely indistinguishable on the basis of the variables included in this study. Depending on which variables were included in any individual DA test, the results with respect to clustering (and hence sub-reach differentiation) were more or less convincing. Sub-reach differentiation was more apparent in the tests that included conductivity, pH, turbidity, temperature, and macroinvertebrate abundance (see Appendix C

Figure A5), for example, than they were in the tests with conductivity, pH, temperature, and nitrogen (see Appendix C Figure A11). Some variables were better at showing sub-reach differentiation than others in this study, and the next section considers this situation in greater detail.

5.2. Discriminating Power of DA Variables for Sub-Reach Differentiation

The DA tests demonstrated that conductivity was consistently the primary driver in sub-reach differentiation (see Table 4.7). Figure 5.1 shows the average loadings for all variables in all of the DA tests, with a larger absolute value of the loading indicating that the variable is better at representing the variance among cases (i.e., discriminating between sub-reaches). The average loading was calculated by dividing the sum of the absolute value of the loading on function 1 across all DA tests by the number of tests. The average was used since the variables were not included in the same number of DA tests (e.g., conductivity was considered in 8 tests whereas pH was considered in 15 tests). Only function 1 was used because it explains most of the variance (see Table 4.1, for example). The results show that nitrogen, macroinvertebrates, and DO were secondary drivers in sub-reach differentiation.

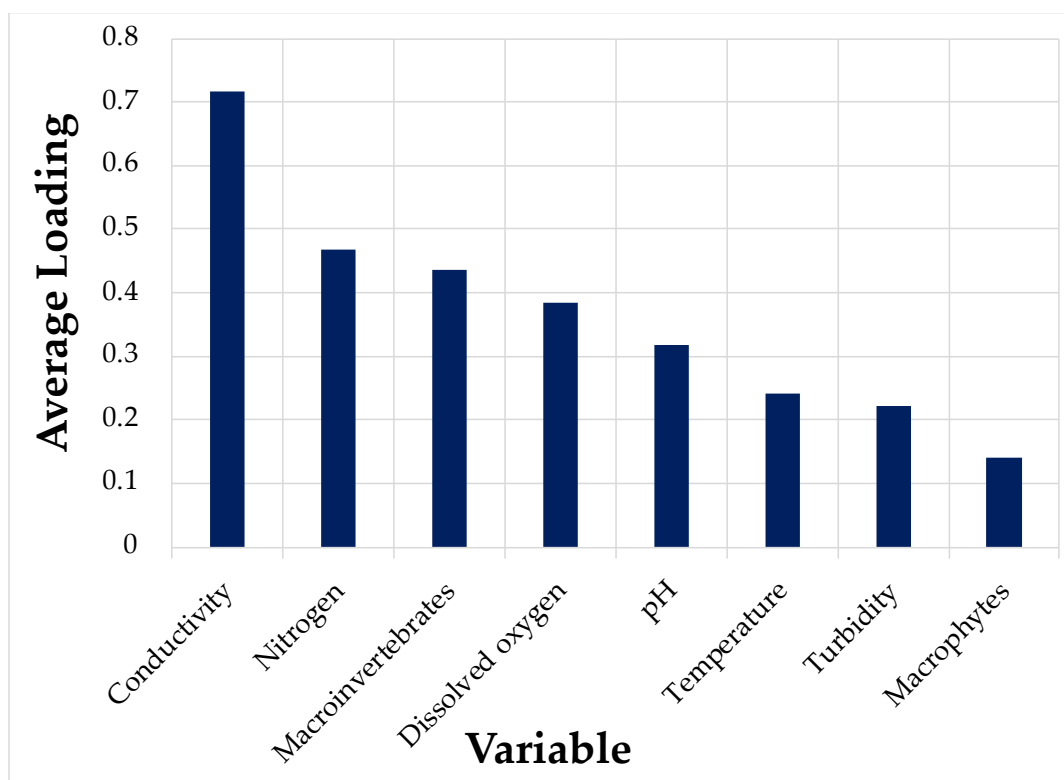


Figure 5.1. Average loading of variables in DA tests. The average loading is the total absolute values of variable loadings divided by the number of DA tests the variable was part of.

In Alderson Creek, conductivity increased in the downstream direction. The source of the creek is groundwater emanating from a spring near XS 35 (in R5), where the water conductivity is small ($300 - 350 \text{ uS cm}^{-1}$). As the water flows downstream, more solutes are picked up leading to larger concentrations ($500 - 550 \text{ uS cm}^{-1}$) at XS 1. Despite regional influences on conductivity due to rock type, climatic conditions, and rain composition, other studies have also documented an increase in conductivity in the downstream direction (Allan and Castillo 2007). There can also be a counter-acting diluting effect due to increases in discharge during rain storms or during the spring freshet (Allan and Castillo 2007; Newbury et al. 1969). Large tributary inputs can increase dilution or if the tributary provides water of high conductivity it will be mixed with the main-stem stream. The data trends at XS 31 are exemplary in this regard because an ephemeral tributary joins Alderson Creek from the east and the tributary waters often displayed elevated conductivities when there was flow (see Figure 4.6). The increases were not noticeable farther downstream (e.g., at XS 30; see Figure 4.6) likely because the tributary flow contribution was small in comparison to the main-stem Alderson Creek. Given the marked downstream increase in

conductivity, it is not surprising that this variable contributes dominantly to differentiating the upstream downstream cross-sections (i.e., R5) from those downstream (e.g., R1 and R2) when used in DA tests. Nevertheless, conductivity does not discriminate between neighbouring sub-reaches farther downstream (e.g., R2 versus R3) because the increases in conductivity are gradually smooth.

In order to determine the discriminating power of secondary variables such as nitrogen and dissolved oxygen, conductivity was removed from further consideration in subsequent DA tests. These tests teased apart whether certain variables influenced clustering of cross-sections into sub-reaches more than others. Nitrogen became dominant when conductivity was not included in subsequent tests (see Appendix C Table A10). Nitrogen concentrations also typically increase in the downstream direction, especially when fertilizers and manure are used on agricultural land (Allen and Castillo 2007; Edwards et al. 2000; Shabalala et al. 2013). In Alderson Creek, nitrogen concentrations increased from the groundwater source to a maximum around XS 25-27 (in R3) and stabilized at that value (approximately 12-13 mg L⁻¹) in the downstream direction. This suggests that there were no further inputs of nitrogen downstream of R3, which coincides with the boundary between the property with cattle grazing (R3) and the properties downstream without cattle grazing (R2 and R1). The data graphs (e.g., Figure 4.17) and DA tests show that nitrogen was effective at differentiating the upstream sub-reaches (i.e., R5 and R4) with small concentrations from those downstream with larger concentrations. But nitrogen did not discriminate between the lower sub-reaches (e.g., R1, R2 and R3) because concentrations were similar (see Appendix C Figure A10 – see also Figure 4.17). Unfortunately, nitrogen measurements were not taken as frequently as many of the other variables, but it is likely that nitrogen would be an even stronger variable in the DA tests if it was measured more frequently and at more sample sites.

Macroinvertebrate counts from the pebble-filled sampling baskets also proved to be an effective explanatory variable in the DA tests, but this was not the case for the kick net samples. It is believed that the basket method yielded a truer representative sample of macroinvertebrate presence in the creek because the pebble composition of the baskets provided ideal habitat for certain macroinvertebrates regardless of the natural substrate. In contrast, the kick net approach disturbs the stream bottom, which in certain locations was sandy or muddy and not ideal habitat

for macroinvertebrates. For example, in R4, which comprises mostly sand and silt, kick net sampling yielded very few counts (indicating the presence but not abundance of invertebrates) whereas the basket samples yielded large counts, more than in other sub-reaches (Figure 4.20 – 22). These results suggest that the conditions in R4 are ideal for supporting macroinvertebrates except for the sandy-silty substrate. In contrast, R5 consistently had very small (often zero) counts using both the basket and kick net methods. Habitat conditions for macroinvertebrates in R5 are not ideal because cattle are allowed unrestricted access to the creek. The banks are trampled, and the substrate consists of muddy organic muck. This is also true for R3, but not quite to the same extent. Sub-reaches with ‘favourable’ stream characteristics (i.e., healthy riparian buffer) had a larger number of macroinvertebrates, especially apparent in R4. Since macroinvertebrates are strongly influenced by water quality, and the DA tests show that macroinvertebrates are an important variable for differentiating between sub-reaches, the downstream trends in macroinvertebrate counts are interpreted as reflective of general water quality conditions in the sub-reaches.

The importance of dissolved oxygen concentration in the DA tests was unexpected given that DO did not demonstrate large spatial variability in the raw data, especially for cross-sections 1 through 30 (see Figure 4.15). Factors that influence DO, such as algal growth processes, cause gradual changes in DO concentrations that were not captured in the bi-weekly measurement strategy adopted in this study (Bailey and Ahmadi 2014). Natural variation in DO is expected as a result of photosynthesis (daytime) and respiration (nighttime), and a diurnal cycle was evident when DO was recorded for one 24-hr period at XS 9 (see Figure 4.16). DO is also expected to differ at cross-sections that have aerated water (i.e., falling from a culvert) or locations where water is still, which explains why sample sites upstream from XS 30 were much different from those downstream. Water was aerated at XS 34 and the McLeod Road sample site because the flow spilled out of culverts, which explains the higher-than-average DO values. In contrast, stagnant water at XS 31 and 32 and the groundwater source at XS 35 explain the reduced DO values at those locations. Differences between these upstream cross-sections were also captured in the DA tests (see Appendix C Figure A8 and Figure 4.30). When these 'abnormal' upstream cross-sections were removed from the analysis to determine if there was further sub-reach differentiation between the sub-reaches, the new test results showed some clustering of the sub-

reach centroid scores, particularly R1, but the casewise results overlapped (see Appendix C Figure A9). This suggests that DO is effective at differentiating some unusual sample sites (e.g., XS 31 and 34) in which DO processes are linked to aeration or stagnation, but in general, DO is not effective at discriminating sites in the downstream direction when there are no other extenuating circumstances. In other words, DO does not appear to be strongly linked to land-use practices related to agricultural production except in the case of human interventions such as emplacement of culverts or watering ponds. However, this conclusion is conditional because the data set used in the analysis was not very extensive.

Temperature and pH were initially thought to be important explanatory variables based on the loadings shown in Table 4.7, however, when averaged for the number of tests, other variables (e.g., conductivity, nitrogen, DO and macroinvertebrates) dominated over temperature and pH with respect to discriminating ability. The pH of water is influenced by many of the same factors as conductivity: soil, geology, and anthropogenic activities (Morosanu et al. 2017). Much like conductivity, there was a slight increase in pH downstream (refer to Figure 4.9), which occurs as stream water equilibrates with gases in the atmosphere (Nakagawa et al. 2009). Carbon dioxide (CO₂) fluctuates in stream water as it balances with atmospheric CO₂, for instance, altering the concentration of hydrogen ions in the water (Nakagawa et al. 2009). Metabolic activity also causes daily fluctuations in CO₂ (i.e., photosynthesis and respiration) and therefore in pH (Nakagawa et al. 2009). None of these sources of pH fluctuation were captured by the bi-weekly measurement protocols in this study. There were minor pH increases year-to-year (see Figure 4.7) but the reason for this is unclear. Perhaps continuous bank degradation is causing leached carbonates, bicarbonates or alkaline compounds to enter the stream. Or, perhaps decreases in atmospheric CO₂ between 2015 and 2017 (Environment and Climate Change Canada 2019) caused decreases in dissolved CO₂ in water, which increases pH. Spatial differences in pH were not apparent with regards to land use (i.e., dissolved mineral inputs on irrigated lands), so although pH was important in many of the DA tests, the ‘clustering’ of sub-reaches was not clearly related to pH (see Figure 4.29).

Temperature was not important in the DA tests (Figure 5.1), which was not surprising given how similar the temperatures were at most of the cross-sections (see Figure 4.3). Temperature is critical for species survival and it fluctuates largely as a result of atmospheric and environmental

conditions close to the site. Temperature is controlled by landscape (i.e., stream slope), stream characteristics (i.e., riparian vegetation or discharge), climatic conditions and air-water interaction (Mayer 2012). Stream temperatures in Alderson Creek follow seasonal variations but demonstrate a lag behind air temperatures seasonally and day to day (see Figure 4.2). Temperature at one cross-section is similar to the adjacent upstream cross-section with minor increases downstream as heat energy accumulates, which is characteristic of most river systems (Bladon et al. 2017). Alderson Creek spans only 2 km and so climatic conditions are uniform throughout its length. Not surprisingly, then, temperature doesn't easily differentiate sub-reaches (see Figure 4.24). Spatial differences that were observed with respect to water temperatures can be attributed to differences in landscape or stream characteristics. For example, ponds and pools, riparian vegetation, and groundwater springs will influence stream temperature (Allan and Castillo 2007), and several sample sites were unique in these characteristics and plotted as outliers. The largest contrast in stream temperatures was between XS 34 and XS 35, despite their proximity because XS 35 was near to the groundwater source whereas XS 34 was below a large watering pond that readily absorbed solar radiation. Temperature is therefore a good indicator of site differences in some instances, but it is not effective in differentiating sub-reaches (see Figure 4.29).

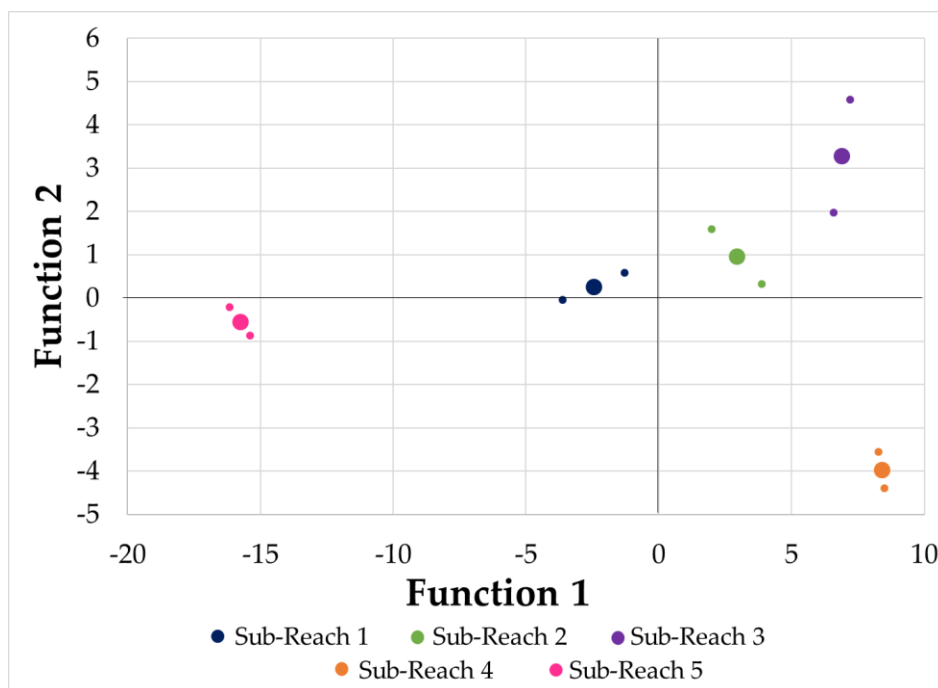
Turbidity and macrophyte density had the least influence in the DA tests (Figure 5.1). Factors that influence turbidity manifest themselves temporally rather than spatially (e.g., rising turbidity after a rainfall event). Some of this temporal variability was evident in the bi-weekly measurements (see Figure 4.10), but the sampling protocols were not frequent enough to discern specific cause-effect relationship. Thus, the turbidity traces have a semi-random look to them, and there is little evidence of spatial trends. The only spatial relationship observed was that turbidity increased when physical disturbances were observed in the creek (i.e., cattle). But these did not align well with property divisions because the fine-grained sediment causing the turbidity increase can be transported over long distances and into downstream sub-reaches. Turbidity was not an effective variable for discriminating sub-reaches.

Macrophyte density is a somewhat unusual variable because it did not figure prominently in the two DA tests for which it was included (smallest loadings in Figure 5.1) despite large differences in the measurements between sampling points. Macrophyte density clearly differentiates R5 from

R4, and differentiates these two sub-reaches from the rest (see Figure 4.19), much the same way as macroinvertebrate count does (see Figure 4.25 and Figure 4.26). The explanation may be due to little consistency in the data for macrophyte density. There was very large scatter around the mean in R1 and R5 (range of 90%) for example, whereas there was minimal scatter around the mean in R4 (range of 50%). Inconsistencies between measurements influence the DA results.

5.3. Optimized Sub-Reach Differentiation

Conductivity, nitrogen, DO, and macroinvertebrates proved to be important variables for differentiating between sub-reaches based on an analysis of the raw data trends as well as the DA tests. Thus, a final series of DA tests was performed using only these key variables with the intent of optimizing sub-reach differentiation. These tests were considered to be the best objective assessment of whether sub-reaches could be discriminated. Figure 5.2 shows the results from one test, which demonstrates that R4 and R5 are different from R1, R2, and R3, that R4 and R5 are different from each other, and that R1, R2, and R3 are less easily differentiated.



There were some limitations in performing this analysis. Two of the variables, macroinvertebrates and nitrogen, were only measured at one cross-section for each sub-reach. This eliminates the ability to see *how* cross-section may cluster into sub-reaches, but it does highlight in *what way* sub-reaches differ from each other with respect to Functions 1 and 2 (e.g., R5 is most distant from R4 with respect to Function 1 but closest to each other with respect to Function 2). In addition, macroinvertebrates and nitrogen were measured at different cross-sections (e.g., nitrogen at XS 1 and macrophyte density at XS 9 in R1), but this spatial separation was ignored in the analysis. The measurements closest in time were selected for the analysis. A second limitation was the number of data points available to be included in the DA test. Figure 5.2 includes only two casewise results representing each sub-reach because nitrogen was measured only in the summer of the final field season and only on two occasions. Thus, only the variables corresponding most closely to the data collection times and locations dictated by the nitrogen sampling could be included in the DA test. Despite these limitations, the results reaffirm the conclusions reached on the basis of the raw data trends (e.g., box-plots) and the many other DA tests regarding the relative differences among R5, R4, and R3/R2/R1.

A similar test was performed excluding nitrogen to incorporate a larger data set (Figure 5.3). In this test, conductivity dominated Function 1 and macroinvertebrate counts dominated Function 2. The results show that R5 is different from all others and has no overlap of casewise scores. R4 is very different from R5 with respect to Function 1 and Function 2. R3 is different from R5 with respect to Function 1 but is different from R4 with respect to Function 2. R1 and R2, in contrast, are essentially the same and transitional between the others.

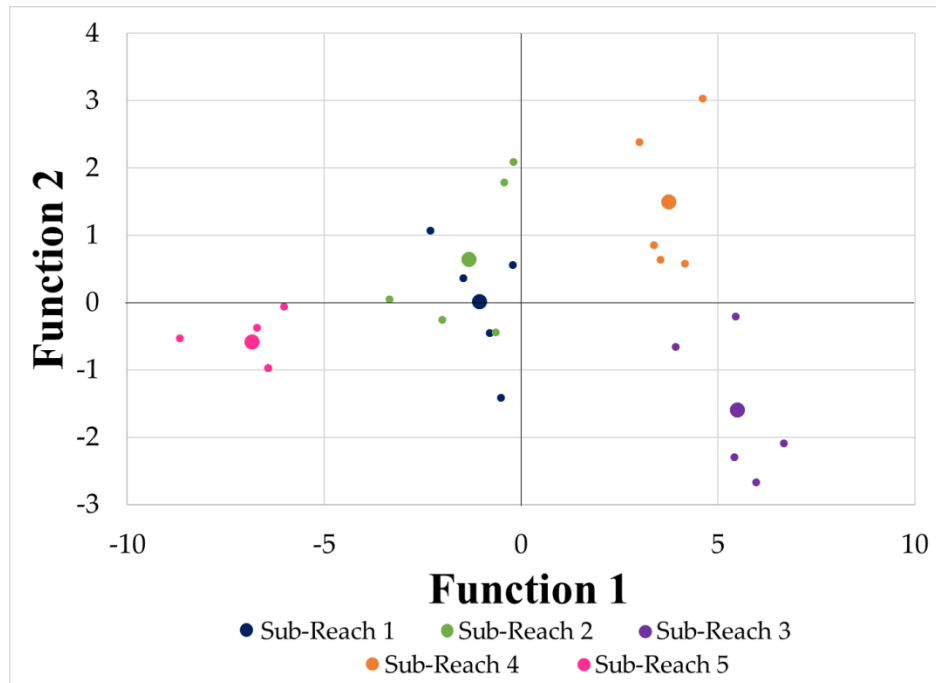


Figure 5.3 Centroids (large circles) and casewise results (small circles) for each cross-section on a combined-group plot. Discriminant functions (x-axis and y-axis) maximize the variance between cross-sections based on the summer conductivity, dissolved oxygen and macroinvertebrate count observations along Alderson Creek. Function 1 is dominated by conductivity and Function 2 is dominated by macroinvertebrate counts.

R3 is both similar and dissimilar to R5 and R4 depending on the function, therefore, it is similar or dissimilar to R5 and R4 depending on the variables with largest loadings: conductivity and macroinvertebrates. There are a number of important observations from this. The first is related to the difference between R3 and R5, but similarity between R3 and R4, with respect to conductivity (Function 1). Conductivity displayed downstream trends and so the results indicate that continuity in the downstream direction is a factor in DA tests. Downstream influences, however, cannot be the *only* factor in sub-reach differentiation because R4 is different from R5 with respect to Function 1, so there must be another influence. Land management, for example, has a strong influence on macroinvertebrate counts, and R3 is similar to R5 with respect to Function 2, but different from R4. Moreover, neighboring sub-reaches R1 and R2 are similar in land management and are essentially the same in DA tests (Figure 5.3). These sub-reaches are also transitional between the others. There is an apparent interaction between downstream trends and land management strategies, and the next sections consider this in greater detail.

5.4. General Downstream Trends versus Localized Effects

In most natural streams, the downstream trends in certain variables are predictable if there are no unusual intervening influences (e.g., tributary confluences, groundwater springs, human modifications). Conductivity and pH, for example, are expected to increase downstream, as was the case in Alderson Creek. These two variables are influenced by changes in stream chemistry as water interacts with its surroundings through bank erosion, hyporheic exchange, leaching processes, and atmospheric interaction. Similarly, mid-day temperature is expected to increase in the downstream direction, all other things kept constant, because the flowing water accumulates heat from solar radiation. In contrast, turbidity is not expected to have a downstream trend at the scale of a river reach if the geology and bed substrate are uniform. However, these trends can be disrupted both temporally and spatially when there are localized effects.

Localized effects were observed at multiple cross-sections along Alderson Creek, with XS 34 and 35 being primary examples (Figure 5.4). The groundwater source of Alderson Creek immediately above XS 35 provided cool water with small conductivity and DO content. This water entered an excavated pond used for livestock watering where the stagnant conditions allowed for heat build-up during hot summer days when solar radiation was intense. At XS 34, positioned at the outlet of the pond, water quality measurements were taken in a large tub situated below the outlet culvert that ran through the small earthen dam holding back the pond water. The highly turbulent water spilling out of the culvert was warm and aerated with large DO content but no change in conductivity. The next major influence occurred after the flow went through another culvert beneath McLeod Road. A small tributary entering Alderson Creek at XS 31 resulted in noticeable increases in conductivity (Figure 4.6) and decreases in DO content saturation (see Figure 4.15), thereby influencing the downstream sample sites below XS 30.



Figure 5.4. XS 35 (left) and the culvert at XS 34 (right). The pond, shown downstream from XS 35 in the left image flows through culvert to XS 34 in right image.

5.5. Sub-Reach Differentiation and Land Management

The working hypothesis for this thesis was that land-management practices have a noticeable impact on stream conditions, and therefore the differentiation of sub-reaches based on biotic and abiotic factors should align roughly with property boundaries, to the extent that those properties are managed differently with respect to land use. The results discussed above indicate that there is sufficient evidence to reject the null hypothesis that land-management practices have no impact on stream quality. Moreover, there is some evidence to support the idea that Alderson Creek can be objectively divided into sub-reaches that map on to property boundaries. In this section, the case will be made that for some sub-reaches, the land-management practices strongly influence water quality and aquatic health of the riparian system.

The DA tests clearly showed that R5 was different from R4, even when taking into consideration the localized influences evident at XS 35, 34, and 32. Land use in R5 consisted of open pasture utilized all-year by a small herd of cattle with unrestricted access to Alderson Creek and the watering pond on the property. There were no shrubs or trees along the riparian corridor, and the watercourse was heavily trampled and degraded. Some of the worst water quality conditions were found in R5, and this was verified by the almost complete absence of macroinvertebrates in this sub-reach. In contrast, R4 had a thick riparian corridor with large cotton woods providing

shade and an understory of ferns and large, broad-leaved plants that kept the ground cool and moist. The property beyond the riparian zone was used for forage crop production and there was no livestock grazing or animal access to the creek. R4 had the best water quality overall, and this was reflected in abundant macroinvertebrate counts. Despite being adjacent sub-reaches, the degraded conditions in R5 were effectively 'remediated' in R4 because of the natural state of the riparian corridor in R4. This suggests that even if an upstream property is not managed effectively, implementing beneficial management practices on the adjacent downstream property can improve aquatic health over a relatively short distance. The extent to which the small tributary entering Alderson Creek from the east at XS 31 influences the water quality in R4 is difficult to evaluate. At certain times of the year, this tributary has significant flow, but during the summer months it often goes dry before reaching the confluence because of infiltration loss to shallow groundwater.

The DA tests also revealed that sub-reaches R1, R2, and R3 were largely indistinguishable from each other, but were distinctly different from R4 and R5. In certain regards, the 'remediated' water from R4 maintained its character in R3, for example, with respect to temperature (Figure 4.3), conductivity (Figure 4.6), pH (Figure 4.9), and DO (Figure 4.15) and the downstream trends were smoothly continuous through R2 and R1. However, it is interesting to note that land use in R3 was similar to R5 (i.e., cattle grazing) although at a lesser intensity given the larger acreage and smaller herd. If land-management practices have a direct and predictable impact on water quality, it would be expected that R3 should cluster close to R5 in DA tests, but Figure 5.3 shows that these sub-reaches are distant and unlike with respect to the key parameters identified as being most effective in differentiating sub-reaches. Arguably, this is due to the remediating role of R4 in providing high-quality water to R3, and thereby buffering the impact of cattle grazing in R3. It is also clear from the macroinvertebrate counts (Figure 4.20 – 22) that R3 had very small values, second only to R5, so aquatic habitat conditions were also quite degraded. Sub-reaches R2 and R1 showed progressive improvement, consistent with the downstream trends as well as land-management practices that were less detrimental to ecosystem health (i.e., forage crop production and fallow fields).

Sub-reach differentiation is therefore influenced by local influences (small-scale), downstream effects (reach scale) and land use (property, or sub-reach, scale). The three scales reflect the

complexities that were observed. For example, it is not easy to differentiate some sub-reaches from others because the land uses are not distinctly different and because there is some transference of quality from upstream. Also, distant sub-reaches tend to be different because of downstream trends that lead to different values, of conductivity and pH for example. However, some sub-reaches are differentiable despite being downstream from one another because land uses are distinctly different. Downstream trends are weakened if an intervening process has a greater influence. This is all made more complicated by localized influences (e.g., tributaries), although, some localized influences are from human interventions (e.g., culverts or man-made ponds).

5.6. Experimental Design Considerations

Sub-reach differentiation as a function of environmental parameters is dependent on spatial scales of influence (local, property, and reach) as well as temporal scales of influence (annual, seasonal, daily). As a result, when and how sampling is performed affects the results and has important implications for the statistical approach. One issue that arose in this thesis research was that the parameters were not all measured at the same locations. For example, nitrogen and macroinvertebrate counts were only measured at one location per sub-reach, which limited the use of these data. Temperature was another example. In-situ temperature pendants were placed at a limited number of locations, which didn't line up with the rest of the data collected manually, so the pendant data weren't as useful in the statistical tests as possible with careful planning.

Another issue with the experimental design was that the parameters were not all measured at the same times. Temperature pendants provided 10-minute intervals of data, for example, but other parameters were measured only once every two weeks. Again, temperature pendant data didn't line up with the rest of the data for statistical tests. Issues with sampling times also occurred with macroinvertebrates and macrophytes, as well as nitrogen and DO. Macroinvertebrates and macrophytes were only measured once per month whereas nitrogen and DO were not part of the original experimental design, so data were limited. This became especially problematic because nitrogen, macroinvertebrates, and DO were potentially powerful variables in DA tests (Figure 5.1) but weren't sampled sufficiently to contribute to sub-reach differentiation (Figure 5.2).

The overarching conclusion with respect to experimental design is that parameters must have the same number of data points for each location in order to be useful for statistical testing. The optimal design, then, would involve collecting all parameters at concurrent times, and ideally at uniform distances throughout the stream. Advances in technology are improving the options for in-situ multi-parameter probes that can record multiple water quality parameters (e.g., the YSI multiparameter electrode used by Boenne et al. 2014). This would be a costly design, however, especially in a large stream system. Even if this were possible, there would remain issues of how to spatially compare large data sets. The 10-minute temperature data gave great detail of the temporal patterns in Alderson Creek (see Figure 4.1), but detailed temperature time series were complex and spatial comparisons were difficult. Since environmental parameters respond to diurnal and seasonal signals, dividing the data seasonally and daily seems appropriate. With temperature, for example, one season will yield different downstream patterns from another season - XS 34 was warmer than XS 35 in the summer, but cooler than XS 35 in the winter (see Figure 4.1). Seasonal divisions were made based on equinoxes and solstices, and only summer data were compared in spatial tests. Days were split into four increments and an average taken for the maximum temperature (12 – 6 pm), minimum temperature (12 – 6 am) and 6-hour transition periods. This made use of most of the data set without suppressing the daily variability. However, when it came to using temperature data in statistical tests, only one data point per measurement day could be used (to align with other parameters). If the experimental design could allow for in-situ multi-parameter probes, all parameters could be divided the same way, then spatially compared. For example, the daily average of all parameters could be used, rather than the daily average of temperature but only the single measurement in time of the other parameters. With the larger data set, it would also be worth testing if sub-reach differentiation would differ with the daily average of all parameters compared to sub-reach differentiation with a single measurement in time, or even how sub-reach differentiation differed with daily maximum or daily minimum data.

Chapter 6. Conclusions

Streams respond to their surrounding environment and to naturally varying stimuli (e.g., solar radiation, water budget, vegetation). The effect that humans are having on streams can also be significant and is of increasing interest and concern. Numerous studies have pursued a better understanding of the relationship between land uses and stream responses. Research designs often focus on a specific response. This may include biological responses, such as macroinvertebrate communities (Kahirun et al. 2019) and fish habitat (Lyons et al. 2000) or hydrological responses, such as water availability (Shrestha et al. 2019) and nutrient loads (Musolff et al. 2016). The scale of human influence on these responses is not well understood, and a better understanding of the scale-dependent influence of land use on stream condition is critical for land management practices and potentially for stream rehabilitation designs.

The conclusions drawn from this thesis contribute to an expanding knowledge about the responses of aquatic ecosystems to agricultural land use and inform existing theories about the importance of spatial scale in streams processes. Alderson Creek is a small, first-order stream that joins Fortune Creek, which provides critical habitat for fish spawning and rearing. Alderson Creek would generally be viewed and classified as first-order stream with uniform conditions along a single reach. However, Alderson Creek traverses five agricultural properties, some used for livestock grazing and some used for forage crop production. An assessment of the quality of aquatic habitat and biophysical characteristics along the length of the stream suggest that this ‘reach’ can be reasonably sub-divided into sub-reaches that align with property boundaries and hence, land use. The primary conclusions from the thesis research are presented below.

Firstly, Alderson Creek demonstrates complex temporal and spatial behaviour in terms of the biological, chemical, and physical attributes relevant to stream health. Small watersheds such as Alderson Creek are characteristically sensitive to weather conditions. Measurements of temperature at 10-minute intervals demonstrated a large degree of variability both temporally and spatially. Diurnal temperature fluctuations during summer were as great as 10°C, which indicates a close connection to atmospheric forcing largely driven by the radiation balance. Furthermore, temperatures increased by almost 2°C from the upstream to downstream cross-sections as heat energy accumulated. Daily fluctuations and spatial variability were seen with

other variables, such as conductivity, dissolved oxygen, and pH. This reality of inherent natural variability in these small systems poses challenges for demonstrating sub-reach differentiation because the trends may be swamped by the natural ‘noise’. This is all made more complicated by localized influences (e.g., tributaries), although, some localized influences are due to human interventions (e.g., culverts or man-made ponds).

Secondly, sub-reaches appear to be an appropriate scale for making land-management decisions because this is the same scale as a small farm. The thesis results indicate that such land-use practices can make a difference to water quality conditions in streams. The spatial differentiation along Alderson Creek roughly aligned with property boundaries in many cases. The use of discriminant analysis showed that measurements at the various cross-sections naturally clustered into groupings consistent with the sub-reaches identified on the basis of visual cues. However, not all sub-reaches were as distinguishable from the others. Some sub-reaches were not clearly differentiated because the land uses were not distinctly different and there was some transference of water quality from upstream. There was no direct correlation that could be made to show that a specific land use will cause a certain biophysico-chemical profile. However, sub-reaches that had distinctly different land uses were easily differentiated despite being downstream from one another, so distinct ‘favourable’ or ‘unfavourable’ land management practices could be differentiated.

Thirdly, certain parameters were better at sub-reach differentiation than others. Some parameters demonstrated no relationship to land management, but others were quite responsive to land management. Conductivity was the strongest driver of sub-reach differentiation, but conductivity displayed a gradual increase downstream, so it did not discriminate well between adjacent sub-reaches. Nitrogen and DO were also strong differentiators. Nitrogen concentrations are related to agricultural land use (Christensen et al. 2011; Shabalala et al. 2013) and did differentiate the ‘best’ and ‘worst’ sub-reaches. DO was not strongly linked to land-use practices related to agricultural production. It was, however, linked to human interventions such as the emplacements of culverts or watering ponds. Moreover, DO is indirectly linked to land-use because DO fluctuates with macrophyte density, for example, which fluctuates in relation to agricultural production (i.e., nutrients increase macrophyte growth). The monitoring of macroinvertebrate counts provided the best evidence for sub-reach differences and for the health

and status of the aquatic and riparian conditions. For example, no macroinvertebrates were found in sub-reach 5 whereas immediately downstream in a natural wetland there were consistently large numbers of macroinvertebrates in sampling baskets. An intervening influence between sub-reach 5 and sub-reach 4 (e.g., a road) allowed for the differences in land use to have a greater influence on stream health.

Fourthly, best-management practices (BMPs), such as fencing and riparian rehabilitation, mitigate the negative effects that agricultural land uses may have on aquatic condition and ecological functioning of a stream. Evidence of this was in sub-reach 4, which was used for crop production and had starkly better aquatic conditions than sub-reach 5 directly upstream. This is attributed to land management, which precluded livestock access to the creek, as well as preserving the riparian buffer zone, which provided shade and an understory of broad-leaved plants that kept the ground cool and moist. The results suggest that stream rehabilitation designs at sub-reach scales may have a positive effect because this is the management scale that successful development of practical tools and guides for BMPs for restoration are likely to occur (i.e., the individual landowner). With the implementation of riparian rehabilitation in sub-reach 5 for example (which includes fencing, replanting, and offstream watering for cattle), the health of the stream should improve (i.e., silt content should decrease and macroinvertebrates should re-occupy the substrate). Moreover, stream health should improve overall downstream even if BMPs are implemented at a sub-reach scale, rather than the entire reach, because of the transference of quality downstream. Likewise, detrimental effects in the middle of a reach due to poor land use practices will transfer downstream (see scenario B in Figure 2.1).

The results of this thesis provide a new interpretation and definition of a stream ‘sub-reach’ that fits well into existing hierarchical frameworks for spatial scales in streams. Specifically, the sub-reach fits between the reach and the habitat/hydraulic zone (see Figure 2.2) Nevertheless, a great deal of future work is required to demonstrate the potential positive effects of implementing BMPs at sub-reach scales (e.g., on sub-reach 5). Fully parameterizing the post-treatment state of the watershed would give an indication of the success of BMPs at sub-reach scales. Alderson Creek is a good candidate as it has a strong set of baseline data. In future work, it is recommended that pre- and post-treatment assessments at sub-reach scales have a ‘control’ system to account for natural variability, such as monitoring a second stream that is comparable

in size, traverses similar substrate and land uses, and experiences similar climate controls, but does not implement BMPs.

Bibliography

- Aljandali A. 2017. Multivariate Methods and Forecasting with IBM® SPSS® Statistics. London, UK: Springer.
- Anderson RJ, Bledose BP, Hession WC. 2004. Width of Streams and Rivers in Response to Vegetation, Bank Material, and Other Factors. *Journal of the American Water Resources Association*. 40(5):1159-1172.
- Allan DJ, Castillo MM. 2007. *Stream Ecology: Structure and Function of Running Waters*. 2nd ed. Dordrecht, NL: Springer.
- Bailey RT, Ahmadi M. 2014. Spatial and Temporal Variability of In-Stream Water Quality Parameter Influence on Dissolved Oxygen and Nitrate within a Regional Stream Network. *Ecological Modelling*. 277:87-96.
- Bailey RG. 1983. Delineation of Ecosystem Regions. *Environmental Management*. 7(4):365-373.
- Bart J. 1998. *Sampling and Statistical Methods for Behavioural Ecologists*. Cambridge, UK: Cambridge University Press.
- Bataineh AL, Oswald BP, Bataineh M, Unger D, Hung IK, Scognamillo D. 2006. Spatial Autocorrelation and Pseudoreplication in Fire Ecology. *Practices and Applications in Fire Ecology*. 2(2):107-118.
- Bell N, Riis T, Suren AM, Baattrup-Pederson A. 2013. Distribution of Invertebrates within Beds of Two Morphologically Contrasting Stream Macrophyte Species. *Fundamental and Applied Limnology*. 183(4):309-321.
- Belsky AJ, Matzke A, Uselmann S. 1999. Survey of Livestock Influences on Stream and Riparian Ecosystems in the Western United States. *Journal of Soil and Water Classification*. 43(1):419-431.
- Bladon KD, Segura C, Cook NA, Bywater-Reyes S, Reiter M. 2017. A Multicatchment Analysis of Headwater and Downstream Temperature Effects from Contemporary Forest Harvesting. *Hydrological Processes*. 32(2):293-304.
- Bledose BP, Carney SK, Anderson RJ. 2011. Scale-Dependent Effects of Bank Vegetation on Channel Processes: Field Data, Computational Fluid Dynamics Modeling, and Restoration Design. In: Simon A, Bennett SJ, Castro JM, editors. *Stream Restoration in Dynamic Fluvial Systems: Scientific Approaches, Analyses, and Tools*. 1st ed. Washington, DC: American Geophysical Union. p.151-165.

- Boenne W, Desmet N, Looy SV, Seuntjens P. 2014. Use of Online Water Quality Monitoring for Assessing the Effects of WWTP Overflows in Rivers. *Environmental Science: Processes and Impacts*. 16(6):151-1518.
- Brierley GJ, Fryirs KA. 2005. *Geomorphology and River Management: Applications of the River Styles Framework*. Malden, MA: Blackwell Publishing.
- Brown MT, Wicker LR. 2000. Discriminant Analysis. In: Tinsley HE, Brown SD, editors. *Handbook of Applied Multivariate Statistics and Mathematical Modeling*. Elsevier Inc. p. 209-235.
- Cao W, Hong H, Zhang Y, Yue S. 2006. Nitrogen Sources and Export on Agricultural Catchments: A Nested Catchment Comparison. *Aquatic Ecosystem Health & Management*. 9(1):9-13.
- Carline RF, Walsh MC. 2007. Responses to Riparian Restoration in the Spring Creek Watershed, Central Pennsylvania. *Restoration Ecology*. 15(4):731-742.
- Christensen VG, Lee KE, McLees JM, Niemela SL. 2011. Relations between Retired Agricultural Land, Water Quality, and Aquatic-Community Health, Minnesota River Basin. *Journal of environmental Quality*. 41(5):1459-1472.
- Clifford HF. 1991. *Aquatic Insects of Alberta: An Illustrative Guide*. Edmonton, AB: University of Alberta Press.
- Collins KE, Doscher C, Rennie HG, Ross JG. 2013. The Effectiveness of Riparian ‘Restoration’ on Water Quality – A Case Study of Lowland Streams in Canterbury, New Zealand. *Restoration Ecology*. 21(1):40-48.
- Couper P. 2007. Fluvial Geomorphology and Semiotics: A Wittgensteinian Perspective of the ‘Divide’ between Human and Physical Geography. *Transactions of the Institute of British Geographers*. 32(3):279-294.
- Courtney LA, Clements WH. 1998. Effects of Acidic pH on Benthic Macroinvertebrate Communities in Stream Microcosms. *Hydrobiologia*. 379(1):135-145.
- Crow GE. 2000. *Aquatic and Wetland Plants of Northeastern North America: A Revised and Enlarged Edition of Norman C. Fasset’s A Manual of Aquatic Plants*. United States: University of Wisconsin Press.
- de Boer DH. 1992. Hierarchies and Spatial Scale in Process Geomorphology: A Review. *Geomorphology*. 4(5):303-318.
- Denis DJ. 2019. *SPSS Data Analysis for Univariate, Bivariate, and Multivariate Statistics*. Hoboken, NJ: John Wiley & Sons Inc.

- Diaz RJ, Solan M, Valente RM. 2004. A Review of Approaches for Classifying Benthic Habitats and Evaluating Habitat Quality. *Journal of Environmental Management*. 73(3):165-181.
- Duan X, Wang Z, Tian Shimin. 2008. Effect of Streambed Substrate on Macroinvertebrate Biodiversity. *Frontiers of Environmental Science & Engineering in China*. 2(1):122-128.
- Edwards AC, Cook Y, Smart R, Wade AJ. 2000. Concentrations of Nitrogen and Phosphorous in Streams Draining in Mixed Land-Use Dee Catchment, North-East Scotland. *Journal of Applied Ecology*. 37(1):159-170.
- Environment and Climate Change Canada. 2019. Historical Data. https://climate.weather.gc.ca/historical_data/search_historic_data_e.html
- Environment Canada. 2008. Canadian Water Quality Guidelines 1987-1997. [accessed April 18th, 2018]. https://www.ccme.ca/files/Resources/supporting_scientific_documents/cwqg_pn_1040.pdf
- Environment Canada. 2012. Canadian Aquatic Biomonitoring Network: Wadeable Streams. Freshwater Quality Monitoring and surveillance Division: Dartmouth (NS).
- Flotemersch JE, Leibowitz SG, Hill RA, Stoddard, JL, Thoms MC, Tharme RE. 2016. A Watershed Integrity Definition and Assessment Approach to Support Strategic Management of Watersheds. *River Research and Applications*. 32(7):1654-1671.
- Frissell CA, Liss WJ, Warren CE, Hurley MD. 1986. A Hierarchical Framework for Stream Habitat Classification: Viewing Streams in a Watershed Context. *Environmental Management*. 10(2):199-214.
- Fryirs KA, Brierley GJ. 2013. *Geomorphic Analysis of River Systems: An Approach to Reading the Landscape*. Chichester, UK: Wiley-Blackwell Publishing.
- Fulton, RJ. 1995. Geological Survey of Canada, "A" Series Map 1880A, 1 sheet. Natural Resources Canada. doi: <https://doi.org/10.4095/205040>.
- Golder Associates. 2014. Evaluation of Aquatic Plants and Controlling Factors in the North Saskatchewan River. Report No. 13-1373-0020. Alberta, BC.
- González-Pinzón R, Haggerty R, Argerich A. 2014. Quantifying Spatial Differences in Metabolism in Headwater Streams. *Freshwater Science*. 33(3):798-811.
- Goodwin K, Caraco N, Cole J. 2008. Temporal dynamics of Dissolved Oxygen in a Floating-Leaved Macrophyte Bed. *Freshwater Biology*. 53(8):1632-1641.
- Government of Canada. 2017. Environment and Natural Resources: Weather, Climate and Hazard Historical Data. Retrieved on November 22nd, 2017 from

http://climate.weather.gc.ca/historical_data/search_historic_data_stations_e.html?searchType=stnName&timeframe=1&txtStationName=Vernon&searchMethod=contains&optLimit=yearRange&StartYear=2016&EndYear=2016&Year=2016&Month=5&Day=15&selRowPerPage=25.

- Gupta, SK. 2011. Modern Hydrology and Sustainable Water Development. West Sussex, UK: Wiley-Blackwell.
- Gurnell AM, Rinaldi M, Belletti, B, Bizzi S, Blamauer B, Braca G, Buijse AD, Bussetini M, Camenen B, Comiti F, et al. 2016. A Multi-Scale Hierarchical Framework for Developing Understanding of River Behaviour to Support River Management. *Aquatic Sciences*. 78(1):1-16.
- Hilsenhoff WL. 1977. Use of Arthropods to Evaluate Water Quality of Streams. Technical Bulletin Number 100, Department of Natural Resources. Madison, WI.
- Hill AR. 2000. Stream Chemistry and Riparian Zones. In: Jones JB, Mulholland PJ. *Streams and Ground Waters*. San Diego (CA): Elsevier Inc. p. 83-110.
- Hugh C. 1991. *Aquatic Invertebrates of Alberta: An Illustrated Guide*. Edmonton: University of Alberta Press.
- Hurlburt SH. 1984. Pseudoreplication and the Design of Ecological Field Experiments. *Ecological Monographs*. 54(2):187-211.
- Kahirun K, Sabaruddin L, Mukhtar M, Kilowasid LMH. 2019. Evaluation of Land Use Impact on River Water Quality Using Macroinvertebrates as Bioindicator in Lahumoko Watershed, Buton Island, Indonesia. *Biodiversitas Journal of Biological Diversity*. 20(6).
- Kauffman JB, Krueger WC. 1884. Livestock Impacts on Riparian Ecosystems and Streamside Management Implications... A Review. *Journal of Range Management*. 37(5):430-438.
- Kelly NE, O'Conner EM, Wilson RF, Young JD, Winter JG, Molot LA. 2016. Multiple Stressor Effects on Stream Health in the Lake Simcoe Watershed. *Journal of Great Lakes Research*. 42(5):953-964.
- Klecka WR. 1980. *Discriminant Analysis*. Newbury Park, CA: SAGE Publications, Inc.
- Lear G, Dopheide A, Ancion P, Lewis G. 2011. A comparison of Bacterial, Ciliate and Macroinvertebrate Indicators of Stream Ecological Health. *Aquatic Ecology*. 45(4):517-527.
- Lee KE, Goldstein RM, Hanson PE. Relation Between Fish Communities and Riparian Zone Conditions at Two Spatial Scales. *Journal of American Water Resources Association*. 37(6):1465-1473.

- Lenat DR. 1988. Water Quality Assessment of Streams Using a Qualitative Collection Method for Benthic Macroinvertebrates. *Journal of North American Benthological Society*. 7(3):222- 233.
- Lillehammer A, Brittain JE, Saltveit SV, Nielson PS. 1989. Egg Development, Nymphal Growth and Life Cycle Strategies in Plecoptera. *Holarctic Ecology*. 12(2):173-186
- Lyons J, Wiegel BM, Paine BM, Undersander DJ. 2000. Influence of Intensive Rotational Grazing on Bank Erosion, Fish Habitat Quality, and Fish Communities in Southeastern Wisconsin Trout Streams. *Journal of Soil and Water Conservation*. 55(3):271-276.
- Majerova M, Neilson BT, Schmadel NM, Wheaton JM, Snow CJ. 2015. Impacts of Beaver Dams on Hydrologic and Temperature Regimes in a Mountain Stream. *Hydrology and Earth System Science*. 19(8):3541-3556.
- Mayer T. 2012. Controls of Summer Stream Temperature in the Pacific Northwest. *Journal of Hydrology*. 475:323-335.
- Miller J. 2015. Off-Stream Cattle Watering Sites (Without Fencing) Protect Riparian Areas and Water Quality. Agriculture and Agri-Food Canada.
- Ministry of Environment. 1998. Interpreting Data. In *Guidelines for Interpreting Water Quality Data*. Retrieved from https://www2.gov.bc.ca/assets/gov/environment/natural-resource-stewardship/standards-guidelines/risc/guidelines_for_interpreting_water_quality_data.pdf.
- Ministry of Environment. 2009. The Canadian Aquatic Biomonitoring Network: Field Manual. Retrieved from https://www2.gov.bc.ca/assets/gov/environment/natural-resource-stewardship/standards-guidelines/risc/cabin_field_manual.pdf.
- Ministry of Environment. 2018. British Columbia Approved Water Quality Guidelines: Aquatic Life, Wildlife, & Agriculture. Summary Report. Retrieved from <https://www2.gov.bc.ca/gov/content/environment/air-land-water/water/water-quality/water-quality-guidelines/approved-water-quality-guidelines>.
- Miranda KM, Espey MG, Wink DA. 2001. A Rapid, Simple, Spectrophotometric Method for Simultaneous Detection of Nitrate and Nitrite. *Nitric Oxide*. 5(1):62-71.
- Moraetis D, Efstathiou D, Stamati F, Tzoraki O, Nikolaidis NP, Schnoor JL, Vozinakis K. 2010. High-Frequency Monitoring for the Identification of Hydrological and Bio-Geochemical Processes in a Mediterranean River Basin. *Journal of Hydrology*. 389:127-136.
- Morosanu G, Zaharia L, Belleudy PH, Toroimac G. 2017. Methodology to Identify the Leading Factors of Rivers' Electrical Conductivity. Case Study: Jiu Catchment (Romania). *Air and Water Components of the Environment*. 2017(2017):26-33.

- Musolff A, Schmidt C, Rode M, Lischeid G, Weise SM, Fleckenstein JH. 2016. Groundwater Head Controls Nitrate Export from an Agricultural Lowland Catchment. *Advances in Water Resources*. 96:95-107.
- Myatt GJ, Johnson WP. 2009. *Making Sense of Data II: A Practical Guide to Data Visualization, Advanced Data Mining Methods, and Applications*. Hoboken, N.J.: John Wiley & Sons.
- Nagle G. 2000. *Advanced Geography*. New York: Oxford University Press.
- Nakagawa Y, Shibaa H, Sato F, Tsuji G. 2009. Influence of CO₂ Partial Pressure and Other Factors on Spatial and Temporal Variation of pH in Two Streams Draining the Watersheds Having different Size of Riparian Zone. *Environmental Science*. 22(3):173-186.
- Newbury RW, Cherry JA, Cox RA. 1969. Groundwater-Streamflow in Wilson Creek Experimental Watershed, Manitoba. *Canadian Journal of Earth Sciences*. 6:613-623.
- Newson MD, Large ARG. 2006. 'Natural' Rivers, 'Hydromorphological Quality' and River Restoration: A Challenging New Agenda for Applied Fluvial Geomorphology. *Earth Surface Processes and Landforms*. 31(13):1606-1624.
- Newson MD, Newson CL. 2000. Geomorphology, Ecology, and River Channel Habitat: Mesoscale Approaches to Basin-Scale Challenges. *Progress in Physical Geography*. 24(2):195-217.
- NRCan. 2017. Advanced Options: Sunrise/sunset Calculator. Retrieved November 22nd, 2017 from <https://www.nrc-cnrc.gc.ca/eng/services/sunrise/advanced.html>.
- Onset Computer Corporation. 2011-2017. HOBO[®] Pendant[®] Temperature Data Logger Manual. Bourne, MA: Onset.
- Palmer MA, Bernhardt ES, Allan JD, Lake PS, Alexander G, Brooks S, Carr J, Clayton S, Dahm CN, Shah JF, et al. 2005. Standards for Ecologically Successful River Restoration. *Journal of Applied Ecology*. 24(2):208-207
- Parkinson EA, Lea EV, Nelitz MA, Knudson JM, Moore RD. 2016. Identifying Temperature Thresholds Associated with Fish Community Changes in British Columbia, Canada, to Support Identification of Temperature Sensitive Streams. *River Research and Applications*. 32(3):330-347.
- Perini K., Sabbion P. 2017. *Urban Sustainability and River Restoration: Green and Blue Infrastructure*. Chichester, UK: John. Wiley & Sons Ltd.
- Quinn J, Cooper AB, Davies-Colley RJ, Rutherford C, Williamson RB. 1997. Land use Effects on Habitat, Water Quality, Periphyton, and Benthic Invertebrates in Waikato, New Zealand, Hill-Country Streams. *New Zealand Journal of Marine and Freshwater Research*. 31(5):579-597. DOI: 10.1080/00288330.1997.9516791.

- Rencher AC, Christensen WF. 2012. *Methods of Multivariate Analysis*. 3rd ed. Hoboken, NJ: John Wiley and Sons, Inc.
- Richter A, Kolmes S. 2005. Maximum Temperature Limits for Chinook, Coho, and Chum Salmon, and Steelhead Trout in the Pacific Northwest. *Reviews in Fisheries Science*. 13(1):23-49.
- Robledo EG, Corzo A, Papaspyrou S. 2014. A Fast and Direct Spectrophotometric Method for the Sequential Determination of Nitrate and Nitrite at Low Concentrations in Small Volumes. *Marine Chemistry*. 162:30-36.
- Roni P, Beechie TJ, Bilby RE, Leonetti FE, Pollock MM, Pess GR. 2002. A Review of Restoration Techniques and Hierarchical Strategy for Prioritizing Restoration in Northwest Watersheds. *North American Journal of Fisheries Management*. 22(1):1-20.
- Roni P, Beechie TJ. 2013. *Stream and Watershed Restoration: A Guide to Restoring Riverine Processes and Habitats*. Chichester, UK: John Wiley & Sons, Ltd.
- Shabalala AN, Combrinck L, McCrindle R. 2013. Effect of Farming Activities on Seasonal Variation of Water Quality of Bonsma Dam, KwaZulu-Natal. *South African Journal of Science*. 109(7/8):1-7.
- Schumm SA, Lichty RW. 1965. Time, Space and Causality in Geomorphology. *American Journal of Science*. 263(2):110-119.
- Shrestha M, Shrestha S, Shrestha PK. 2019. Evaluation of Land Use Change and its Impact on Water Yield in Songkhram River Basin, Thailand. *International Journal of River Basin Management*. Published online: 05 Feb 2019. doi: 10.1080/15715124.2019.1566239.
- Steel A, Sowder E, Peterson EE. 2016. Spatial and Temporal Variation of Water Temperature Regimes in the Snoqualmie River Network. *Journal of the American Water Resources Association*. 52(3):769-787.
- Stone ML, Roeske K, Chintapenta LK, Phalen L, Kalavacharla V, Ozbay G. 2016. Water Quality Analysis of Agriculturally Impacted Tidal Blackbird Creek, Delaware. *Frontiers in Environmental Science*. 4. doi: 10.3389/fenvcs.2016.00070.
- Taccogna G, Munro K. 1995. *The Streamkeepers Handbook: A Practical Guide to Stream and Wetland Care*. Salmonid Enhancement Program, Dept. Fisheries and Oceans. Vancouver, BC.
- Talling JF. 2008. Electrical Conductance – A Versatile Guide in Freshwater Science. *The Freshwater Biological Association*. 2:65-78.

- Thorp JH, Covich AP. 2010. Ecology and Classification of North American Freshwater Invertebrates. 3rd ed. London, UK: Elsevier.
- Thorp JH, Covich AP. 2015. Thorp and Covich's Freshwater Invertebrates: Ecology and General Biology. 4th ed. US: Academic Press.
- Viswanathan VC, Molson J, Schirmer M. 2015. Does River Restoration Affect Diurnal and Seasonal Changes to Surface Water Quality? A Study Along the Thur River, Switzerland. *Science of Total Environment*. 532:91-102.
- Waldron MC, Wiley JB. 1996. Water Quality and Processing Affecting Dissolved Oxygen Concentrations in the Blackwater River, Canaan Valley, West Virginia. United States.
- Walker J. 2016. Sub-reach Characterization of Alderson Creek to Determine Microhabitats Within a Small Riparian System. Thesis (BSc), University of British Columbia Okanagan, Kelowna, BC. 123 pages.
- Wallace JT, Grubaugh JW, Whiles MR. 1996. Biotic Indices and Stream Ecosystem Processes: Results from an Experimental Study. *Ecological Applications*. 6(1):140-151.
- Ware WB, Ferron JM, Miller BM. 2013. Introductory Statistics: A Conceptual Approach Using R. New York, NY: Routledge.
- Welch PS. 1952. Limnology. 2nd ed. New York, NY: McGraw-Hill Book Company, Inc.
- Wolter C, Buijse AD, Parasiewicz P. 2016. Temporal and Spatial Patterns of Fish Response to Hydromorphological Processes. *River Research and Applications*. 32(2):190-201.
- Woolsey S, Capelli F, Gonser T, Hoehn E, Hostmann M, Junker B, Paetzold A, Roulier C, Schweizer S, Tiegs S, et al. 2007. A Strategy to Assess River Restoration Success. *Freshwater Biology*. 52(4):752-769.

Appendix A: Instrument Calibration

Temperature

The temperature pendants were calibrated at the beginning of each deployment season, prior to placing them in the creek. Temperature pendants were calibrated by tying them to a weight and submerging them in a large container of ice water. The ice-water bath was left for the day to heat up slowly while temperature was recorded simultaneously by all the pendants at 15-minute intervals. Once the ice melted, hot water was added to spike the temperature, and the system was left to cool down. Several cycles of cooling with ice and heating with hot water were recorded over the course of several days, simulating a range of temperature changes from just above freezing to about 50° Celsius. During the initial set of calibrations in 2015 and 2016, small differences in several pendant recordings were noted, and this was believed to be due to density stratification of the water according to temperature (relative to the position of the pendants in the container). During the 2017 calibration, a small recirculating pump was used to keep water moving and to prevent thermal stratification. In addition, a copper-plated sensor was used as a ‘standard’ and the signal was recorded by an Onset HOBO 4-channel logger (model number U12-008). The accuracy of this sensor was $\pm 0.25^{\circ}\text{C}$ in comparison to the $\pm 0.53^{\circ}\text{C}$ for the pendants.

The raw temperature data for all pendants were plotted against a ‘true’ temperature, and a regression analysis was performed. The ‘true’ temperature was the mean of all pendants for 2015 and 2016 whereas the ‘true’ temperature in 2017 was the value from the copper-plated probe. Regression statistics were used to evaluate whether the pendant temperature deviated significantly from the true temperature. As an example, the regression equations for pendant 1 (T1) are shown from 2016 and 2017 in Figure 0.1 A) and Figure 0.1 B), respectively, where y is the temperature recorded by T1, and x is the true temperature. The r-squared values of 0.9997 and 0.9995 (2016 and 2017, respectively) indicate very small variance of temperatures recorded by pendant 1 compared to the true temperature, and the gains and offsets indicate a one-to-one correlation.

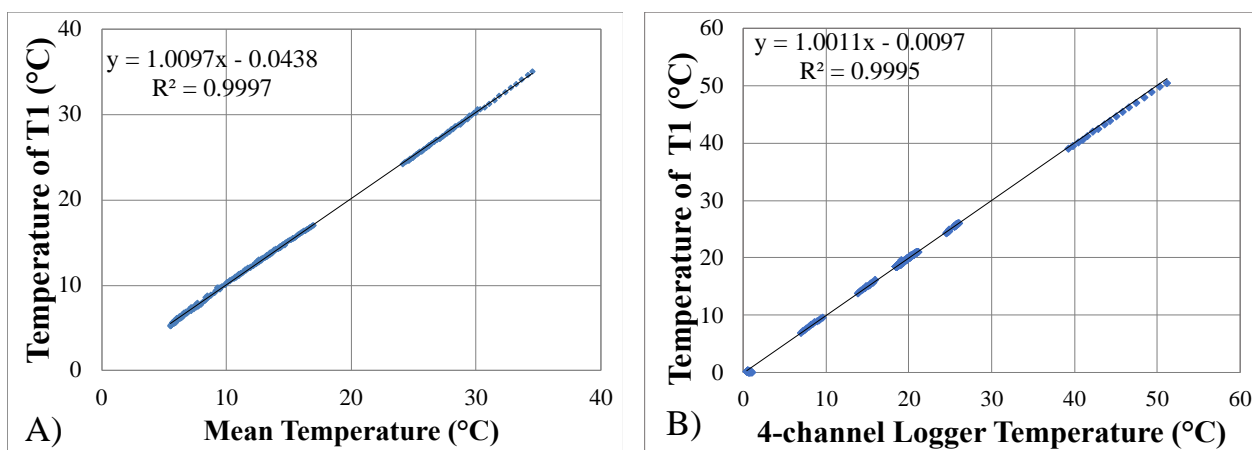


Figure 0.1. Regression analysis for the calibration of temperature pendant 1 in A) 2016 and B) 2017. Temperatures recorded by pendant 1 are plotted against the mean of the temperatures recorded by all pendants for 2016 and plotted against the temperatures recorded by the copper-plated 4-channel logger for 2017.

Regression residuals were calculated and plotted against the true temperature values to evaluate the relative performance of each of the pendants (2016 in Figure 0.2A) and 2017 in Figure 0.2B)). Most residuals were between -0.7°C and $+0.7^{\circ}\text{C}$, which is approximately the accuracy of the pendants (Table 3.3). The exceptions are for warm temperatures beyond the range of interest of this study (i.e., above 30°C). The calibration results for 2017 are considered more reliable because of the use of a circulation pump in the water bath, whereas in 2016 there was likely thermal stratification that may have influenced pendant results depending on position within the tank. The residuals indicate that there is a trending deviation away from the copper-plated standard above 30°C , although all pendants responded in similar fashion.

Temperature pendants are also sensitive to solar radiation. A laboratory experiment testing the extent of the response of the pendants to the sun demonstrated that pendants left exposed to the sun recorded temperature maximums up to 3°C warmer than pendants that were shaded from the sun. In Alderson Creek, several pendants were shaded naturally (i.e., tree cover, culverts) and other pendants were deeply immersed in aquatic weeds and likely did not see the sunshine during the summer, which suggests that shielding may not have been an issue. An in-stream experiment comparing daily temperature maximums of shaded versus non-shaded pendants at each sample site was not carried out, however, and some temperature maximums may be exaggerated by up to 3°C .

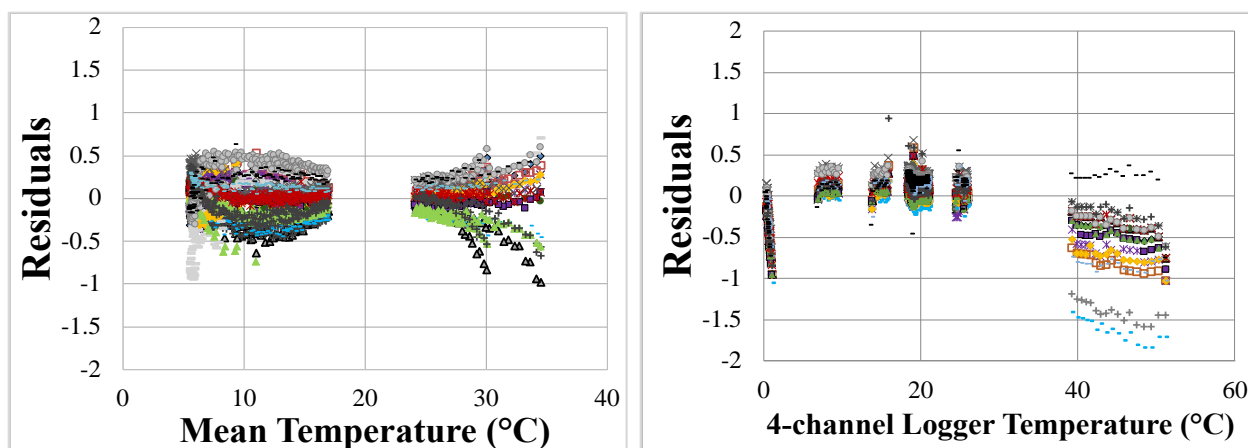


Figure 0.2. Residuals of temperature pendant data plotted against the true temperature to evaluate variance in A) 2016 and B) 2017. Degree of variance was used to confirm calibration and accuracy of the temperature pendants.

Conductivity, Turbidity, pH, Dissolved Oxygen

PCTestr 35 handheld probes were calibrated as per the manual instructions using the calibration function on the meter and a set of standards. BDH® pH reference buffers included 4.01, 7.01 and 10.01 pH standards. Conductivity standard was an in-house salt solution made of 0.759 grams of KCl salt in 1 L of water to get a 0.01 M solution, corresponding to a conductivity of 1413 μS at 25°C. The meters were calibrated several times throughout the field collection season.

The HACH 2100Q turbidimeter comes with a StablCal ampule kit, which included three calibration standards: 20, 100, and 800 NTU, and a 10 NTU verification standard. The 20, 100 and 800 NTU standards were read using the calibration function on the turbidimeter, and the 10 NTU standard was read to verify the calibration. Turbidimeter calibration was done several times throughout the field collection period, in addition to when batteries were replaced and when the lightbulb was replaced.

The DO meter was calibrated with a small amount of room-temperature water in a narrow-neck bottle. A stopper sealed the bottle while it was shaken vigorously for several minutes to attain fully air-saturated water. This acted as the 100% DO standard required to calibrate as per the DO meter calibration function.

Appendix B: Nitrogen Concentration Calculation

The molar concentration of KNO₃ (10 mM) was used to calculate the nitrogen concentration from absorbance. For instance, if c_1 is the molecular concentration of the KNO₃ stock solution (mM), v_1 is the volume of the KNO₃ stock solution (mL), and v_2 is the volume of e-pure water (mL), c_2 will be the concentration of nitrogen in the mixed standard (mM) and can be calculated by $c_1v_1=c_2v_2$. The concentration of nitrogen can be converted to milligrams per litre with the molar mass of KNO₃, which is 101.1032 g/mol. An example calculation of the concentration of nitrogen in the standard made up of 50 μ L KNO₃ (0.05 mL) in 100 mL of e-pure is as follows:

$$c_1 * v_1 = c_2 * v_2$$

$$10 \text{ mM} * 0.05 \text{ mL} = c_2 * 100 \text{ mL}$$

$$0.5 \text{ mM} * \text{mL} = c_2 * 100 \text{ mL}$$

$$c_2 = 0.005 \text{ mM}$$

$$\text{Converted to mg/L: } c_2 = 0.005 \text{ mM} * \frac{1 \frac{\text{mol}}{\text{L}}}{1000 \text{ mM}} * \frac{101.1032 \text{ g}}{\text{mol}} * \frac{1000 \text{ mg}}{1 \text{ g}}$$

$$c_2 = 0.506 \text{ mg/L}$$

The concentrations of nitrogen (mg/L) in each standard were plotted against the absorbance given by the spectrophotometer to obtain a calibration curve. The calibration curve trendline equation was used to convert absorbance to concentration for creek samples, where the x in the $y = mx+b$ slope equation was absorbance of creek samples, and y was nitrogen concentration in mg/L.

Appendix C: Discriminant Analysis Results

The following results are discriminant analysis (DA) tests that were not presented in the results chapter. The combined-group plot and loadings tables are shown for each test.

Discriminant Variables: Conductivity, temperature, pH, turbidity (excluding XS 34/35)

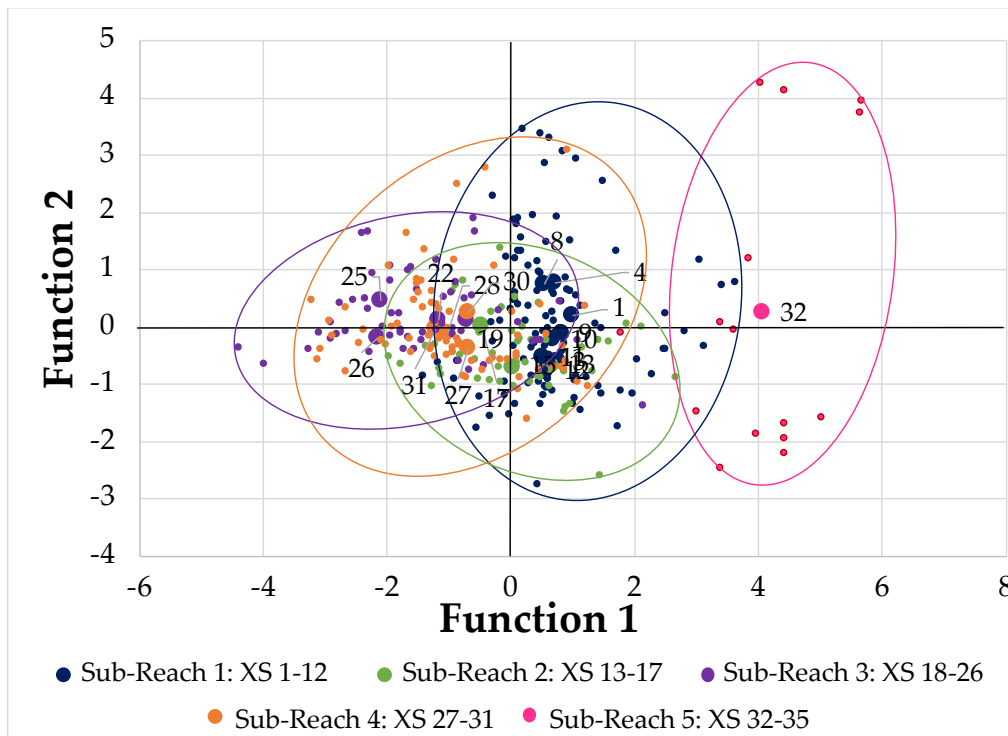


Figure A1. Centroids for each sampling site (i.e., cross section) on a combined-group plot. Discriminant functions maximize the variance between cross-sections based on the summer pH, turbidity, temperature, and conductivity observations along Alderson Creek. Cross-sections 34 and 35 are excluded to identify how remaining sample sites cluster. Centroids and casewise results are shown to see how well 32 is differentiated from other sample sites.

Table A1. Loadings of each parameter on the respective functions, shown for the analysis that included pH, temperature, turbidity, and conductivity (excluding XS 34 and 35). The larger the loading, the stronger the correlation between the variable and the discriminant function. The sign (+/-) indicates the direction of the relationship.

	Function 1	Function 2
pH	0.462	1.022*
Temperature	0.597	-0.154
Turbidity	0.318	0.412
Conductivity	-0.964*	0.442

Discriminant Variables: Temperature, pH, turbidity (excluding R5)

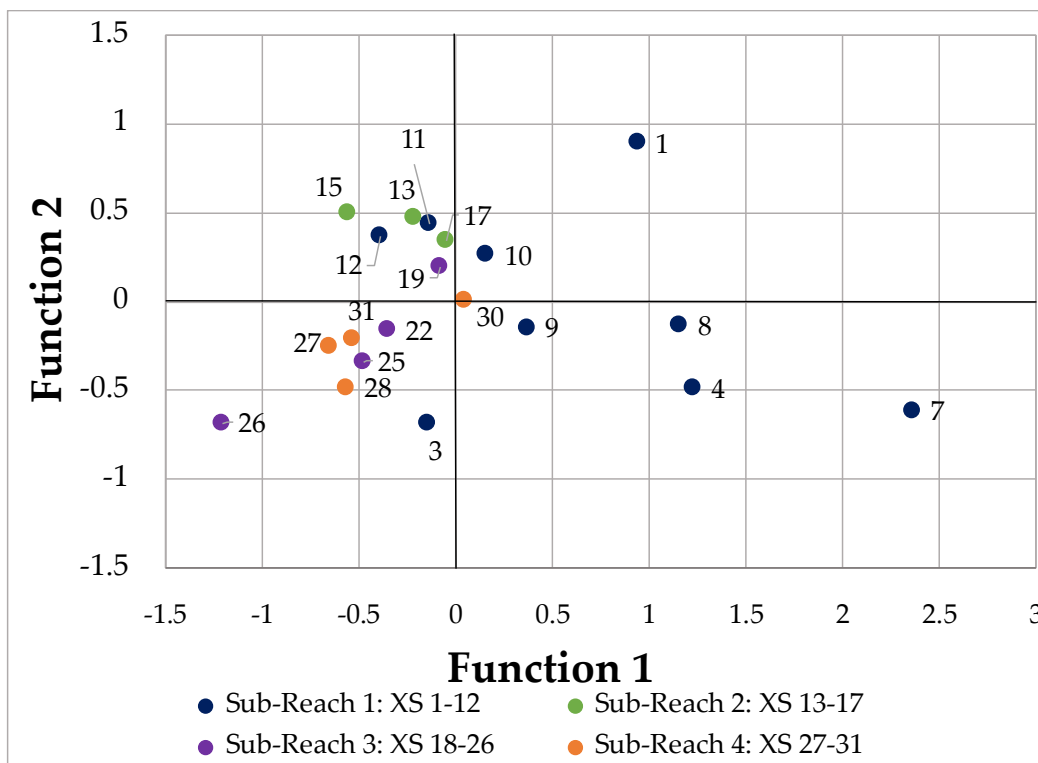


Figure A2. Centroids for each sampling site (i.e., cross section) on a combined-group plot. Discriminant functions maximize the variance between cross-sections based on the summer pH, turbidity, and temperature observations along Alderson Creek. Sample sites in sub-reach 5 are excluded to identify how remaining sample sites cluster.

Table A2. Loadings of each parameter on the respective functions, shown for the analysis that included pH, temperature, and turbidity (excluding R5). The larger the loading, the stronger the correlation between the variable and the discriminant function. The sign (+/-) indicates the direction of the relationship.

	Function 1	Function 2
pH	0.863*	-0.124
Temperature	0.165	0.953*
Turbidity	-0.050	-0.164

Discriminant Variables: Conductivity, temperature, pH, turbidity (excluding R5)

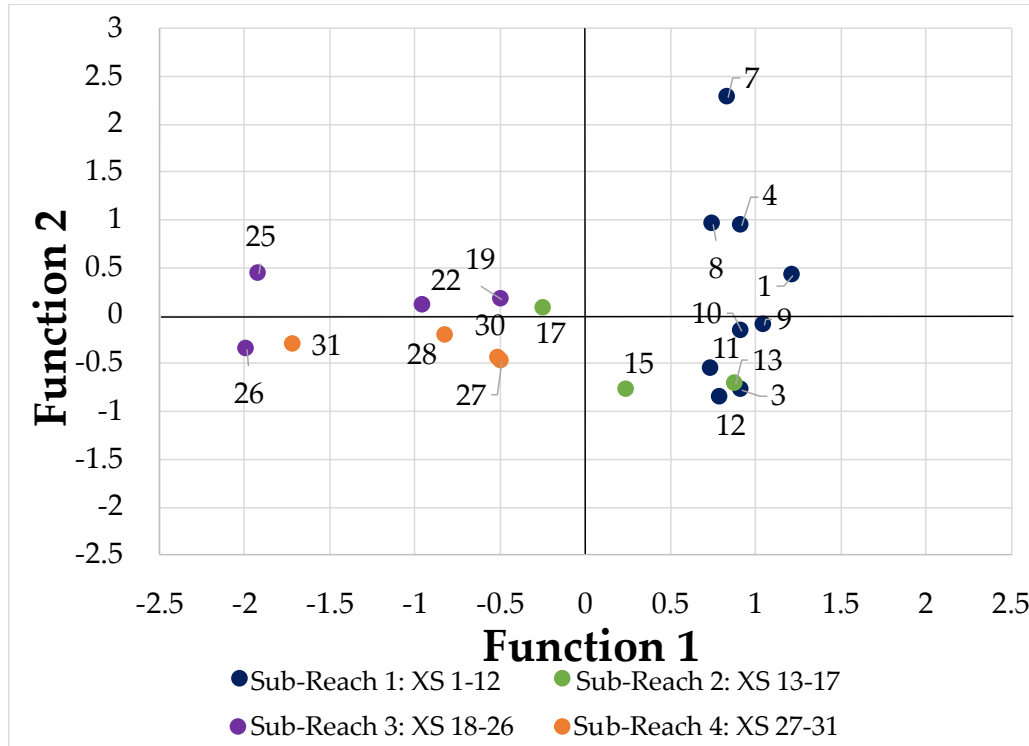


Figure A3. Centroids for each sampling site (i.e., cross section) on a combined-group plot. Discriminant functions maximize the variance between cross-sections based on the summer pH, turbidity, temperature, and conductivity observations along Alderson Creek. Sample sites in sub-reach 5 are excluded to identify how remaining sample sites cluster.

Table A3. Loadings of each parameter on the respective functions, shown for the analysis that included pH, temperature, turbidity, and conductivity (excluding R5). The larger the loading, the stronger the correlation between the variable and the discriminant function. The sign (+/-) indicates the direction of the relationship.

	Function 1	Function 2
pH	0.389	0.736*
Temperature	0.248	0.006
Turbidity	-0.091	0.057
Conductivity	-0.745*	0.339

Discriminant Variables: Macrophyte density, pH, temperature

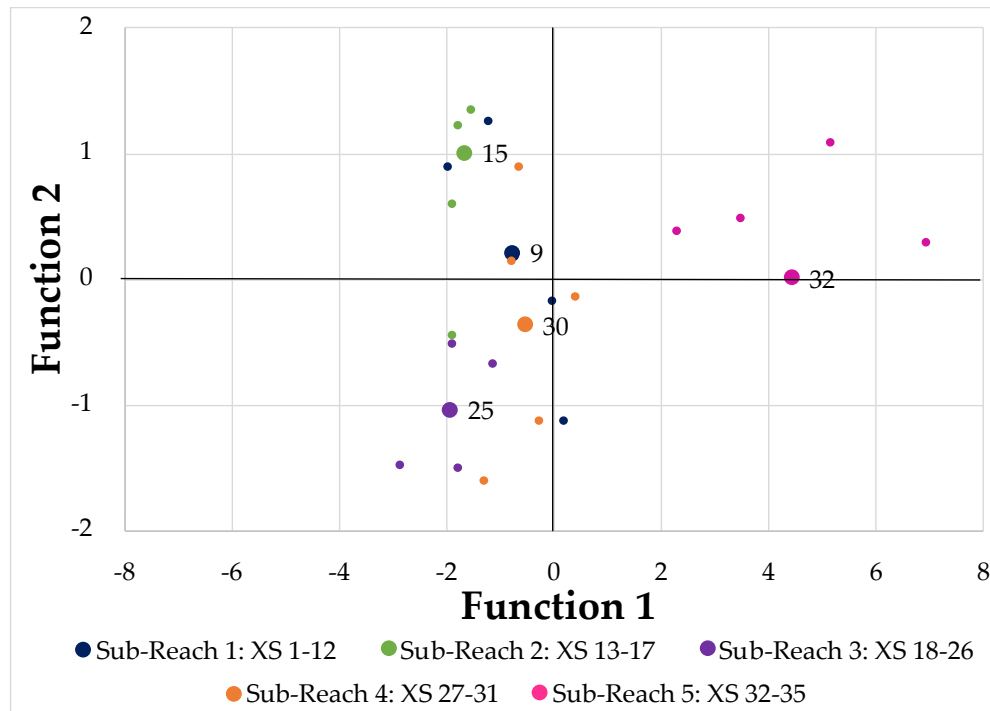


Figure A4. Centroids for each sampling site (i.e., cross section) on a combined-group plot. Discriminant functions maximize the variance between cross-sections based on the summer pH, temperature, and macrophyte density observations along Alderson Creek.

Table A4. Loadings of each parameter on the respective functions, shown for the analysis that included pH, temperature, and macrophyte density. The larger the loading, the stronger the correlation between the variable and the discriminant function. The sign (+/-) indicates the direction of the relationship.

	Function 1	Function 2
pH	0.699*	-0.244
Temperature	0.228	0.962*
Macrophyte Density	-0.167	-0.484

Discriminant Variables: Macroinvertebrates in control baskets, pH, temperature, turbidity, conductivity

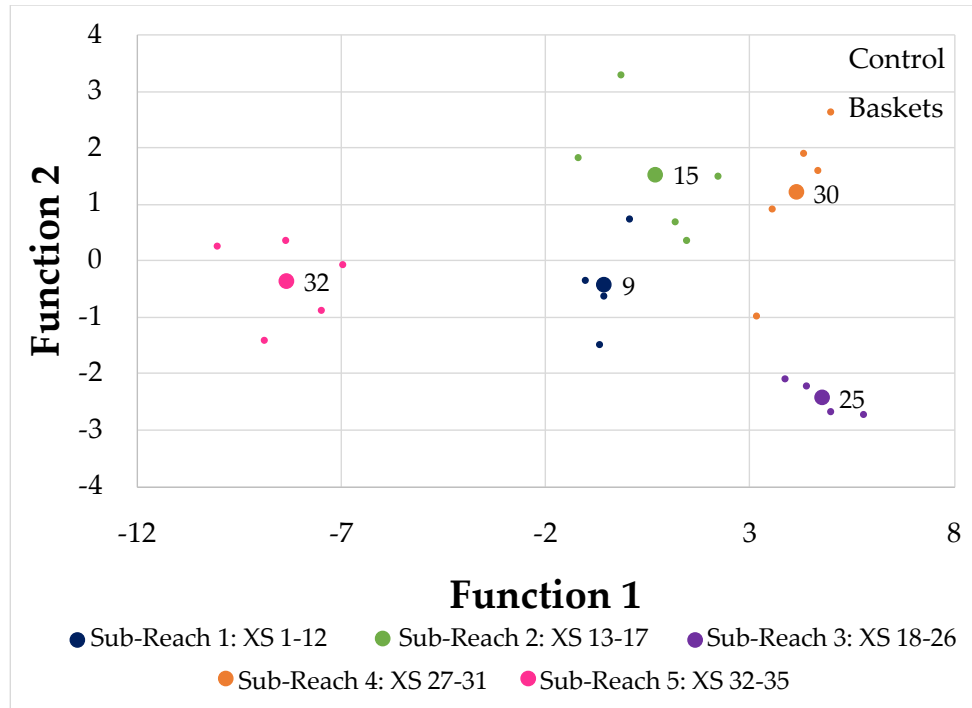


Figure A5. Centroids for each sampling site (i.e., cross section) on a combined-group plot. Discriminant functions maximize the variance between cross-sections based on the summer pH, temperature, turbidity, conductivity and macroinvertebrate counts in control baskets along Alderson Creek.

Table A5. Loadings of each parameter on the respective functions, shown for the analysis that included pH, temperature, turbidity, conductivity and macroinvertebrate counts in control baskets. The larger the loading, the stronger the correlation between the variable and the discriminant function. The sign (+/-) indicates the direction of the relationship.

	Function 1	Function 2
Macroinvertebrate Abundance	0.166	0.64*
pH	0.177	-0.193
Turbidity	0.059	0.021
Temperature	-0.129	0.43
Conductivity	0.624*	-0.275

Discriminant Variables: Macroinvertebrates in cumulative baskets, pH, temperature, turbidity, conductivity

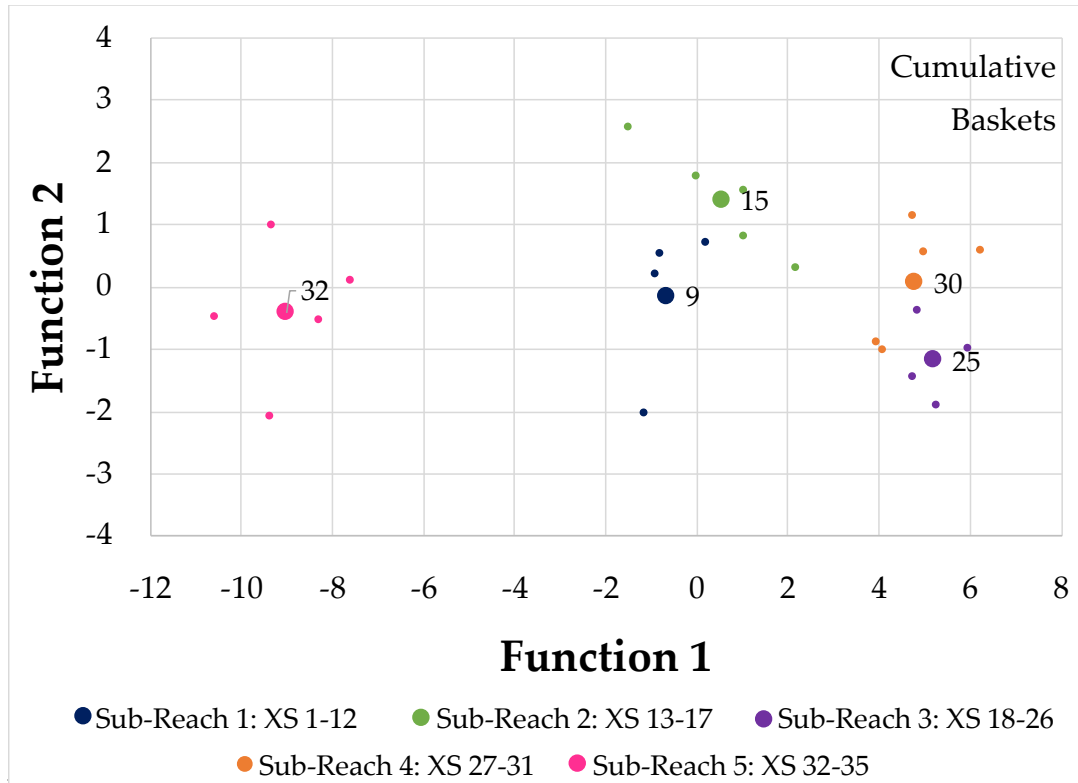


Figure A6. Centroids for each sampling site (i.e., cross section) on a combined-group plot. Discriminant functions maximize the variance between cross-sections based on the summer pH, temperature, turbidity, conductivity and macroinvertebrate counts in cumulative baskets along Alderson Creek.

Table A6. Loadings of each parameter on the respective functions, shown for the analysis that included pH, temperature, turbidity, conductivity and macroinvertebrate counts in cumulative baskets. The larger the loading, the stronger the correlation between the variable and the discriminant function. The sign (+/-) indicates the direction of the relationship.

	Function 1	Function 2
Macroinvertebrate Abundance	0.135	0.289
pH	-0.158	-0.608
Turbidity	0.052	0.177
Temperature	-0.118	0.684*
Conductivity	0.571*	-0.603

Discriminant Variables: Macroinvertebrates in kick nets, pH, temperature, turbidity

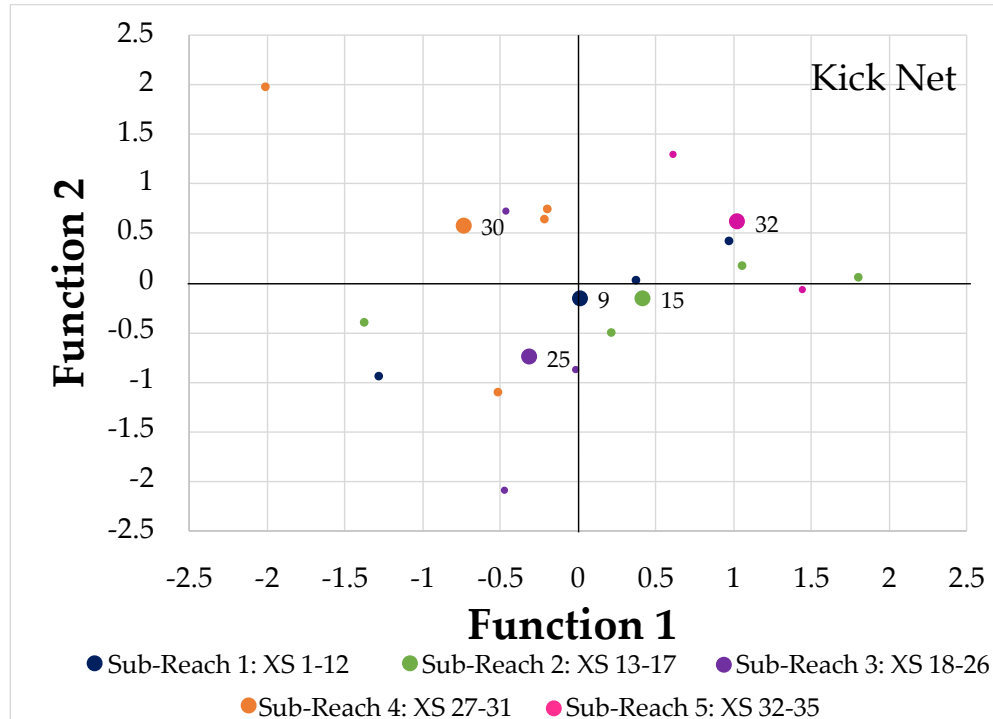


Figure A7. Centroids for each sampling site (i.e., cross section) on a combined-group plot. Discriminant functions maximize the variance between cross-sections based on the summer pH, temperature, turbidity, and macroinvertebrate counts in kick nets along Alderson Creek.

Table A7. Loadings of each parameter on the respective functions, shown for the analysis that included pH, temperature, turbidity, and macroinvertebrate counts in kick nets. The larger the loading, the stronger the correlation between the variable and the discriminant function. The sign (+/-) indicates the direction of the relationship.

	Function 1	Function 2
pH	0.339	0.417
Temperature	0.473	0.549*
Turbidity	-0.552*	0.398
Macroinvertebrate Counts	-0.367	-0.166

Discriminant Variables: DO, pH, temperature

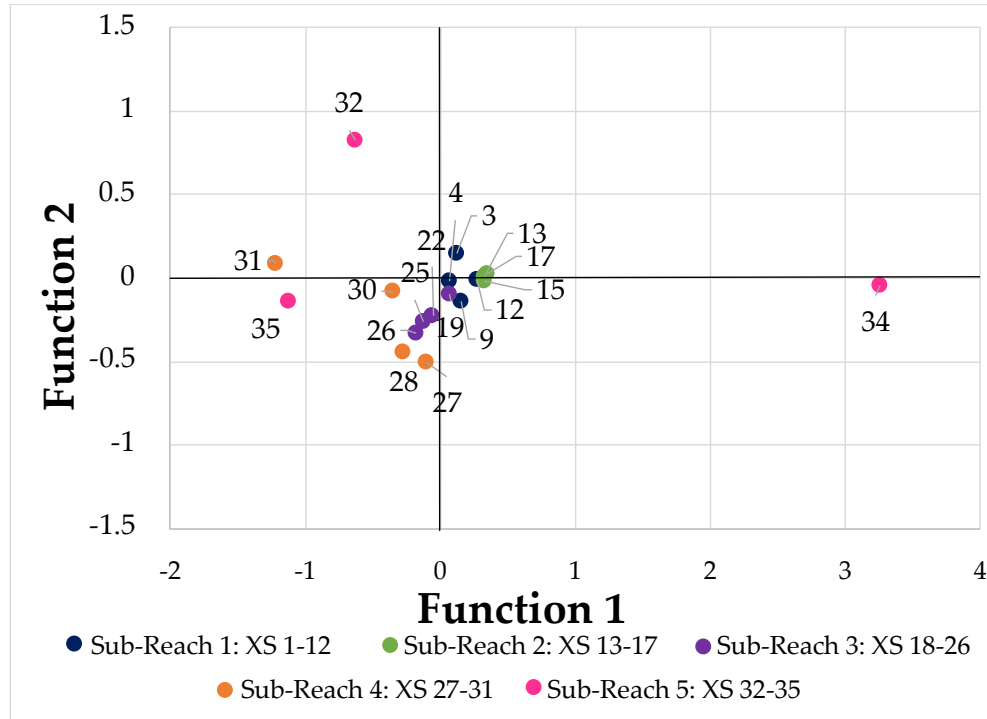


Figure A8. Centroids for each sampling site (i.e., cross section) on a combined-group plot. Discriminant functions maximize the variance between cross-sections based on the summer pH, temperature, and DO observations along Alderson Creek.

Table A8. Loadings of each parameter on the respective functions, shown for the analysis that included pH, temperature, and DO. The larger the loading, the stronger the correlation between the variable and the discriminant function. The sign (+/-) indicates the direction of the relationship.

	Function 1	Function 2
pH	-0.061	0.745*
Temperature	0.349	0.742
DO	0.911*	-0.406

Discriminant Variables: DO, pH, temperature, conductivity (excluding R5)

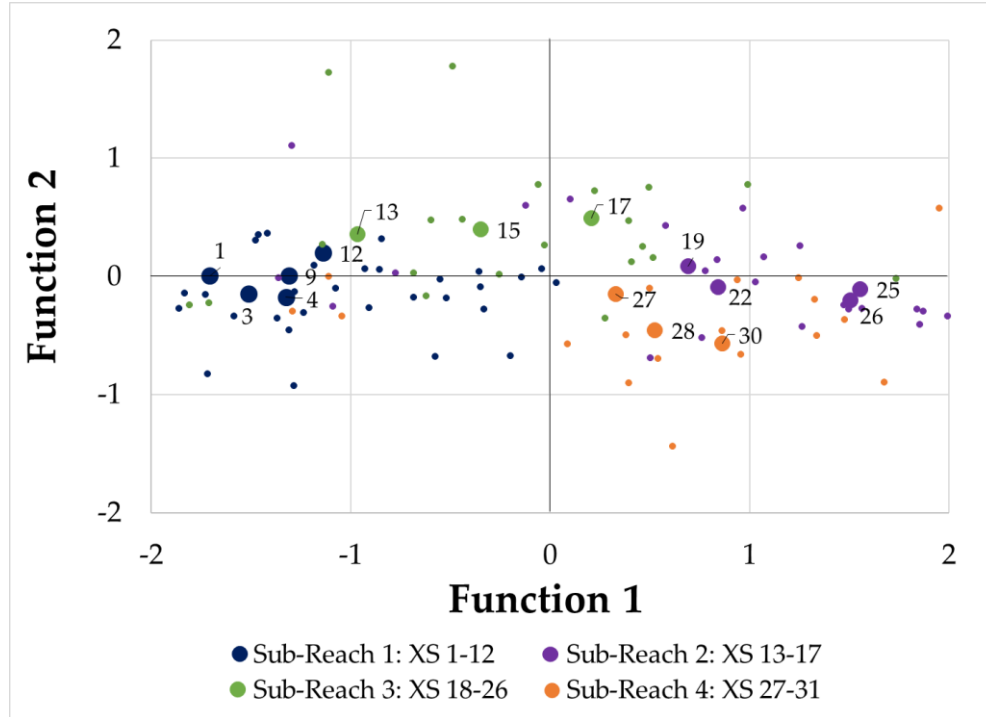


Figure A9. Centroids for each sampling site (i.e., cross section) on a combined-group plot. Discriminant functions maximize the variance between cross-sections based on the summer pH, temperature, conductivity, and DO observations along Alderson Creek. Sample sites in sub-reach 5 are excluded to identify how remaining sample sites cluster. XS 31 was also excluded since it was an outlier for R4.

Table A9. Loadings of each parameter on the respective functions, shown for the analysis that included pH, temperature, conductivity, and DO (excluding R5). The larger the loading, the stronger the correlation between the variable and the discriminant function. The sign (+/-) indicates the direction of the relationship.

	Function 1	Function 2
pH	-0.124	0.01
Temperature	-0.138	0.354
Conductivity	0.77*	0.082
DO	-0.036	0.859*

Discriminant Variables: Nitrogen, pH, temperature

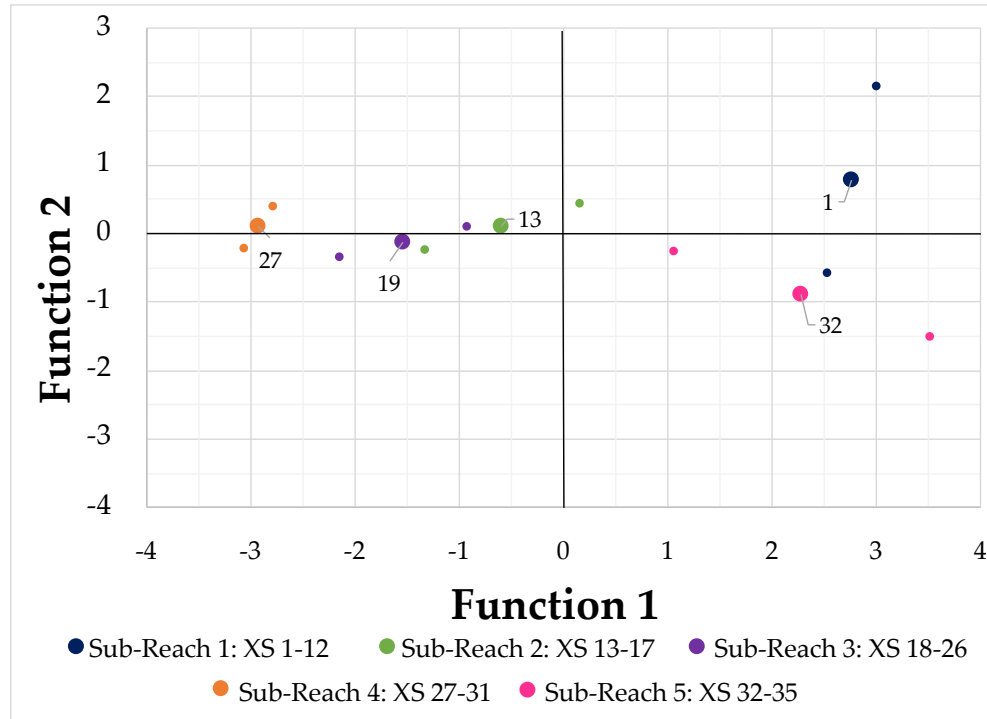


Figure A10. Centroids for each sampling site (i.e., cross section) on a combined-group plot. Discriminant functions maximize the variance between cross-sections based on the summer pH, temperature, and nitrogen observations along Alderson Creek.

Table A10. Loadings of each parameter on the respective functions, shown for the analysis that included pH, temperature, and nitrogen. The larger the loading, the stronger the correlation between the variable and the discriminant function. The sign (+/-) indicates the direction of the relationship.

	Function 1	Function 2
pH	0.203	0.776*
Temperature	0.091	0.253
Nitrogen	-0.69*	0.676

Discriminant Variables: Nitrogen, pH, temperature, conductivity

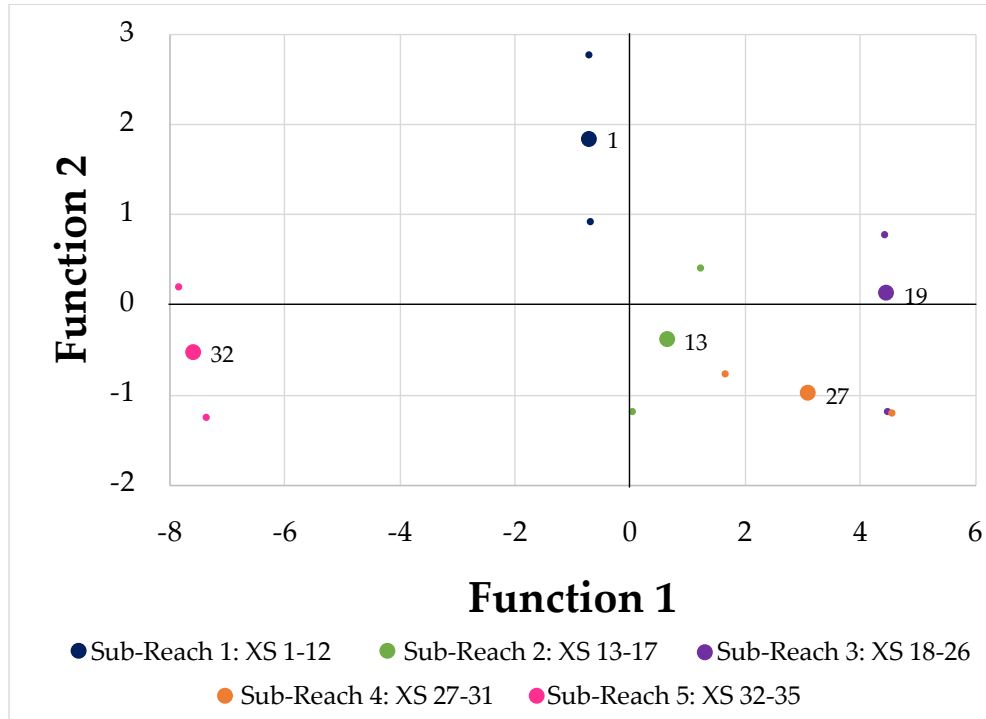


Figure A11. Centroids for each sampling site (i.e., cross section) on a combined-group plot. Discriminant functions maximize the variance between cross-sections based on the summer pH, temperature, conductivity, and nitrogen observations along Alderson Creek.

Table A11. Loadings of each parameter on the respective functions, shown for the analysis that included pH, temperature, conductivity, and nitrogen. The larger the loading, the stronger the correlation between the variable and the discriminant function. The sign (+/-) indicates the direction of the relationship.

	Function 1	Function 2
pH	-0.029	0.589*
Temperature	-0.02	0.191
Conductivity	0.279*	0.055
Nitrogen	0.246	-0.388